Faculdade de Engenharia da Universidade do Porto

NEEM – Non-metallic Electrodes for EEG Monitoring

Francisco Machado Dutra

20/09/2020

Faculdade de Engenharia da Universidade do Porto

NEEM – Non-metallic Electrodes for EEG Monitoring

Francisco Machado Dutra
up201809045@fe.up.pt

Dissertation carried out within the scope of
Master in Biomedical Engineering

Superviser: José Carlos Fonseca

20/09/2020

Resumo

Neste trabalho foi desenvolvido um novo tipo de elétrodo não-metálico para a realização de medições de eletroencefalografia.

Este é fabricado em poliuretano revestido com um filme de polímero condutor designado por poli(3,4-etilenodioxitiofeno), PEDOT, o qual tem demonstrado bastante interesse nos últimos anos devido à sua estabilidade ao ar e condutividade.

Neste trabalho foram produzidos filmes de PEDOT pelo método da polimerização por fase de vapor com o uso de oxidantes de Fe(III). Posteriormente, foram adicionados aditivos como piridina, um copolimero, PPG-PEG-PPG, e ainda foi analisado um pós-tratamento com ácido sulfúrico, com o objetivo de melhorar a condutividade dos filmes. Por fim, foi selecionado o melhor filme, para o a caraterização física e eletroquímica e para o revestimento de elétrodos multipino de poliuretano para eletroencefalografia. Obtiveram-se valores de condutividades entre 209 a 268 S/cm.

Estes elétrodos, por sua vez, foram avaliados por testes eletroquímicos *in-vitro* e *in-vivo,* e, de seguida, foram testados por aplicação em duas posições, frontal e occipital, no escalpe de vários voluntários.

Nos registos eletro-encefálicos conseguiu-se obter resultados bastante semelhantes aos obtidos com elétrodos de Ag/AgCl com gel, apresentando coeficientes de correlação de Spearman acima dos 76% entre o elétrodo de Ag/AgCl e PEDOT. Em termos de densidade espectral os espectros são idênticos tanto na posição frontal e occipital, ou seja, os elétrodos de PEDOT conseguiram registar de forma análoga em vários pontos da cabeça.

Palavras-chave: Eletroencefalografia, PEDOT, elétrodos

Abstract

In this work, a new type of non-metallic electrode was developed to perform electroencephalography measurements. It is made of polyurethane coated with a conductive polymer film called poly (3,4-ethylenedioxythiophene), PEDOT, which has shown considerable interest in recent years due to its stability and conductivity.

For this work, PEDOT films were deposited by using vapor phase polymerization, using Fe (III) oxidants. Subsequently, additives such as pyridine, a copolymer of PPG-PEG-PPG were added, and a post-treatment with sulfuric acid was also analyzed in order to improve the conductivity of the films. Finally, the best film was selected and the physical and electrochemical characterization was carried out. Finally, the PEDOT coatings were applied to polyurethane multipin electrodes for electroencephalography. Conductivity values between 209 to 268 S / cm were obtained.

These electrodes, in turn, were evaluated by electrochemical tests in-vitro and in-vivo, and then they were fixed in two positions of the scalp, frontal and occipital, and tested for EEG acquisition.

In the electro-encephalic registers it was possible to obtain results very similar to those obtained with gel Ag/AgCl electrodes, presenting Spearman correlation coefficients above 76% between the Ag/AgCl and PEDOT electrodes. In terms of spectral density, both spectra were identical in both the frontal and occipital positions, meaning that the PEDOT electrodes were able to record the EEG signal in several points of the scalp.

Key words : Electroencephalography, PEDOT, electrodes

Agradecimentos

É com grande satisfação que expresso nesta dissertação o mais profundo agradecimento a todos aqueles que tornaram possível a sua realização.

Ao meu orientador Prof. Dr. José Carlos Magalhães Duque da Fonseca pela oportunidade de trabalhar num projeto tão interessante e pela sua disponibilidade, pelos conhecimentos transmitidos e incentivo demonstrado ao longo de todas as fases do projeto.

Queria agradecer ao professor Haueisen por se ter disponibilizado receber-me no seu laboratório, embora tal não tenha afinal sido possivel

À instituição que tornou possível o sucesso deste trabalho: o Departamento de Engenharia Metalúrgica e de Materiais da Faculdade de Engenharia do Porto.

A todos os colegas de laboratório e pessoas que contribuíram para este estudo.

Aos meus amigos pelo seu apoio, incentivo e amizade.

À minha família que me ajudaram ao longo do meu percurso académico e que sempre acreditaram em mim.

Table of contents

List of figures

List of tables

Abbreviations, Acronyms e Symbols

List of abbreviations and acronyms

A/D	*Analog-to-digital*
Ag/AgCl	*Silver/silver chloride*
Au	*Gold*
ECoG	*Electrocorticogram*
EDOT	*3,4-ethylenedioxythiophene*
EEG	Electroencephalogram
EIS	*Electrochemical impedane Spectroscopy*
$Fe(Tos)_3$	*Iron(III)-toysolate*
$FeCl_3$	*Iron(III) chloride*
H2SO4	*Sulfuric Acid*
ICP	*Intrisically conductive polymer*
PEDOT	*Poly(3,4-ethylenedioxythiophene)*
PEDOT:PSS	*poly(3,4-ethylenedioxythiophene) polystyrene*
PEG-ran-PPG	*Poly(ethyleneglycol)-ran- poly(propylene glycol)*
PPy	Polypyrrole
PU	Polyurethane
PSS	Polystyrenesulfonic acid
Pt	*Platinum*
qEEG	*Quantitative electroencephalography*

SRy	*Surface resistivity*
VPP	*Vapor Phase Polymerization*

List of symbols

µV	Microvolt
C	Carbon
Cl^-	Cloride
dB	Decibel
e	Electron
eV	Electronvolt
Fe^{3+}	Iron (III)
h	Hour
H	Hydrogen
Hz	Hertz
K^+	Potassium
kΩ	Kilohm
min	Minute
mm	Milimeter
mV	Milivolt
MΩ	Megaohm
N	Nitrogen
Na^+	Sodium
nm	Nanometer
O	Oxygen
ºC	Celsius
S	Sulfur
S/□	Siemens per square
S/cm	Siemens per centimeter
sec	Second
Wt%	Weight of solute per weight of solvent
Ω/□	Ohm per square
Ω/cm	Ohm per centimeter

Chapter 1

1. Introduction

1.1. Background

The term *electroencephalogram* (EEG) was introduced for the first time by a German psychiatrist named Hans Berger, who recorded the potential fluctuations from the brain in a systematic form [1]. This electrical activity of the brain can be recorded with three types of electrodes, namely scalp, cortical and depth electrodes [2]. Starting with the scalp electrodes, these ones can register EEG signals on the scalp surface of a subject. Cortical electrodes are fixed on the surface of the brain, which is termed as an *electrocorticogram* (ECoG). Depth electrodes have the form of small needle capable of recording brain activity inside the neural tissue of the brain.

Measurements from all types of electrodes give rise to a changing potential that can be represented as a sum of the field potentials produced by different nerve cells. These records vary with the region of the brain [1].

The brain is divided in three main parts *cerebrum, brainstem and cerebellum*, **figure 1. 1**. The brainstem has three major functions, like connecting the cerebral cortex, spinal cord, and *cerebellum*; it is the responsible centre for the visceral functions such as, controlling the blood flow and respiration; finally, it works as an integration centre of some motor reflex. The *cerebellum* controls the somatic muscle system and operates with the *brainstem* and cerebral cortex to regulate and provide synchronous muscle movements. The *cerebrum* is a major part of the central nervous system and it is responsible for many functions of the nervous system [3].

The *cerebrum* is also a paired structure with right and left cerebral hemispheres in opposite sides of the body, meaning that voluntary movements of the right hand are controlled by the left cerebral hemisphere. The surface layer of the hemisphere is called the *cortex,* which receives sensory information from skin, eyes, ears and other receptors that caused movements or responses to these stimuli [3].

The hemispheres consist of several layers. The outer layer is composed by large groups of nerve cells and has a thickness of about 1 cm. It is named *cerebral cortex* and consist of a convoluted

surface with *gyri* (ridges) and *sulci* (valleys). In the deep layers of the hemispheres there are myelinated *axons (*white matter*)* and cell bodies called *nuclei*[3].

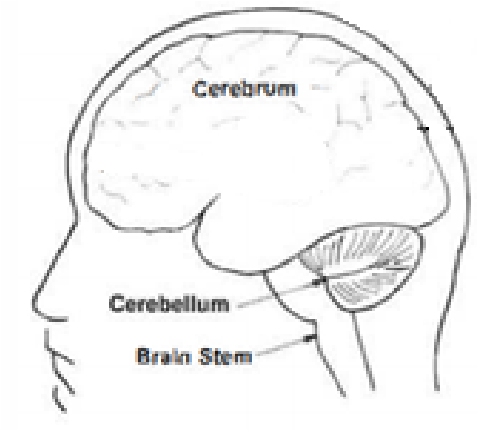

Figure 1. 1- Division of the human brain. Adapted from [2]

Neurons are classified in two main types pyramidal and nonpyramidal. Pyramidal cells of the cerebral cortex are organized vertically, with their long apical dendrites running parallel to one another; this orientation causes a current flow and potential differences that can be measured at the cortical surface [4]. Consequently, this forms a dipole as the extracellular medium near the soma acts as a source (+) and the upper part of the apical dendritic tree behaves as a sink (-).In **figure 1. 2**, it is possible to see a current flow in a pyramidal neuron. Non-pyramidal cells do not interfere, considerably, to the surface records, since their trees are radially arranged, over their cell bodies, in a way that charge differences between the dendrites and the cell body produce fields of current flow of zero when summed from a relatively distance on the cortical surface [3].

In addition, the influence of a specific dendritic *postsynaptic potential*[1] (PSP) on the cortical surface recording depends on its excitatory (-) or inhibitory (+) sign and its location in relation to the measurement site. The effect of each PSP impacts the orientation of the current dipole. Meaning that, continuing synaptic input creates a series of potential dipoles and resulting current flows that are staggered but overlapped in space and time. On the scalp potentials of any form can be created by one population of presynaptic fibres and cells on which they terminate, depending on the proportion that are inhibitory or excitatory, the level of the postsynaptic cells in the cortex, and so forth.

When multiple synaptic endings on the dendritic tree of each cell turn active, current flows in any direction in the dendritic tree on whether the synapses are excitatory or inhibitory. The source-sink previously discussed between dendrite and cell is a constantly shifting current dipole, where variations in dipole orientation and strength produce wavelike fluctuations in the surface field potential. When this sum of dendritic activity is negative relative to the cell, the cell is depolarized and quite excitable. When it is positive, the cell is hyperpolarized and less excitable [3].

The dipole produced by just one pyramidal cell cannot be measured with the electrodes attached to the scalp. Though, when a large number of dipole units approximately 60 million, synchronously discharges their action potentials, potentials in the scale of the μV are large enough to be recorded with the non-invasive EEG electrodes [5]. To sum up, the EEG is the macroscopic measure of the synchronous activity of a large population of neurons.

[1]The electric potential at a dendrite or other surface of a neuron after an impulse has reached it across a synapse.

Measurements of the electric recording from the scalp (outer surface of the head, EEG) or exposed surface of the brain (ECoG) results in oscillations produced inside the brain, also known as *brain waves*. *Brain waves* on the surface of the brain can reach 10 mV in amplitude in relation to an indifferent electrode like an earlobe electrode, but in the scalp the amplitudes only reach 100 μV. The frequencies depend on the kind of activity of the cerebral cortex which can vary between 0.5 to 100 Hz [2, 3, 6].

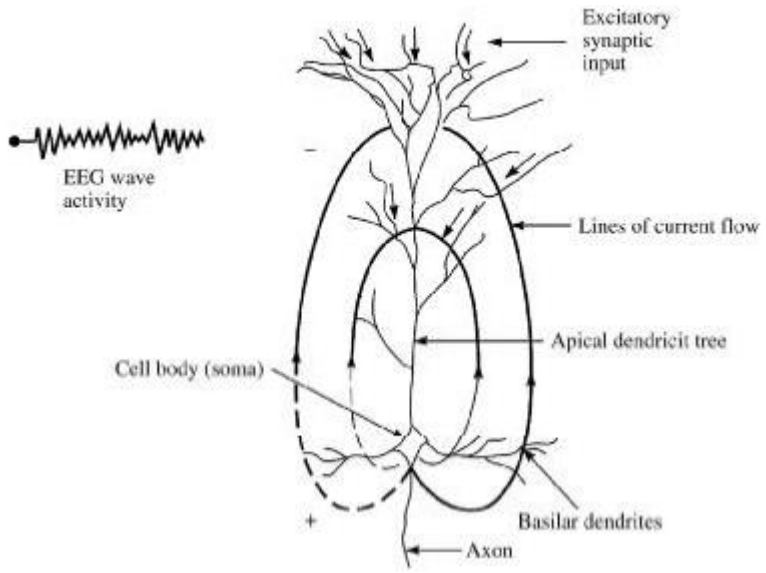

Figure 1. 2- Current flow in a pyramidal neuron [1]

As for EEG electrodes, they must be small, easily affixed to the scalp without disturbing the contact skin, comfortable and they must stay in place for sometimes long periods of time. Most EEG electrodes are made of silver/silver chloride (Ag/AgCl) which need a gel application and a previous skin preparation before starting EEG monitoring [7]. A new kind of EEG electrodes are starting to be used, called dry electrodes as they are gel-free sensors; they do not need skin preparation, consequently requiring less time for the recording preparation.

EEG is a good diagnose method for many neurological diseases such as cerebrovascular lesions, ischemia, tumour, epilepsy and problems caused by a trauma [1]. An EEG test is done by keeping the patient still to reduce artifacts from any movement of the electrode and muscle activity (face, neck, ears). Scalp electrodes are mostly formed by bulk metal electrodes coupled with gels. Though, these materials have a hard time to match the soft textured tissues of the skin and the roundness [8]. Subsequently, causing discomfort, irritation and, sometimes, adverse immune responses [8]. Therefore, a need for softer materials in scalp electrodes is emerging [8].

Measurement and/or stimulation requirements are necessary for the communication between electronic devices and biological tissues [9]. The electrode materials are extremely important for the transfer of the signal from the tissue to the recording apparatus since they influence the redistribution of charges (capacitive) and transfer of electrons and ions (faradaic) at the double layer that forms between the electrode and electrolyte (surrounding biofluid) [10, 11]. The charge injection capacities and the impedances are found to be the most important for stimulation and sensing [9]. Metals, metal alloys, metal oxides, doped semi-conductors, conductive polymers, and carbon nanomaterials have been investigated [9].Conducting polymers have been sometimes

replacing the metals for biomaterials applications due their softer nature (1 MPa to 5 GPa modulus, 5%–500% elastic strain limit) and biocompatibility [9]. Specifically, conducting polymers like poly(3,4-ethylenedioxythiophene) (PEDOT) and polypyrrole (PPy), are a appealing material because of their low electrochemical impedances [10].

Recent advances in conductive polymers have demonstrated that they could successfully replace conventional metals in EEG applications [9]. Dry polymer-based electrodes, like those built with thin layers of poly(3,4-ethylenedioxythiophene) polystyrene, PEDOT:PSS, on films of polyimide had a stable mechanically interface and they were able to conform to the scalp [12]. Moreover, the electrodes from this kind demonstrated to be useful in measuring EEG waveforms that were not detected by conventional materials [13, 14]. Additionally, other promising dry electrodes were processed with conductive elastomeric composites to further increase conformability and adhesion to the skin [15].

1.2. Scope, specific objectives and research approach

The goal of this work is the development and test of a new class of non-metallic and conformable bio-electrodes for non-invasive EEG signal monitoring. The new electrodes will increase the comfort of the patient during the exam, due to the deformation ability and they will avoid dermatitis due to metal contact (developed by some patients during long-term exams). Finally, they will enable to perform simultaneous electric and magnetic field measurements on the head without interferences, even with close electrodes, since PEDOT does not interfere with magnetic fields.

Here, a flexible polyurethane (PU) thermoplastic substrate will be coated with a thin layer of a conductive polymer, PEDOT, in order to obtain a conformable and conductive non-metallic electrode. A mechanical, electrical, and chemical characterization of the new composite will be undertaken, and in-vivo EEG signal acquisition will be carried on, to validate the concept.

The work involves the development of the fabrication technique for the electrodes, laboratory electrical and mechanical characterization, and in-vivo tests. The in-vivo tests will consist in the acquisition of EEG signals in volunteers and comparison with the signals obtained with commercial electrodes.

1.3. Structure of the report

This report is divided in seven chapters:

I. Introduction – a brief introduction of the work was explained is provided;
II. Fundamentals of electroencephalography – introduction of the electroencephalography system, electro-encephalic signals, EEG electrodes and technique, and artifacts;
III. Conductive Polymers – conductive polymers basic concepts, PEDOT and different polymerization processes;
IV. Enhancing the conductivity of PEDOT films- review of different studies of techniques that increase the conductivity of PEDOT;
V. Materials and Methods
VI. Results and Discussion
VII. Conclusion and Future Developments

Chapter 2

2. Fundamentals of electroencephalography

In this chapter the fundamentals of electroencephalography topics such as the anatomy of cerebrum, the bio-eletrical signals generation and transmission, neurological disorders, brain waves classification, acquisition of electroencephalic signals will be explained. Furthermore, the parameters for EEG measuring, electrode positioning and montages, and artifacts are other themes that are presented as well.

2.1. Anatomy and function of the cerebrum

As stated before, the brain is divided in three parts the *cerebrum*, *cerebellum* and the *brain stem*. Though, the *cerebrum* will be the most studied in this chapter since electric signals are generated on the scalp [2, 3].

The *cerebrum* is divided in two hemispheres, right and left and each hemisphere is sub-divided in four lobes named *frontal, temporal lobes*, *parietal* and *occipital lobes*. In each lobe, as a specific sensory information is processed like hearing, touch, vision and motor activity, **figure 2. 1**. The frontal lobe is important for problem solving, speech, movement and also associated to emotions.

Parietal lobe as a sensory function which receives sensory inputs coming from the hands, legs, and other parts of the body and also is important for language processing. Vision and visual memories take place in the occipital lobe.

Finally, the temporal lobe is the hearing centre as well as the storage place for long-term memory.

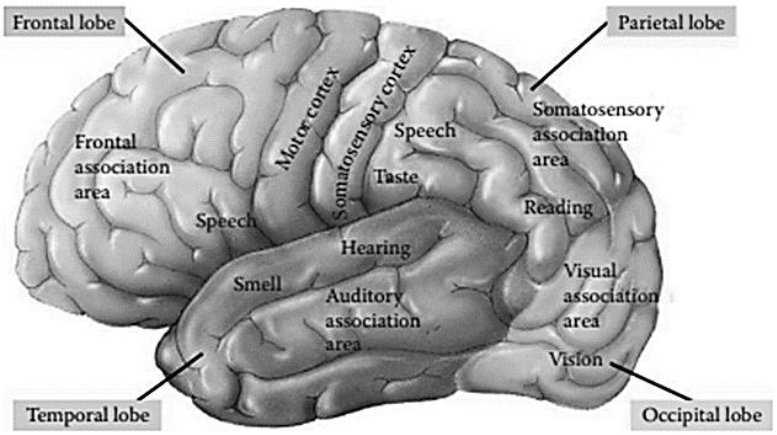

Figure 2. 1- Functional diagram of brain lobes. [4]

2.2. Bio-eletrical signals generation and transmission

Bioelectric signals that come from ECG (electrocardiographic) or EEG are generated by actions of various synchronized cells. Bioelectric signals, are propagated in nerve cells and muscle cells and they are the result of, basically, an excitation in the cell membrane that, when under specific conditions, generates an action potential [2, 3].

In EEG, neurons are responsible for these bioelectrical signals. A neuron has a nucleated cell body and several terminations. The terminations that can conduct impulses to the cell body are called dendrites. Axons are the parts that conduct the impulses away from the cell body.

As detailed before, pyramidal cells are in charge of the current flow and the potential variations registered in the cell membranes are responsible for the propagation of bioelectrical signals along the neurons. The formation of these bioelectric potentials come from an ionic nature of the semipermeable membrane of the cells which is selective to ions such as Na^+, K^+ and Cl^-[2, 3].

When a cell, such as a neuron, is excited its membrane does not permit the flow of K^+ and Cl^- but does allow the entrance of Na^+ resulting in a higher concentration of this ion inside the cell membrane. As Na^+ is a positive ion, in the resting state (resting potential), a cell will have a more positive charge in the inner surface of its membrane and a negative charge on the outside. This resting potential is about -90mV with the reference at the outer side of the cell. As stated before, when the flow of ions causes a potential difference between the inner and outer membrane of the cell of -60mV, depolarization happens. Consequently, the cell potential changes to a maximum value of +20mV. After that, the cell potential decreases to the resting potential (repolarization). All this complex process of discharging and recharging gives place to different voltage waveforms which can be measured with electrodes [2].

Another feature of this process is the refractory period which is the amount of time before the cell can again be stimulated for another action potential. This is related with the metabolic processes within the cell that takes time and energy for the completion of the action potential development [2].

2.3. Application of EEG in Neurological Disorders

A disorder in any component of the nervous system (brain, nerves and the spinal cord) that produces an impact on the structural, biochemical, or electrical nature is named a neurological disorder. Common symptoms of neurological disorders might consist of seizures, paralysis, muscle weakness, poor coordination, altered levels of consciousness, loss of sensation, pain and confusion [16].

The causes of disorders may come from a genetics, environmental and lifestyle problems (traumas, spinal cord, brain or nerve injury) and poor nutrition [16]. Additionally, a problem with another body system may cause, subsequently, a problem in the nervous system. For example, if there is a problem in the circulatory system, blood vessels may be unable to supply blood to the brain, causing serious problems in the nervous system, like stroke. Though, it is not possible, in some situations, to identify the cause of a neurological disorder. A few examples of neurological disorders are Parkinson's disease, Alzhemier's disease, epilepsy and others.

Epilepsy is one of the most common neurological diseases. Seizures ("abnormal, excessive, or synchronous neuronal activity in the brain results in transient epochs" [16]) are the characteristic symptom of epilepsy and could be recurrent and unprovoked [17]. This disorder is the most known brain illness within children and places third among adults after Alzheimer's disease and stroke. Furthermore, it is not very well understood what causes this disorder but some causes like brain tumour, stroke head trauma, accidents, falls, infection, and the genetic factor can provoke the appearance of epilepsy. This disease, currently, it has no cure though it can be controlled with medication [16]. The measurements of an epileptic brain have been registered with EEG and it was possible to determine a nonlinear signal with deterministic properties [17]. With a mathematical modelling of the nonlinear brain behaviour it may be possible to identify and prevent the seizures and control them to not happen in early stages of the neurological disease [16].

2.3.1. Abnormal Brain Activity Monitoring

Conventional EEG techniques are based on visual inspection of patterns from EEG measurements. This implies observation of changes in wave shapes, frequencies, and transitions of states that are not present in healthy subjects. Frequency analysis is specifically related to measurements of changes of the sub-band order, termed *spectral analysis*. Distinct types of neuronal disorders have different kind of spectral changes. For example in a subject that suffers a *traumatic brain injury* there is a significant decrease in the overall brain signal strength and epileptic subjects show very high activity at a focal point [16].

EEG abnormities can be classified in a variety of ways that are distinguished by abnormal expressions of normally occurring rhythms, like asymmetries of normal rhythms; inherently abnormal rhythms, for example 'slow' delta and theta rhythms in an adult who is awake; *periodic patterns*, burst-suppression patterns[1]; epileptiform abnormalities (spikes, sharp waves and others); and finally, abnormal 'super-architecture' (different/abnormal sleep state cycling) [18]. In the next **figure 2. 2** it is possible to see a clear EEG example of an abnormality, which has an evident slowing in the waves on the top that corresponds to the left hemisphere. This example is from a subject that has a postictal change[2] after a seizure.

[1] "burst suppression describes an electroencephalographic (EEG) pattern consisting of a continuous alternation between high-voltage slow waves (occasionally sharp waves) and depressed(or suppressed) electrographic activity."[21]

[2] Postical change is the altered state of consciousness after an epileptic seizure

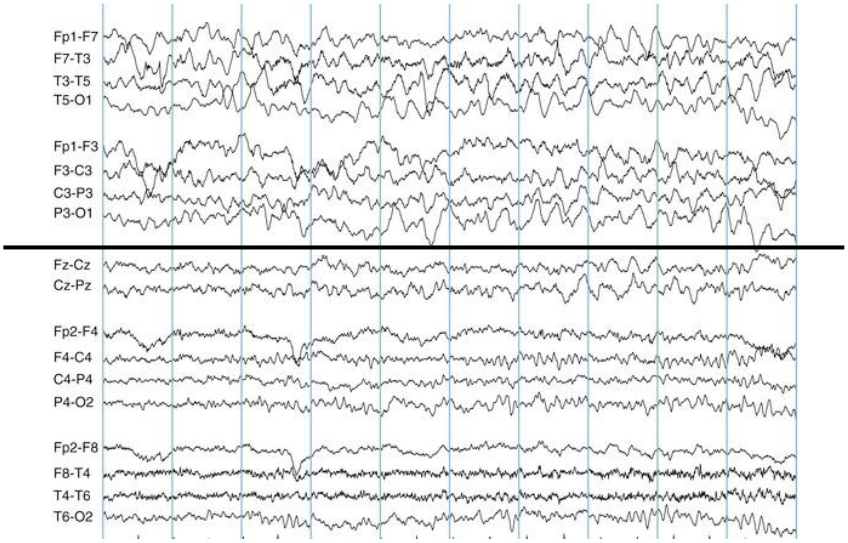

Figure 2. 2- EEG after a seizure. Slowing in the waves on the top (left hemisphere).Adapted from [4]

Lately, other techniques based on signal digitization and processing have been proposed, including quantitative electroencephalography (qEEG) [16].

qEEG covers techniques involving computer algorithms and methods for quantification, analysis, diagnosis, discrimination of clinical disease subtypes, and prediction of treatment response medicine. Firstly, it needs digital recording of EGG as an unavoidable preliminary step for digital storage of the signals. qEEG substantially boosts the capacity of conventional EEG techniques. Though, both techniques complement each other: conventional EEG is used to aid the diagnosis of a disease, while qEEG precisely discriminates individuals by analysing EEG features into clinically significant subgroups [19]. The results of qEEG are represented in a form of topographic brain mappings with colour maps in 2D and 3D, which gives a better visualization and evaluation, as seen in the next figures**, figure 2. 3 and figure 2. 4.**

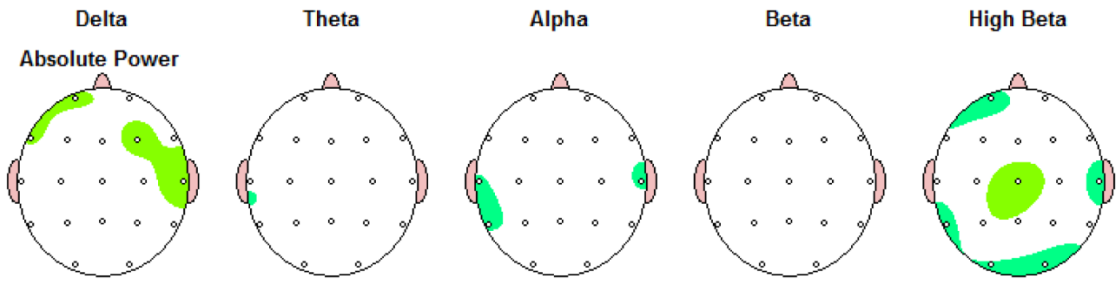

Figure 2. 3-Normal qEEG [20]

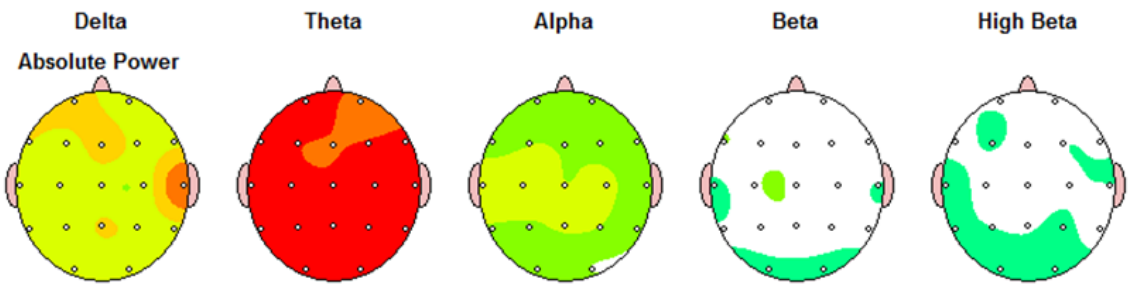

Figure 2. 4-Very High Theta In Dementia Patient [19]

2.4. Classification of the brain waves

EEG is a result of simultaneous synchronized discharges of different neurons that can be measured at the scalp, the so-called brain waves. These brain waves acquired at the scalp have a peak-to-peak amplitude up to about 100 μV and a range of frequencies lying between 0.5 - 50 Hz. Brain waves can be classified in the frequency domain in five bands: delta, δ (0.5-4Hz); theta, θ (4-8Hz); alpha, α (8-13Hz); beta, β (13-22Hz); and gamma, γ (22-30Hz) [2, 3].

2.5. Acquisition of electroencephalic signals

Bio-electrodes play an important role in the acquisition of bioelectric signals before the amplification and displaying the signals. The conversion of the ionic conduction to electronic conduction of these signals must be done in a manner that the recording tissue is not damaged and also, no noise is add to the signal. Furthermore, they have to be biocompatible, easy to apply and comfortable. All these specifications are applied for surface electrodes like the EEG ones.

2.5.1. Electrode-Electrolyte Chemical Interface

The body fluid can be seen as an electrolyte, since it contains ions, and when an electrode is applied to a specific body region an electrode-electrolyte interface is formed [2]. This electrode-electrolyte interface results from electrochemical interfacial reactions that can be represented as

$$C \leftrightarrow C^{n+} + ne^{-} \quad (2.1)$$

$$A^{m-} \leftrightarrow A + me^{-} \quad (2.2)$$

Where C is cation, *n* is the charge of C, A is anion and *m* is the charge of A. This is only possible if the electrode in the interface can be oxidized to form a cation and one or more electrons. Then, the cation can be discharged to the electrolyte and the electron remaining act as a charge carrier in the electrode. The anion coming to the interface can be oxidized to a neutral atom, with a trade of one or more electrons to the electrode[2].

This interface can be exemplified as a metal placed into a solution with the same ions of the metal. The ions are cations and the solution, which has anions, will maintain neutrally of charge in the surrounding. When there is the initial contact of the metal with the solution the reaction represented by equation 2.1, starts immediately. Either the reaction goes to the left or the right, depending on the concentration of cations in solution and the equilibrium conditions, the local concentration of cations in the solution at the interface changes [2]. This will, then, influence the anion concentration as well. The net result is that neutrally of charge is not equal in this region in

comparation to the rest of the solution, meaning that in this electrolyte surrounding has a different electric potential. A potential designated by *half-cell potential*.

These distributions of ions in the electrolyte in the metal-electrolyte interface gives raise to the formation of an electronic double layer. Where, at the surface metal there is a one type of charges dominant and the opposite charge is distributed in excess in the near by electrolyte.

The half-cell potential of any electrode takes into consideration that, the hydrogen electrode is zero, at 25ºC, since it would not be possible to have a connection between the electrolyte and one terminal of the potential-measuring system. So, the value of the hydrogen electrode is necessary to measure the half-cell potential [2].

Though, the half-cell potential of an electrode only indicates its resting state, meaning when there is no net current flowing. Thus, when a current exists what is observed is the difference between the measured half-cell potential and the equilibrium zero-current half-cell potential resulting on the overpotential. This overpotential, impacts the performance of electrodes, which is termed polarization [2].

In an ideally polarizable electrode charges are accumulated at the interfacial layer, generating a high impedance, particularly at low frequencies. Thus, these electrodes are not adequate for transmission of electro-encephalic signals at low frequencies [2]. Examples of these electrodes are platinum (Pt) or gold (Au).

The non-polarizable electrodes permit the free movement of currents in the electrode-electrolyte interface without the alteration of the potential. These ones are preferred for biomedical applications. A common example is the Ag/AgCl electrode [2].

Perfectly polarizable electrodes and non-polarizable electrodes are described theoretically, though there is not a true application of them in real applications[2]. Meaning that the existing electrodes are an approximation of perfectly polarizable electrodes and non-polarizable electrodes.

2.5.2. Electrodes for EEG

Electrodes for EEG are capable of capture changes in electrical brain activity in a non-invasive form. These ones then, can be divided into wet, dry and non-contact [1].

2.5.2.1. Wet electrodes

Wet electrodes are the most used for EEG and the most common are made from Ag/AgCl, Au, Pt, Tin and stainless steel. They are operated with conductive gels and prepared as disposable surface electrodes, reusable disc-electrode or saline-based electrode. Disposable surface electrodes are composed of a Ag/AgCl pre-gelled disc and adhesive pad and reusable disc-electrode is smaller than disposable but they can be attached to the scalp through the hair [1]. The reusable disc-electrodes are made of Ag/AgCl or gold-plate silver and are used with collodion and gauze with electrode gel. The saline-based electrode is shaped as a shell electrode with a saline-soaked sponge. The sponge is kept wet with saline during the EEG recording.

2.5.2.2. Dry electrodes

One drawback of the wet electrodes is the influence of the gel that dirties the scalp and may short-cut adjacent electrodes [1]. Additionally, the gel is very sticky, which makes the hair and scalp filthy and the preparation time for the exam long [21].

The dry electrodes can be divided in two categories invasive and non-invasive but both have a spike array form. The invasive ones cause skin or tissue reaction like allergic reaction, rash or skin irritation and are composed of microscale pillars that can be made of silicon [22], carbon nanotube [23], or conductive polymer [8]. Their distinction from the non-invasive relies in a slight penetration into the epidermis of the patient. The non-invasive ones are made of micro- or macro-scale conductive pins and are the most used [1], since they increase the contact area to lower the impedance without penetration. *Chen et al.,* [8], used flexible polymer dry electrodes fabricated with ethylene propylene diene rubber to measure EEG signal on skin. *Grozea et al.* ,[24], produced a non-invasive dry electrode made of flexible silver-coated polymer bristles. *Liao et al.* [25], built a dry electrode with 17 spring contact probes for measuring EEG signals without skin penetration.

2.5.2.3. Non-contact electrodes

As the name says, these electrodes are capacitive electrodes that can perform an EEG measurement by keeping a distance between the electrode and the skin. The advantage is to reduce preparing procedure for capturing EEG signals, thought they provide small amplitude signals and are very sensible to motion artifacts [1].

2.6. Measuring technique

An EEG measurement recording system consists of the electrodes, amplifier with filters, A/D (analog-to-digital) converter and a recording device. From a general point of view, an EEG measurement circuit potential measures the difference between a signal or active electrode and a reference electrode [6]. In addition, a third electrode is needed, named ground electrode, to subtract the same voltages in the active and reference points. Many EEG instruments have 128 or 256 active electrodes [6].

Amplifiers are needed in the EEG to make bio-signals compatible with A/D converters but some requirements need to be applied, as they must give an amplification selective to the bio-signal, reject noise and interference signal, and provide protection from voltage and current surges for both patients and electronic equipment [6, 26].

The amplifier gain, defined as the ratio between output and input signal, must offer a good signal quality and enough voltage level to be further processed. Other parameters such as gains of 100-100000, sampling rate or good signal-to-noise ratio are necessary [26]. To further decrease the impact of noise from external sources, amplifiers must have high common-mode rejection ratios, at least 100dB, (common-mode rejection ration is the ratio of the gain of differential mode, desirable signal, over the gain of the common mode, initial input signal between input and ground) and high input impedances of 100 MΩ[26].

An EEG recording can be performed in a special electrically shielded room, to avoid the 50/60 Hz alternating current line noise, or not, for example in a clinical purpose. In this case the amplifiers run on batteries and cables that lead to the computer, unfortunately their frequencies can be picked up in an EEG measuring. One way to avoid this problem, it is the usage of low-pass filters with a cut-off bellow 50/60 Hz or the application of a notch filter (filter with a narrow band around 50/60 HZ) for a better quality recording.

The A/D converters are capable of converting samples from the analogue channel, at a fixed time interval, into a digital signal and store them in the computer's memory. The resolution of the converter is given by the smallest amplitude that it can sample and this is achieved by dividing the voltage range of the A/D converter by 2 raised to the power of the number of bits of the A/D

converter [27]. Usually, A/D an converter has a minimum of 12 bits (4096 value levels) and the ability to resolve 0.5 μV is the recommendation [28]. For an efficient signal recording the sampling rate, should be higher than twice the signal frequency (Nyquist theorem) [6].

Analogue filters are also important components in an EEG measuring. The high-pass filter will reduce the noise related with low frequencies from bioelectric flowing potentials, like breathing. The low pass-filter will avoid interference related with high frequency noise and aliasing. For each one, a cut-off frequency of 0.1-0.7 Hz is needed [27].

Finally, after all data is collected digital filtering is necessary to have good signal properties [6].

2.7. Electrode positioning and montages

Remembering the anatomy of the cerebellum, electrode positioning is made according with a standard named 10-20 electrode placement system [29]. The head is divided in pre-defined distances from prominent skull landmarks (nasion, preauricular points, inion) to better cover all regions of the brain. The label 10-20 designates proportional distance in percentages between ears and nose where points for electrodes are chosen. The electrode placements are labelled according near brain areas: F (frontal), C (central), T (temporal), P (posterior) and O (occipital). In addition, on the left side of the head odd numbers are indicated with the letters and on the between nasion and inion the letters are represented with a Z. **Figure 2. 5**, shows a representative electrode positioning.

The set of all active electrodes with the reference and ground electrodes and their positions in the scalp is called montage. Four types of montages exist namely the bipolar, the referential, the average and the Laplacian [2]. Bipolar montage measures the difference between two adjacent electrodes. In the referential montage, each channel measures the difference between one electrode and a reference electrode. For the average montage, each channel measures the difference between one electrode and the average of all electrodes. In the Laplacian montage, each channel measures the difference between one electrode and weighted average surrounding electrodes.

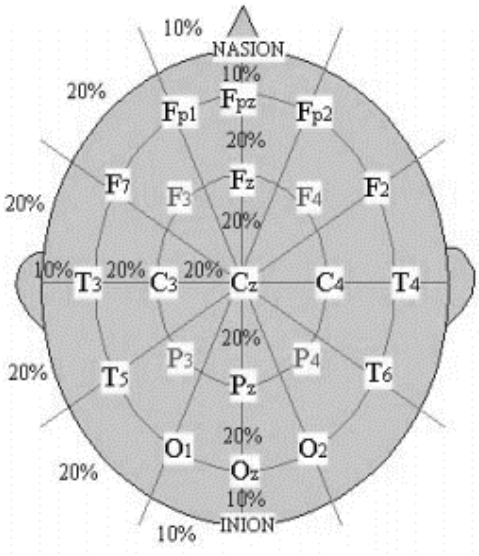

Figure 2. 5- 10-20 Electrode placement system

2.8. Artifacts

In an EEG measurement, signal distortions occur quite often. These can be represented as signals with higher amplitude and a distinct waveform in comparison to other signals. Artifacts can be from two sources patient related or technical [6]. Patient related artifacts come from the patient body functions and technical artifacts are introduced by the experimental equipment. All these artifacts, then are examined by the trained technicians and removed.

2.8.1. Patient related artifacts

2.8.1.1. Ocular Artifacts

Ocular artifacts are formed by a vision related stimulus like eye movements and blinks. These artifacts (eye blink, eyeball movements, and extraocular muscle activities) are localized in the frontal lobe [16].

Eye blink artifacts may give alterations in both the amplitude and the frequency content of the EEG, changing then, the classification accuracy. These artifacts are introduced in the alpha frequency and can be viewed as muscle artifacts [16].

2.8.1.2. Electromyogram Artifacts

The EMG artifacts are found when electrical current is generated by the contraction of muscles. This also represents neuromuscular activities. When subjects are submitted to an EEG they are instructed to avoid movements as much as possible during signal recordings.

An example of an EMG artifact is the hand/leg artifact, which cause a slow drift in the EEG amplitude. This drift is usually high compared to brain activities [16]. Another example is the facial muscle artifact like swallowig.

2.8.1.3. Electrocardiogram Artifacts

ECG artifacts occur because there is a potential difference during depolarization and repolarization in the cardiac muscle cell. The ECG influence depends on the length and width of a person's neck [16]. These artifacts appear on every subject, while their magnitude and location may vary depending on the subject. It is possible to remove cardio artifacts using an ECG signal with specific ECG artifact mitigaton [16].

2.8.1.4. Other Bio-Artifacts

Any form of distraction capturing the subject's attention (noise coming from outside, people moving inside the lab, telephone calls) should be avoided while capturing EEG signals and eliminating then, any artifact from the acoustic noise.

2.8.2. Technical artifacts

2.8.2.1. AC or Power Line Artifacts

Power line artifacts have a significant peak of about 50/60 Hz in the power spectrum. High-impedance electrodes can influence the wire running from them to behave like a antennae that captures electrostatic noise [16]. Shielding the power source can reduce the electrostatic noise.

2.8.2.2. DC Noise

A DC offset is frequently observed in recorded signals and they are formed by the hardware[16]. For each trial, the DC noise may differ in amplitude.

2.8.2.3. Artifacts due to High Impedances

A high impedance of EEG electrode (>5kΩ) may produce artifacts. The EEG is a weak signal, with an amplitude up to 100 uV so the contact resistance of electrodes is generally kept bellow 5kΩ to avoid high-impedance artifacts [30].

Chapter III

3. Conductive Polymers

In this chapter, an introduction to the different conductive polymers will be introduced as well as examples of the most used conductive polymers in the literature.

3.1. Conductive Polymers

Conductive polymers are considered as " the 4th generation of polymeric materials", which shows the enormous importance of these chemical compounds [31]. Conductive polymers can be divided in two groups *extrinsically conductive polymers* and *intrinsically conductive polymers* (ICPs)[32]. Extrinsically conductive polymers are blends of conductive additives such as metallic fibbers or carbon modified with duromers or thermoplastic polymers [32].

Polyacetylene was the conductive polymer that started the progress in ICPs. This conductive polymer, like others, has a conjugated backbone and it can be doped [33].

In conjugated polymers a π system[1] is formed along the polymer backbone. The carbon atoms normally involved in the formation of the polymer backbone form three σ-bonds with nearby atoms and the remaining *p* orbitals, usually p_z orbitals, are involved in the π system.

In polyacetylene, the simplest conjugated polymer, each carbon is σ-bonded to two neighbouring carbon atoms and one hydrogen atom, leading to a π electron per carbon. Thus, the carbon-carbon bonds were equally long, the remaining π electrons would be found in one half filled continuous band. Though, Peierls' theorem states that one-dimensional, equally spaced chain with one electron per ion is unstable [34]. So, the symmetry of the system is reduced, and the orbital levels are rearranged in a way that the filled orbitals are lowered. In the case of polyacetylene, the lattice distortion leads to a repeat of unit with two carbon atoms close together and the next two carbon atoms farther apart. Consequently, the repeat unit can be described as —CH=CH— instead of —CH— . The electronic result is an energy gap between a completely filled π band and an empty π^* band. The energy savings due to the new gap outweighs the energy cost of rearranging the carbon atoms. Then, it is formed a characteristic bond-alternating-structure of the conjugated polymers. Therefore, conjugated polymers do not have partially filled bands, which are typically considered as semiconductors [31].

[1]Is a system of connected p orbitals with delocalized electrons in a molecule for better stability

Conjugated polymers, as other inorganic semiconductors, have very low conductivities in their pristine state [32]. Though, it is possible to introduce charges into these materials and to radically change their electronic properties in two ways, namely by chemical doping or electrochemically.

In chemical doping the term *doping* in the context of conductive polymers, refers to a chemical reaction either oxidation or reduction [32]. In both cases, there are the formation of new electronic states and the new semiconducting material can now be considered conductive. Both electron donating (n-type) and electron accepting (p-type) dopants, or reducing agents and oxidants, have been used to introduce charges in conjugated polymers to provide conductivity. After doping, conjugated polymers go from the insulating state to the semi-conducting or even metallic conductor state [33], **Figure 3. 1**.

In the case of electrochemically induced conductivity, the counterion is elicited from the surrounding solution.

The charges in polymers and oligomers are stored in novel states as polarons, bipolarons, or solitons [34].

A polaron is created when an electron is added or removed from the conjugated chain. This modification results in a chain deformation and a change in the energy level structure. One electronic level is moved from the valence band into the gap with its two electrons and an additional level is moved from the conducting band into the gap. In the case of an electron polaron, the added electron is stored in the newly created level in the conduction band. In the case of a hole polaron, an electron is moved from the newly created level to the valence band. In both cases a half-filled level is created with spin ½. The energy difference between the band edge and the newly created states depends on the gap and the chain length.

Bipolarons are a combination of two polarons with the same charge. The bipolaron additionally has two levels in the gap. In the case of a negative bipolaron both levels are fully occupied and for positive bipolaron both levels are empty. In either case the spin is zero and due to their charge, bipolarons are presumed to be near their counterions.

Solitons occurred in degenerated polymers [35]. Degenerated polymers have an interchange of single and double bonds along the polymer chain results in the same structure. Solitons are states in the center of the band gap associated with an inter-change of single and double bonds. Solitons can be filled with one electron (neutral soliton, spin ½), with two electrons (negatively chaged soliton, spin zero) or empty (positively charged, spin zero).

ICPs are synthetic polymers made of elements like C, S, N, O and H, have low density and good mechanical properties as other plastics. Modifying the processing conditions (the doping species or changing the chemical structure of the conjugated polymer chains) different electronic structures and properties of conductive polymers can be created [36, 37]. Additionally, employing different electrochemical potentials ICPs can be oxidized or reduced [38]. As a result, ICPs have many applications such as electrical wires of circuits, electrodes for electronic devices, actuators, sensors and others [33].

Though, ICPs have some drawbacks such as their stability, conductivity and processability [33]. In terms of stability polyacetylene is a good example since it has a high oxidation rate in air resulting in a fast degradation, in spite of its good conductivity (10^5 $S.cm^{-1}$)[33]. However, other conductive polymers like polypyrrole (PPy), polyaniline (PANi), polythiophene and their derivates display a better stability in ambient conditions due to their heteroaromatic rings.

ICPs cannot be processed by usual processing techniques for plastics (coating, printing, extrusion and melt spinning) since they degrade at temperatures below their melting point. Additionally, their conjugated backbone is rigid and the strong Coulombic attractions between the

polymer cations or anions and counter anions or cations make these conductive polymers insoluble and intractable in the conductive state.

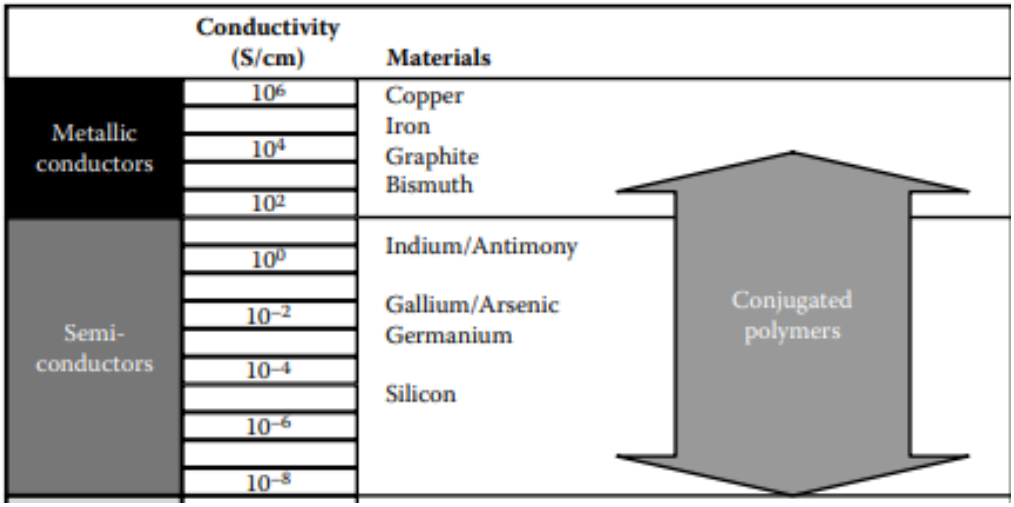

Figure 3. 1- Electric conductivity of semiconductors, and conductive materials. Adapted from [3]

3.2. Polyaniline (PANi)

PANi, the first conductive polymer to be dispersed in a solvent in a conductive state [33], when doped with a bulky organic anion such as *d,l*-camphorsulfonic acid (CSA) or dodecyl benzene sulfonic acid (DBSA), can be mixed in organic solvents like *m*-cresol and chloroform [33, 39]. This is explained by the presence of bulky organic anions, which lowers the Coulombic attractions with the positively charged PANi chains and permits the entrance of solvent molecules into the polymer chains. Moreover, the interchain interactions in the conjugated polymer chains can also be lowered with the attachment of side chains. If these side chains are anions, the conductive polymer can be doped by side chain cations [40].

3.3. Polypyrrole (PPy)

After the discovery of the conductivity of PANi another emerging group of electrically conductive polymers appeared named polypyrroles (first conductive poly(heterocycles)) was proposed [32]. The electric conductivity of polypyrroles depends of the degree of doping by iodine like the one represented in **figure 3. 2**.This polymer has been applied for industrial applications as conductive polymer anode in capacitors and corrosion inhibitor in base coatings [32].

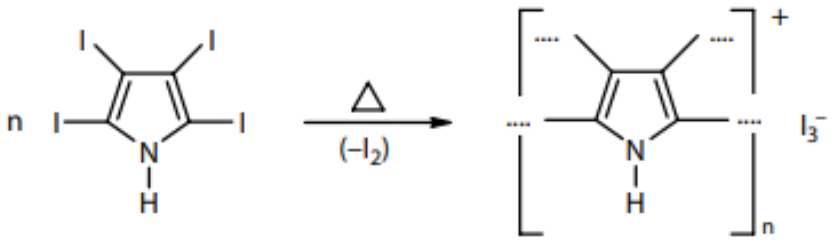

Figure 3. 2- Conductive, doped polypyrrole. [3]

3.4. Polythiophene

Polythiophene was considered a good candidate as a conductive polymer, when in 1967, A.G. Davies and co-authors studied the acid catalysed polymerization of furan, pyrrole and thiophene heterocycles [41]. They concluded that the conductivity of this last polymer in comparison to others already known (PANi and PPy) is ionic.

Few years later, in 1982, Tourillon and Garnier electropolymerized thiopenhe on platinum electrodes in acetonitrile with perchlorate or tetrafluoroborate counterions, obtaining conductivities of 10-100 S/cm [42]. This achievement started a new era for polythiophene as a promising conductive polymer for technical applications. In spite of the high conductivity achieved with this polymer, Garnier and Tourillon's could not solve the long-term environmental stability in air and humidity of the doped, bipolaron state, **figure 3. 3**.

Another issue of polythiophene at the time was its processability. For example, highly conductive, electrochemically prepared doped poly(alkylthiophene)s could not be dissolved in solvents like ketones or halogenated hydrocarbons, to a reasonable degree [43].

These drawbacks led to the polythiophene and its derivatives to be considered semiconductors and not conductors with high conductivity [32]. One of the pre-requisites for a truly conductive polymer is the long-term environmental stability against air and humidity of the doped, bipolaron state.[32]

Later, from 1986 to 1988, a group of chemists from Hoechst AG started to work with oxygen substituents at the 3- and 4-position in the thiophene moiety to stabilize the doped, bipolaronic state in polythiophenes by their electron donating properties [32, 44]. The oxygen-bearing substituent stabilizes the free radical and positive charge carrying forms by further electron delocalization, as seen in **figure 3. 4**.Subsequently, numerous patents and studies describing these conductive polymers appeared [45-47]. Though, these polymers did not fulfil the stability in the doped state due to the effective conjunction length needed for an adequate mesometric stabilization of the highly conductive bipolaron.

Then, researches from Bayer, Friedrich Jonas and Gerhard Heywang, found that it was necessary to extend the thiophene structures to bicyclic ring systems, meaning, ring closure of two alkoxy substituents, forming then dioxolane-, dioxane-, or dioxepane 3,4- anellated thiophenes, **figure 3. 4** [32]. This discovery resulted in molecules with an extended mesometric stabilization by two oxygen atoms with less steric strain compared with others previous polythiophenes. On their first attempt, they started with the dioxolane derivative 3,4-methylenedioxythiophene (MDOT, represented as I in **figure 3. 4**) but they could not produce significant amounts of this compound [32]. At that moment, Bayer researchers abandoned MDOT

and extended the ring size of the anellated dioxolane to the six-membered dioxane ring in 3,4-ethylenedioxythiophene,EDOT, representaded as II in **figure 3. 4**. This was a great accomplished.

The polymerization to PEDOT by the action of iron-III chloride ($FeCl_3$) demonstrated to be a polythiophene with a high conductivity and stability in the doped state. The patent application of the inventors Jonas, Heywang, and Werner Schmidtberg was introduced in Germany on April 22, 1988 [48]. Next, numerous studies and patents appear after its discovery.

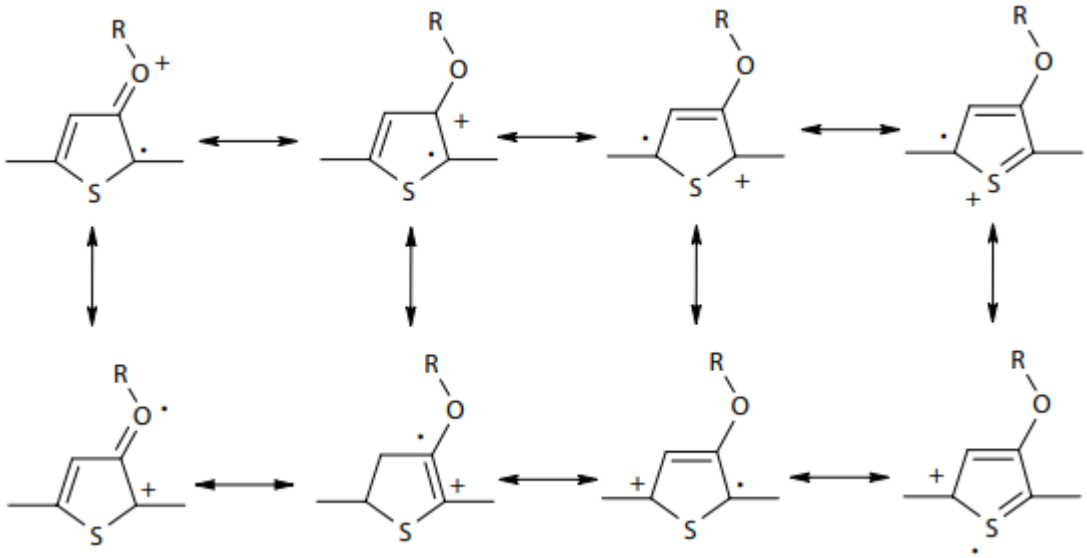

Figure 3. 3 - Radical cation (polaron) mesomeric stabilization with oxygen contribution. [3]

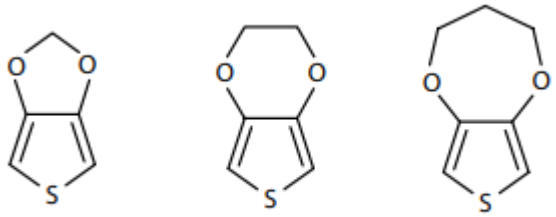

Figure 3. 4- Bicyclic dialkoxythiophenes for stable conducting polythiophenes. [3]

Chapter IV

4. Poly(3,4-ethylenedioxythiophene) (PEDOT)

In this chapter, a description of the conductive polymer used in this work will be performed. Firstly, the polymerization of PEDOT will be described, as well as, the oxidants utilized for the polymerization. Secondly, three common polymerization processes of PEDOT are going to be reported and then, a major attention, is going to be dedicated to the technique employed in the work.

4.1. EDOT to PEDOT – Oxidative Polymerization

EDOT can suffer from oxidation by weak oxidants and it is completely destroyed by very strong oxidants [32]. As for example, in mixtures of nitration agents like high concentrated nitric acid with EDOT, a rapidly dark blue colour will appear and disappear in instants [32]. For better understanding the EDOT oxidation, **figure 4. 1** illustrates the synthesis of PEDOT-tetrachloroferrate in the presence of $FeCl_3$ (oxidant). This synthesis gives rise to an insoluble powder with a high conductivity.

In chemically polymerized PEDOT, a salt will contain the oxidation agent (cation) and its anion, the counterion for the polymerization of PEDOT. Some examples of oxidants are iron (III)-salts, iron(III)-sulfonates, polystyrenesulfonic acid (PSS) , manganese (in form of manganese oxide) [49], cerium (IV) (in form of sulfate $Ce(SO_4)_2$) [50] and others [51, 52]. Iron(III)-salts have been widely used as oxidation agents of PEDOT [48, 53, 54] and iron(III)-sulfonates, like the salts of toluene sulfonic acid, both are soluble in organic solvents like ethanol or n-butanol. Furthermore, these solvents can dissolve large amounts of iron(III)-toysolate ($Fe(Tos)_3$) without being oxidized by Fe(III) [32]. PEDOT:toysolate films prepared by chemical polymerization have shown conductivities higher than 1000 S/cm [55].

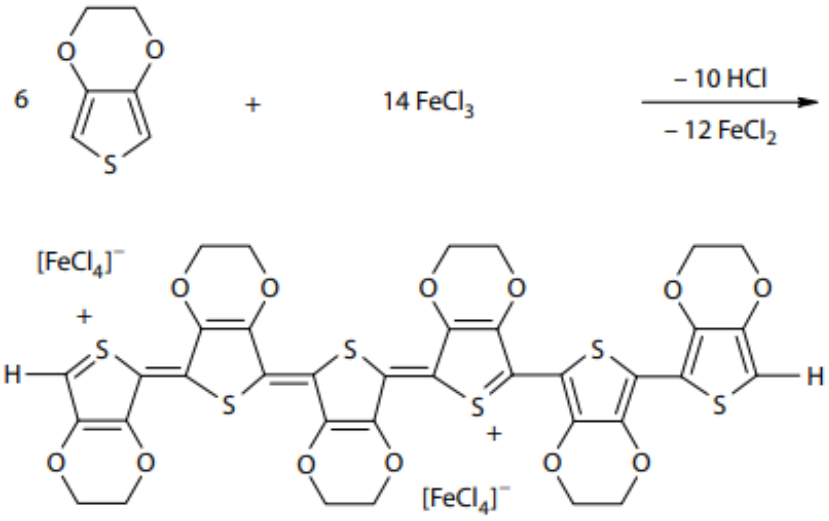

Figure 4. 1- PEDOT-tetrachloroferrate synthesis. [3]

4.2. Polymerization Processes of PEDOT

4.2.1. Solution Polymerization (*in-situ*)

In-situ PEDOT polymerization was the first polymerization process for production of conductive films [48]. This process uses ionic oxidants like iron-III, manganese-IV, or other oxidants. In addition, other metal oxidants can come from other compounds such as peroxides [32]. With this technique PEDOT is obtained in a insoluble form and the oxidant, besides operating oxidatively for polymerization and doping, also works as the source for the counterion (from $FeCl_3$ the tetrachloroferrate-III ($FeCl_4^-$) or from $Fe(Tos)_3$ the tosylate) [32].

In this process, six guidelines have to be respected [32]:

1. *Chemicals* - in literature iron-III oxidants, are preferred, and they need to be soluble with alcohols like ethanol or n-butanol since EDOT miscibility in water is limited. A widely used oxidant for *in situ* PEDOT synthesis is the iron-III toluenesulfonate;

2. *Mixing the solution* – an homogeneous solution must be formed. Then, the mixture can be filtered.

3. *Coating in the solution*- after the addition of EDOT, the polymerization starts within 5 to 10 minutes or when a gel is formed, the coating process stops. Production of films following the gel formation will have an inhomogeneous and undesired result.

4. *Drying the film* – films should be dried at about 50ºC for low periods of time (about 5 minutes). Then the film is left to dry at room temperature. In this step EDOT continues to polymerize and the films change color.

5. *Washing* – the substrates with PEDOT films are washed with water to remove any Fe in excess.

6. *Conductivity* –the conductivity of the films produced are measured. Conductivities of 500 S/cm are easily achieved.

If the substrate is a glass, it is necessary to previously form an adhesion layer for the PEDOT film. This prevents the PEDOT layer to peel off during the washing step. This adhesion layer must have a thickness of 10 to 20 nm. When PEDOT:PSS is used as the adhesion layer it is spin-coated onto a glass and next baked at 200ºC for 10 min. In the case that γ-Glycidoxypropyltrimethoxysilane is used as the adhesion layer, this is spin-coated onto a glass substrate or the substrate is simply dipped in the solution.

4.2.2. Coating with PEDOT:PSS

Poly(3,4- ethylenedioxythiophene):polystyrene sulfonate (PEDOT:PSS) is a polyelectrolyte that can be dispersed in water and some polar organic solvents. A polyelectrolyte is a conductive polymer that uses its polymer anions as the counter ions and the polymer anions stabilize the conjugated polymer cations in water and polar organic solvent [33, 56, 57]. In the case of PEDOT: PSS the dispersion is due to the stabilization of the hydrophobic PEDOT chains by the surfactant PSS anions. Moreover, PSS is commercially available in a substantial range of molecular weights and forms durable films [32].

For formation of PEDOT:PSS films water is the solvent of choice [32, 58] since it is inert to most oxidation or reduction agents. As a result, common deposition techniques like slit coating, drop casting, bar coating, spin coating, electrospinning and spraying can be applied to obtain uniform PEDOT: PSS films. Though, some requirements have to taken into consideration like viscosity of the solution, the surface tension, and the adhesion to the substrate [32]. These requirements can be fulfilled by different grades of PEDOT: PSS available from H.C. Starck Clevios GmbH namely Clevios™, by addition of water or dispersible additives. There are also, already in the market, various ready-to-use formulations optimized for specific applications and deposition techniques [50].

The most used oxidizing agents for PEDOT:PSS are peroxodisulfates, especially with monovalent cations such as Na, K, or ammonium [59-61].

After PEDOT:PSS films formation, they can be subjected to high temperatures by using a hot plates at 100 ºC or infrared radiation (IR) to remove excess water, due to their thermal stability [32]. Another process can be vacuum or a combination of the other two techniques with vacuum.

4.2.3. Vapour Phase Polymerization

Vapour Phase Polymerization (VPP), was first reported by *Mohmammdi et al.* , [62], where pyrrole in its vapour phase was put in contact with $FeCl_3$ vapour under vacuum resulting then in a polymer thin film. With this process the problems related to ICP, like solubility and solvent/substrate compatibility, were solved.

Looking at the **figure 4. 2**, the VPP process is an oxidative polymerisation method. First an oxidant (Fe^{3+}) mixed in a solvent is adsorbed/absorbed onto a substrate. Next, this substrate is put inside of a chamber with a monomer that is evaporated slowly from a container. Then, polymerization starts when the monomer gas reaches the substrate. Additionally, both the monomer and the oxidant can be optimized for a specific application, which gives this process an advantage to others polymerization process. Furthermore, the rate of polymerization can be controlled by different parameters. On one hand, the concentration of the oxidant or the addition of additives,[63, 64]. On the other hand the concentration of the monomer, temperature, pressure. These characteristics bring a lot of interest to the industry, since VPP can be applied in

a large-scale manufacturing, and different ICP thin films can be produced with specific properties (conductivity, optical properties and others) [65, 66].

In VPP, as in other PEDOT polymerization process, the oxidation strength of the oxidant of choice will play an important role in the final polymer [67, 68]. The cation Fe^{3+} is the most used and it is paired with anions such as chloride (Cl^-), tosylate (Tos^-) [69] and sulphonates [70], which will dope the ICP. $FeCl_3$ has been the salt of choice to polymerize many monomers [71, 72], but $Fe(Tos)_3$ has demonstrated more interest due its lower effective oxidation power [70, 73]. The difference of anions in $FeCl_3$ and $Fe(Tos)_3$ leads to a change in the polymerization rate. In the literature, it has been reported that the $Fe(Tos)_3$ has a slower rate of polymerization, which leads to a formation of smooth and longer polymer chain. Thus, resulting in films with a better conductivity due to the charge transport along the polymer chain and between connected grains of ordered polymer that can occur faster due to lower amount of structural or chemical defects [74].

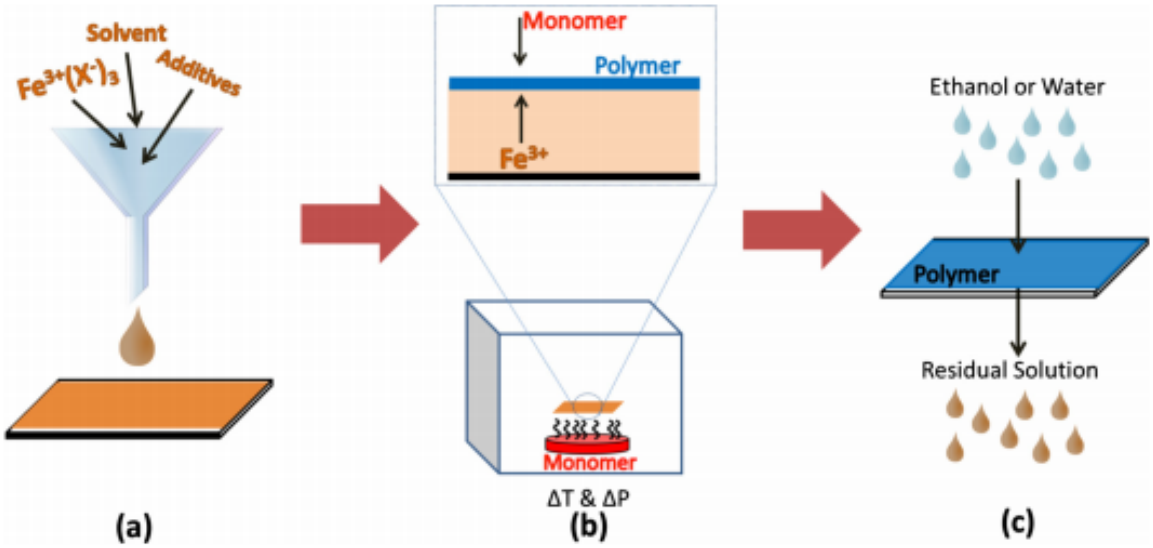

Figure 4. 2- The VPP process involving (a) deposition of the oxidant solution (onto the substrate, black), (b) exposure of the oxidant to monomer vapor at a certain temperature and pressure, where oxidant/monomer is moved/condensed at the interface to initiate polymerization, and (c) washing away excess oxidant and monomer. [5]

Chapter V

5. Techniques for enhancing the conductivities of PEDOT films

Many studies have been focused on gaining an efficient control of the oxidation level of PEDOT polymerization in order to enhance the conductivity of PEDOT films [75, 76]. Therefore, this enhancement of the oxidation level can be accomplished by modelling it with different techniques that are going to be introduced in this chapter. Parameters like morphology, the grain size, the inter-chain-interactions and the rate of polymerization will have an impact on the electrical transport properties of the final PEDOT film [77, 78].

5.1. Pyridine

A study of Winther-Jensen and West, 2004, [79], demonstrated that the addition of a volatile base, namely pyridine, into the oxidant solution of $Fe(Tos)_3$ prior to exposing the monomer EDOT, lead to an increase of 1000 S/cm in conductivity. They found that the polymerization of EDOT generates high acidic products (pH< 0.5), which makes the monomer unstable, with the formation of non-conjugated polymer, suppressing then, the polymerization of EDOT. By rising the pH of the oxidant solution, they were able to prevent this and an increase of conductivity was obtained. Moreover, this high acid concentration derives from the presence of Fe (III) that when the organic solvent evaporates decreases even more the pH and further promotes the mentioned reactions. In this study, a 40 wt%(weight of solute per weight of solvent, in percentage) $Fe(Tos)_3$ solution, in butanol where the substrate, poly(ethylene terephalate) (PET) was immersed. Then, 0.5 mol of pyridine per mol of $Fe(Tos)_3$ was added to the oxidant solution.

Another study investigated the influence of pyridine in the surface roughness and transparency of PEDOT films. *Truong, T.L., et al.* , 2007, [80] also used a 40wt% $Fe(Tos)_3$ in butanol and 0, 0.25, 0.5 and 0.75 molar ratio of pyridine/ $FE(Tos)_3$ were added to the oxidant solution. They reported that the thickness of the PEDOT film decreases with the increasing pyridine concentration 191 nm to 25 nm. This decrease in film thickness comes from the difficult reduction of Fe^{3+} to Fe^{2+} due to the presence of pyridine. It was supposed that pyridine coordinates with the $Fe(Tos)_3$ through the

successive substitution of pyridine with the alcohol ligands via the un-bonded electrons. Then, by controlling the polymerization rate of PEDOT with the concentration of pyridine, they could minimize the formation of defect sites, by the rapid polymerization kinetics that have a negative effect on the conductivity of the films. They reported that a molar ratio of pyridine/$Fe(Tos)_3$ higher than 0.5 translates in a decrease in conductivity. They supposed that an excess of pyridine will act as an impurity, which may well accumulate in the PEDOT coating and disturb the movement of charge carriers, which then decreases the conductivity [80].

5.2. The importance of water in the polymerization process

The two most used oxidants in VPP, $FeCl_3$ and $Fe(Tos)_3$, both have an affinity for water absorption which leads to the formation of crystals in the conductive films [81, 82]. There are two forms of overcoming this problem, first by eliminating the atmospheric water content within the chamber or a surfactant is added to avoid any absorption of water by the oxidant. Although, without the absorption of atmospheric water, the oxidant cannot successfully participate in the polymerization process, which impacts the electro-optical properties of the film. Recently *Fabretto et al.* , [83], reported that water vapour plays a crucial role in PEDOT polymer formation using VPP under vacuum. They reported that without the presence of water there was no formation of a conductive film, but by adding water within the chamber, the water acts as the effective proton scavenger, deprotonating the EDOT dimers for the polymerization to take place.

Hence, there must be some water to assist EDOT polymerization but not too much. On one hand, the lack of water prevents the polymerization of PEDOT. On other hand, an excess of water promotes the formations of crystals on the final films that translates in a decrease of conductivity. Thus, surfactants like the amphiphilic copolymer poly(ethyleneglycol)-ran-poly (propylene glycol) (PEG-ran-PPG), can be added to the oxidant solution as a solution to this problem. This surfactant has hydrophobic PPG blocks and hydrophilic PEG blocks and can act as a crystallization inhibiting agent [84]. Moreover, the co-polymer can slow down the polymerization rate of PEDOT by reducing the effective reactivity of the oxidant [84] and has a similar effect as pyridine (raising of the pH) but it does it by complexing with the iron [85].

In *Zuber, K., et al.*, 2008, [84] an interesting and extensive study was published in regards to the influence of PEG-ran-PPG in the EDOT polymerization by VPP.. The first conclusion they reported was that with a relative humidity (RH) higher than 50% the crystallization area of the films produced was predominant. Then, by adding 5 wt% of PEG-ran-PPG they were able to inhibit both crystal formation and the rapid polymerization [84]. Another interesting conclusion regarding crystal formation was that as EDOT monomer begins to polymerize, these sites act as heterogeneous nucleation points which promote an increased level of water vapour condensation. The subsequent increase in water vapour absorption by the oxidant leads to an increased level of crystal formation [84].

Another extensive study with a derivate of PEG-ran-PPG, the PEG-PPG-PEG, used glass samples coated with $Fe(Tos)_3$ in *n*-butanol. In this study, the main goal was to find the sources of water under their chemical vapour deposition (CVD) and for that they used the vacuum vapour phase polymerization (VVPP). They stated that water can come from three sources [73]:

1. The oxidant solution;
2. A small proportion of water in the hydration shell on the co-polymer;

3. Water which is coordinated with the metal Fe(III) centres of the oxidant is retained in a useable/accessible form [73].

They were able to solve the presence of water in the first two sources of water by desiccating one or the other, prior to the junction of the two, and conductive films were produced. However, if the sources were both desiccated before the mix of the two, water was still present in the form of the third source of water and a film would also be generated. Curious, if both two first sources were desiccated after the mix of the two, no film was formed. Concluding that, the strong co-ordination bond of PEG moiety with metal ions, [86, 87], results in a synergistic interaction with the coordinated water within the Fe (III) centre of the oxidant. Then, this available water will serve as a proton scavenger when $Fe(Tos)_3$ is operated as an oxidant [73] and polymerization is able to occur.

5.3. Sulfuric Acid (H_2SO_4)

Many studies have been dedicated to improving the oxidation level of PEDOT by means of reducing agents such as sodium borohydride ($NaBH_4$), hydrazine hydrate($N_2H_4{\cdot}H_2O$), hydrogen iodide (HI) and H2SO4 [77, 88-90].

Jia, Y., et al., 2019, [91], observed that by putting the PEDOT film in contact with a 1 M H_2SO_4 solution at 160ºC for 5 min (oxidant solutions were $Fe(Tos)_3$ in n-butanol), lead to an enhancement of the conductivity from 480 S/cm to 1000 S/cm. This was achieved, firstly by a formation of a more homogeneous surface structure. Secondly, by using UV-Vis-NIR absorbance spectroscopy they registered a pronounced absorption band at about 870 nm after the addition of H_2SO_4, which indicates an increase in the oxidation level. The formation of polaron and bipolaron bands are reported, in literature, to be at >800 nm for PEDOT [78, 92]. Thirdly, by the Sulphur (2p) XPS spectra, there was also an increase in intensity at 166 to 168 eV compared to the films without H_2SO_4, which is caused by the further doping of PEDOT with HSO^{4-} resulting in the high oxidation level of PEDOT [91]. Moreover, because of the four electronegative oxygen atoms from HSO^{4-} compared with Tos^- it moves the S(2p) to a high binding energy [89, 93].In the S(2p) signals of PEDOT, it is found a peak of the sulfur atom at 163–166 eV from the thiophene units and if $Fe(Tos)_3$ it is the oxidant of choice, other peak it is pronounced at 166–170 eV from the sulfonates of Tos [94].

Another interesting study of the usage of H_2SO_4 post-treatment of PEDOT films is the one by Xia, Y., K. Sun, and J. Ouyang, 2012, [78]. PEDOT:PSS films were formed on glass or PET substrates and, after their formation, 150 µl of H_2SO_4 (1M) were dropped on the sample at 160ºC. They reported that the thickness of the films was reduced after the addition of H_2SO_4 and conductivity increased by three times. They extensively described that H_2SO_4 treatment causes replacement of some PSS^- with HSO^{4-} counter anions in the PEDOT chains.

One particularity of this study was that they repeated the addition of H_2SO_4 several times and in each layer formed the thickness of the films was higher and the conductivity was even higher than the layer before. The highest conductivity reported was 3065 S/cm and they registered no considerable change in conductivity after 2 months.

5.4. Post-synthesis Heat Treatment

Zuber et al.,2018, [95] studied the influence of a heat treatment on PPy and PEDOT films, after their formation, in order to improve the adhesion of the films to the substrate. They were able to expand the time of polymerization but it has been shown that this has detrimental effects on the formation of PEDOT films [96]. Additionally, they were expecting that, due to the elevated temperature and the presence of the short chain oligomers and residual monomer in the oxidant layer, polymerization would be able to continue during the heat treatment. Thus, an oxidant solution of $Fe(Tos)_3$, PEG− PPG−PEG and ethanol was spin-coated on borosilicate glass and, after VPP, they treated the samples at 70ºC for different times. They reported that they were able to raise the oxidation level of PEDOT, which would result in a better conductivity, though the conductivities of the samples decreased along the time (0h, 2.5h, 5h and 7h). This result comes from the fact that a significant presence of PEG− PPG−PEG produced an impairing inter-grain hopping in the conductive polymer grain boundaries [97], which gives an decrease in conductivity . Therefore, as a drawback of creating a more robust conductive film is the occurrence of a film with less conductivity.

Chapter VI

6. Materials and Methods

In this chapter, the methodology to produce PEDOT films will be introduced with a description of solutions preparation, the synthesis of the samples, the parameters employed before VPP process and then, a theoretical description of four-point method for conductivity measurements will be made. In this work, some techniques to enhance the conductivity have been tested like the addition of pyridine or PEG-PPG-PEG, the multideposition by VPP and H_2SO_4 post-treatment. Next, the techniques for the physical characterization of the best PEDOT film will be presented. Finally, there is the electrochemical characterization of the electrode for EEG as well as the parameters for the EEG recording.

6.1. Methodology to produce PEDOT films

6.1.1. Solutions preparation

Solutions of $FeCl_3$ and $Fe(Tos)_3$ were prepared with concentrations of 20 and 40 wt% in methanol or ethanol.

For pyridine tests, pyridine was added to the 40wt% $Fe(Tos)_3$ solution, with a pyridine/Fe(III) molar ratio of 0.5. For PEG-PPG-PEG tests, a concentration of 25wt% was dissolved in a 26.6wt% solution of $Fe(Tos)_3$, methodology from [98].

In the post-treatment H_2SO_4 , samples were immersed in H_2SO_4 for 30 minutes and then heated in an oven at 120ºC for 20 minutes in a closed flask. This protocol was based on [78].

6.1.2. Synthesis of PU samples

Samples of polyurethane (made from U1419 resin, Sika) were used as substrates. The two components of the resin were mixed and cast in a Teflon® mould with 2 mm of thickness, see **figure 6. 1**. Then, a leveller was used to obtain a film with a uniform thickness. The resin was left for 4 hours to cure.

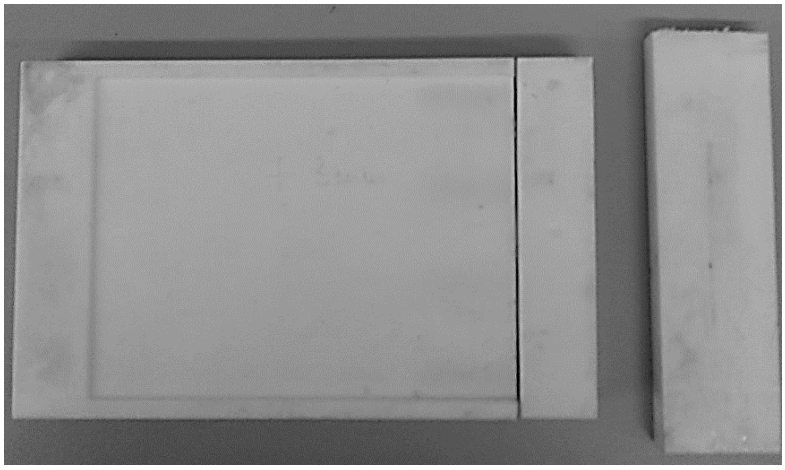

Figure 6. 1- Teflon® mold on the left and leveler on the right

Afterwards, small rectangles of 1 cm width and 2 cm length were cut and a hole was made on them, **figure 6. 2** . A Teflon® rope was attached to the rectangles with the purpose of hanging them during immersion in the oxidant solution and afterwards, in the VPP process.

Figure 6. 2- Example of a sample

Next, the samples were cleaned by immersing them for 5 minutes in 2-propanol, ≥99.8% (ROTIPURAN®) and then, they were placed at 50ºC for 30 mins to dry. After 30 mins, the samples were left to cool and weighed.

6.1.3. Optimization of the parameters prior to VPP

6.1.3.1. Choice of the solvent and concentrations of the oxidant solutions

The samples are first immersed in a solution in order to adsorb the oxidant. In this work, $FeCl_3$ and $Fe(Tos)_3$ solutions were studied. In a first approach, 20wt% and 40wt% concentration of each oxidant were the interesting concentrations for this work. Second condition a solvent had to be chosen either methanol or ethanol.

The samples were immersed in the oxidant solution for 1 minute and dried with a blow dryer until the excess oxidant was evaporated.

6.1.3.2. Drying technique and time

The first parameters to analyse were the drying technique and drying time, after an established immersion time of 1 minute. There was a need to study the drying technique because it was noticed that an uneven film was often obtained after exposure in the VPP chamber. In order to avoid these effects, the sample was slowly rotated during the blow drying.

Another relevant step in the preparation of the samples prior to VPP was the drying time after immersion in the oxidant solutions. When samples were removed from the solution, a liquid film remained on the samples. Samples were dried for different times (30 secs, 1 min and 2 mins) because water has a crucial role in the polymerization of PEDOT.

6.1.3.3. Immersion time in the oxidant solution

After the study of the drying time, it is important to evaluate the effect of the immersion time in the oxidant solution The samples were immersed for 10 and 30 s, 1, 5 and 10 minutes.

6.2. VPP process

For the VPP process, samples were hanged inside a round bottom flask, which is immersed in polyethylene glycol hot bath to control the temperature. The temperature of the samples inside the flask was set to 65ºC and 4 drops of 3,4-Ethylenedioxythiophene *(*Sigma-Aldrich®*)*,97%, EDOT, were added to the bottom of the round-bottom flask, see **figure 6. 3.** A small nitrogen stream was applied during the whole polymerization process. Samples were left for 1 hour inside the flask.

Then, the samples were removed, and washed 2 times for 5 minutes. First time in 70 % alcohol and then in water to remove residues. Then, they were dried for 10 minutes at 50ºC and let to cool down.

6.3. VPP process repetition

One attractive feature about this technique is the possibility of the repetition of the VPP process to increase the thickness of the film. This was first tested only with $Fe(Tos)_3$. Additionally, this procedure was also tested with the additives to enhance conductivity, such as pyridine and PEG-PPG-PEG.

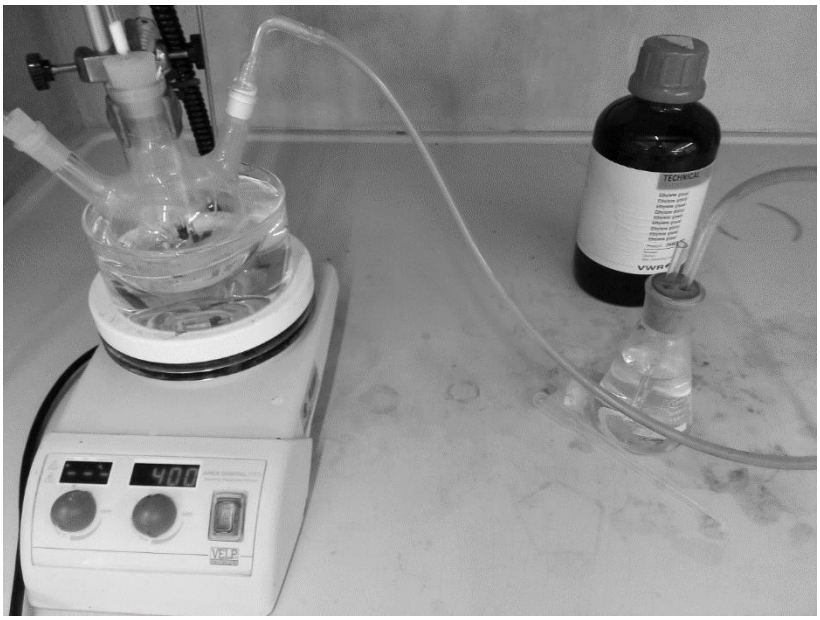

Figure 6. 3- VPP montage

6.4. Surface Resistivity measurements

After VPP, PU coated samples were removed, washed, dried and surfaces resistivities were measured. For these measurements, a four-probe homemade laboratory equipment was utilized, **figure 6. 4**.

Samples were submitted to different current values (I) applied by the exterior probes and the voltage (V) is measured between the internal probes. A potentiostat Gamry G300 (Gamry Instruments, USA), **annex 1**, and the Gamry framework were used to control the current/potential measurements, which were registered and displayed in graphs like in **annex 2**.

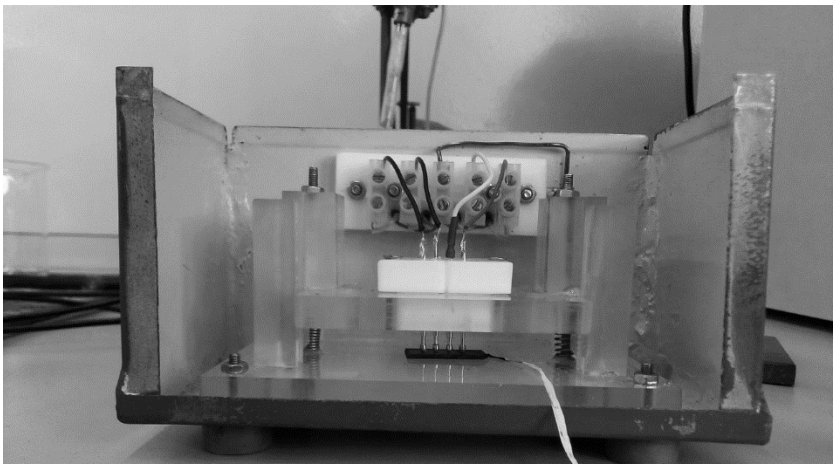

Figure 6. 4- Four probe equipment

In the four-point theory, assuming that the samples have a semi-infinite volume, and if the space between each probe is *s*, then resisitivty is given by: [99, 100]

$$\rho_0 = 2\pi s \frac{V}{I} \tag{6.1}$$

The value of ρ_0 , in the earlier equation, represents the measured value of resistivity. However, the samples have a finite volume, hence it is necessary to make some adjustments to the value of ρ_0. In this work, the thickness is in the micrometric range, thus considerably lower than 5s, then the value of ρ_0 can be calculated by:

$$\rho_0 = 2a\pi s \frac{V}{I} = a\rho_0 \tag{6.2},$$

where, *a*, it is a correction factor for the thickness, t, which is calculated from equation 6.3:

$$a = K\left(\frac{t}{s}\right)^m \tag{6.3},$$

K it is the value of *a* when (t/s)= 1. For a value of *m* equal to 1 *K* has the value of 0.72. Thus:

$$a = 0.72\frac{t}{s} \tag{6.4}$$

Returnig to the initial equation:

$$\rho = 2a\pi s\frac{V}{I} = 4.53t\ \frac{V}{I}, \text{ for t/s<=0.5} \tag{6.5}$$

In this work, t/s, is ≤ 0.5 because *s* is 2 mm and t is is always in the nm range. If both terms of the earlier equation are divided by *t* superficial resistivity can be calculated in Ω/cm:

$$R_s = \frac{\rho}{t} = 4.53\frac{V}{I}, \text{ for t/s<=0.5} \tag{6.6}$$

This equation is independent of the geometry of the samples, meaning that it is going to be dependent in the material. Using a general equation of resistivity:

$$R = \rho\ \frac{l}{wt} \tag{6.7}$$

If w=1 (a square) then:

$$R = \frac{\rho}{t} = R_s \tag{6.8}$$

Then, *Rs*, can be understood as a resitance of a square sample and, for that reason, it can be expressed in Ω/□. Though, this equation does not account for the effects of the frontiers's samples to the probes. Consequently, to obtain the most exact measurement it is essential to apply a corretion factor:

$$Rs = C\frac{V}{I} \tag{6.9},$$

where, *C* is the correction factor.

Testing, then, each measurements with the four probles in midle of the samples:

$$\rho = 4.53t\ \frac{V}{I} * C = 4.53t\ \frac{V}{I} * f_1 f_2, \text{ for t/s<=0.5} \tag{6.10},$$

$f1$, is the finite thickness corretion and $f2$, the finite width corretion. In this work, as refered earlier *t* is lower than *s* so, $f1$= 1 and the quation is only dependent of $f2$. To resolve the value of $f2$, it was necessary to used a plot, where a series of lines dependent of the difference between of the witdh (d) and *s* are calculated and represented in **annex 3**. The final value of $f2$ was 0.63.

In this type of samples it is more convenient working with condutivity, which can be represented as :

$$\kappa = \frac{1}{\rho} = \frac{1}{R_s * t} \qquad (6.11),$$

and it is expressed in S/□. In each condition 4 samples were measured.

6.5. Physical characterization

6.5.1. Scanning Electron Microscopy (SEM)

The SEM applies a focused beam of high-energy electrons to generate a variety of signals on solid specimens. The signals that come from the electron-sample interactions[1] show information about the sample like external morphology (texture), chemical composition, and crystalline structure and orientation of materials in the sample.

These signals consist of dissipated energy that is produced in the solid sample when a beam of high-energy electrons is applied to the sample. This energy is split up in secondary electrons, which give information to produce SEM images, backscattered electrons, diffracted backscattered electrons, they are important to determine crystal structure and orientations of minerals, photons, visible light and heat, **figure 6. 5**.

In most applications, data is collected over a determined area of the surface of the sample, and a 2-dimensional image is generated and exhibits spatial variations in the different properties before mentioned. Secondary electrons and backscattered electrons are most used for imaging samples [101], because they highlight the morphology and topography on samples. Whereas backscattered electrons are mostly used for clarifying contracts in composition in multiphase samples [101].

In this work a Quanta 400 FEG ESEM SEM equipment was used.

6.5.2. Energy-Dispersive X-Ray Spectroscopy (EDS)

An EDS system has a sensitive x-ray detector and a software to record and analyse energy spectra. Thus, the detector can separate characteristic x-rays of different elements into an energy spectrum and the software identifies specific elements. EDS is able to identify the chemical composition of materials of a certain zone and create maps with element composition. An EDS detector has a crystal that absorbs the energy of incoming-x-rays by ionization, generating free electrons in the crystal that become conductive and produce electrical charge bias. The x-ray absorption then converts the energy of individual x-rays into electrical voltages of certain size. This ones after corresponding to the characteristic x-rays of the element [102]. An EDAX Genesis X4M system coupled to the SEM equipment was used in this work.

[1] "Electrons accelerated onto a material result in a number of interactions with the atoms of the target sample. Accelerated electrons can pass through the sample without interaction, undergo elastic scattering and can be inelasticaly scattered. Elastic and inelastic scattering result in a number of signals that are used for imaging, quantitative and semi-quantitative information of the target sample and generation of an X-ray source."[100]

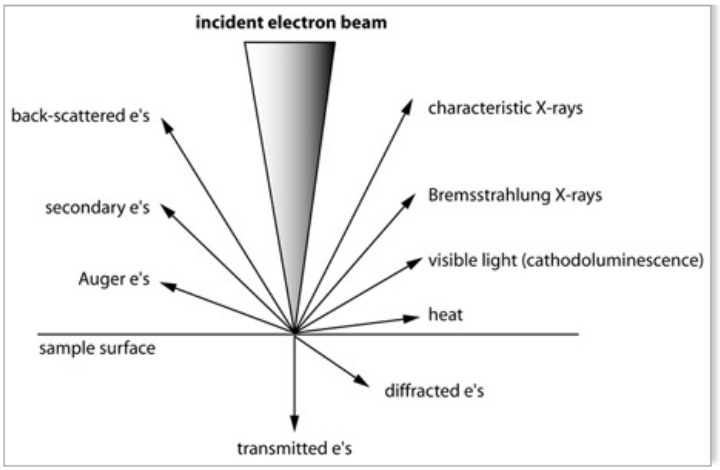

Figure 6. 5 - SEM high-energy electrons dissipated on top of a sample surface

6.5.3. Fourier-Transformed Infrared Spectroscopy (FTIR)

FTIR is a preferred method of infrared spectroscopy [103]. This applies infrared radiation onto a sample, which is either absorbed or passes through the sample. The resulting signal at the detector is a spectrum representing a characteristic molecular "fingerprint" of the sample.

The term FTIR derives from the fact that a Fourier transform, a mathematical process, is required to convert raw data to the spectrum. FTIR spectra were recorded on a Fourier transform infrared spectrometer (JASCO FT/IR - 4100) assembled with an ATR (ATR PRO410-M) accessory. The spectra were obtained after the accumulation of 64 scans, acquired with a resolution of 4 cm $^{-1}$.

6.6. Electrochemical characterization techniques for EEG electrodes

6.6.1. Electrochemical Impedance Spectroscopy (EIS) in-vitro and in-vivo

EIS is a technique to measure electrical impedance. The impedance is a complex quantity, $Z(\omega)$, which can be represented by its amplitude and phase angle. Moreover, the impedance can be described as $Z(\omega)= \nu(\omega)/I(\omega)$ where $\nu(\omega)$ is the transform of an alternating potential signal applied to the system and $I(\omega)$ is the transform of the alternating current signal that results. The impedance is a function of the frequency of the signal [104].

In order to evaluate EIS of a system a small amplitude sinusoidal excitation potential needs to be employed and the impedance measured represents the ability of the interface to resist to electrical current flow [105].

Another general representation of impedance is $Z(\omega)=|Z|e^{i\theta}$. Its magnitude or modulus is $|Z|$, and its phase angle is θ. Both $|Z|$ and θ are functions of frequency. With an increased contribution of the imaginary part, the angle increases. For a capacitor, the impedance is imaginary, the phase angle is -90º and the current is out of phase with the voltage by 90º [104].

Though, in a resistor, the impedance is real, the current and the voltage are in phase, and the phase angle is zero. Meaning that, a large phase angle indicates that the impedance is mainly capacitive, whereas for small angles, it is resistive.

6.6.1.1. *In-vitro* experiments

In an EIS measurement different values of impedance and phase angles are measured for frequencies ranging from 0,01 Hz– 10kHz and the signal probe was 5 mV (RMS). These values are represented in a Bode magnitude plot, log(|Z|), and Bode phase plot, θ, as a function of frequency.

In this study, the measurements were performed by using a potentiostat G300 and the software Gamry Framework (Gamry, USA).

The experiments were performed by immersing the PEDOT coated samples in a 1% saline solution (to mimic the sweating conditions). The impedance vs frequency measurement allowed to study the charge transfer kinetics.

A three electrode system was used has it is possible to see in **figure 6. 6**. The reference electrode is an Ag/AgC electrode, the counter electrode is a Pt electrode and the working electrode is the PEDOT sample.

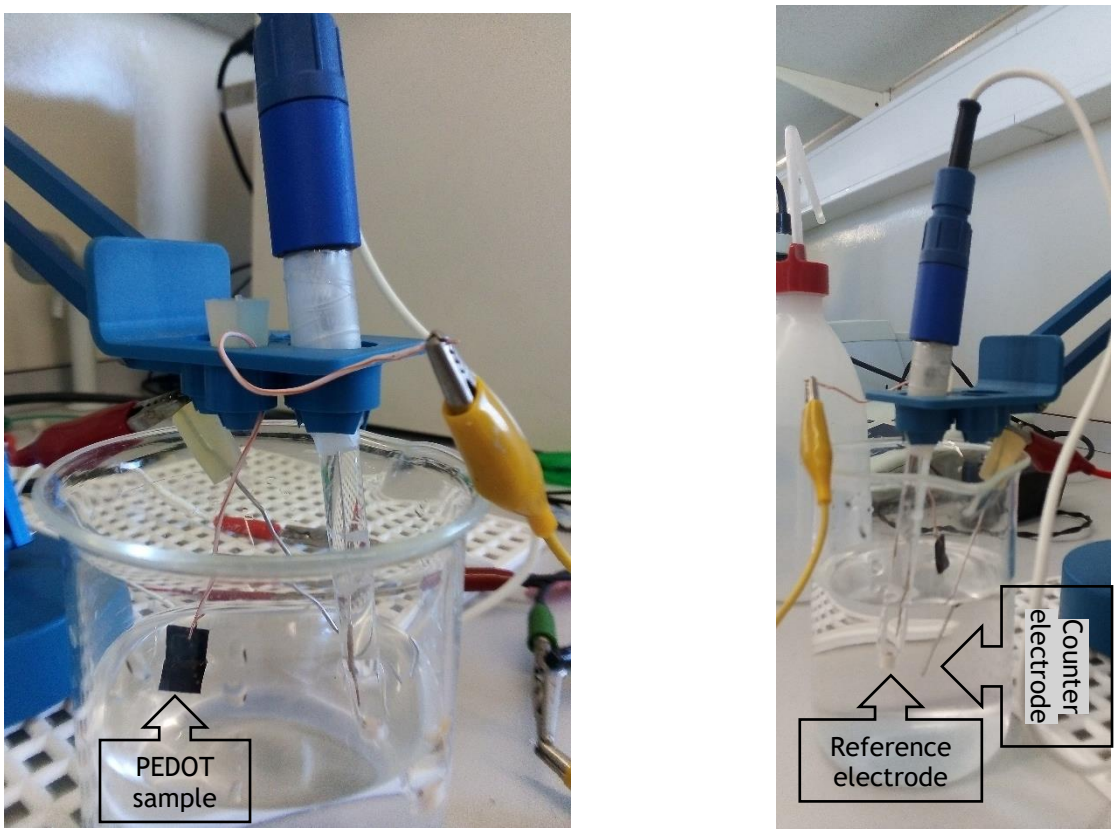

Figure 6. 6- EIS montage *in-vitro*

6.6.1.2. In-vivo experiments

The same kind of impedance tests were performed in-vivo, by applying the electrodes to the forearm of the patient, in order to study the charge transfer with the skin contribution. Here two measurements were done one closer and another farther to the reference. A two electrode system was used, with a Ag/AgCl disposable electrode with gel being used as the reference and the new electrode as the working electrode, **figure 6. 7.**

Figure 6. 7-EIS montage in-vivo. Red wire with PEDOT pin electrode. White wire the AgCl reference electrode

6.7. EEG Data

6.7.1. PEDOT pin for EEG recording

The multipin electrode for EEG recording, has it is possible to see in **figure 6. 8**, presents a complex shape, very different from the rectangle samples. This brought one additional difficulty to cover it completely because when the pin was immersed in the solution small bubbles were formed on the base plate, which inhibited the oxidant solution to get there. As a result, when the pin was exposed to VPP there was a lack on film formation on the base plate, as it is noticeable in **figure 6. 9**. One solution for this problem was to make the immersion of the multipin in the oxidant solution and apply ultra-sounds to help taking out the bubbles formed. After that, a complete covering in the multipin was successfully accomplished.

Each multipin was coated with two layers of PEDOT and then the electrical connection with a copper wire was accomplished by gluing it with a home-made glue composed of 50% or 70% (w/w) graphite powder and araldite® glue [106].

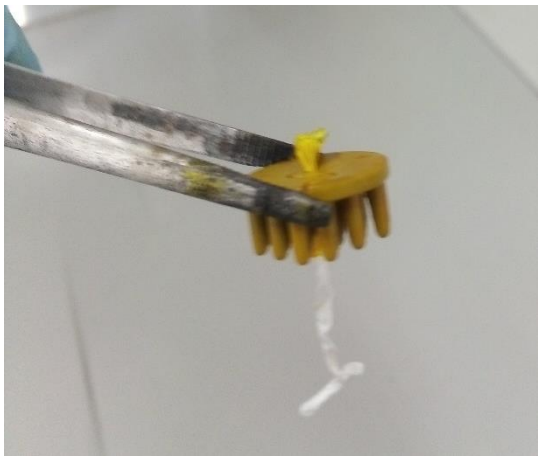

Figure 6. 8-PEDOT pin with $Fe(Tos)_3$

Figure 6. 9-PEDOT pin after VPP

6.7.2. EEG Monitoring and Acquisition

For the EEG measurements, the tests were performed in the frontal and occipital areas of the brain, in the Fp1 and O1 positions of the system 10-20. Conventional and PEDOT-coated electrodes were applied, in close positions (2cm apart) has it is noticeable in **figure 6. 10** and in **figure 6. 11**. The goal is to compare the performance of each electrodes in the recording of the same electro encephalic signal.

Additionally, a reference Ag/AgCl conventional electrode was positioned in the frontal Fp1 position, 10-20system, and the ground in the temporal bone near the mastoid.

The acquisition of EEG signals was guaranteed by the eego™ mini-series amplifier and the eego64 software (Eemagine, Medical Imaging Solutions).

Before each acquisition, every impedance is measured by the software amplifier. The test progresses when the impedances are below 20 or 90 kΩ for AgCl electrodes or PEDOT electrodes, respectively.

Three different kinds of test signals were recorded: resting state EEG, alpha activity, and eye blink artifacts. For all EEG episodes, the sampling rate was constant at 1024 samples/second. Alpha activity was induced by asking the subject to close the eyes.

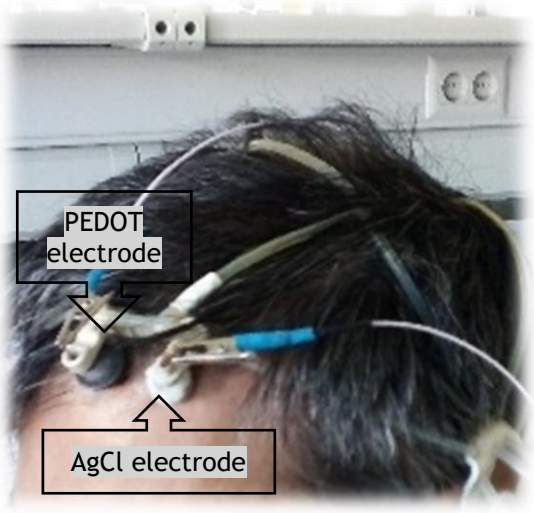

Figure 6. 10-EEG recording in Fp1 position

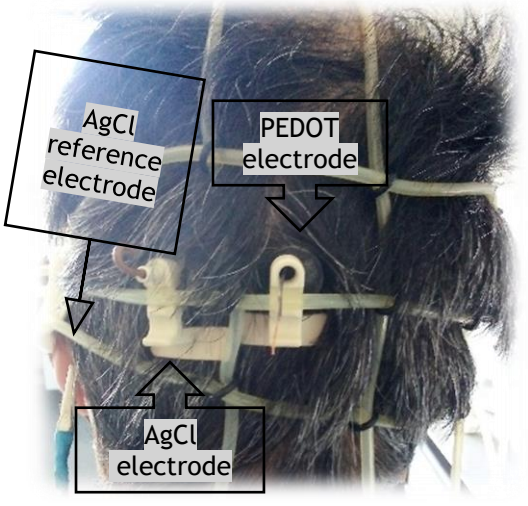

Figure 6. 11- EEG recording in O1 position

6.7.3. Digital Signal Processing

Analog signals, like EEG, are continuous and can be observed with different precision degrees. On the other hand, digital signals are discrete, and their values are quantified with a specific resolution.

The conversion from analogue to digital signal happens with a process known as sampling. This process is limited by the maximum frequency, which can be represented, and it is expressed by a sampling rate, in hertz (Hz or samples per second). At least two samples are necessary in each cycle for a specific frequency to record the signal amplitude. The relationship between the signal frequency and sampling rate is given by Nyquist theorem, which says that the sampling rate must be, at least, two times higher than the maximum frequency of the analysed signal [107].

The maximum frequency of EEG signal is 30 or 40 Hz, though 70 Hz is also possible to observe. To avoid any kind of aliasing in the recorded signal it is proposed a sampling rate of 1024 Hz [107]. Next, the signals are processed with MATLAB (MathWorks Inc., MA) with a specific algorithm.

In MATLAB, a band-pass Butterworth filter with a cut-off band from 0.5Hz to 40Hz is most used for this application. In the first 10 seconds the signal is eliminated to avoid any kind of artefacts.

6.7.4. Fourier Transform and power spectral density (PSD)

The Fourier Transform theorem describes that any finite and continuum wave can be decomposed, with a certain precision, by the sum of sine and cosine with determined amplitudes and phases. Furthermore, a signal can be formed with different frequency components, spectrum. This spectrum is a histogram of amplitudes in function of the frequencies [107].

The Discrete Fourier Transform, DFT, acts over digital data and has an efficient algorithm for its computation known as Fast Fourier Transform, FFT.

The PSD is normally represented as a function of the frequency based in the Transform Fourier. It uses the Welch method, which develops non-overlapping windows of waves, tapering to the extremes of the window, applies the FFT for each window, then, computes the average. Finally, the square of the value converts to an amplitude of power units. Thus, allowing the study of a transductor or amplifier response to every frequency. [108]

6.7.5. Signal evaluation parameters

The Root Mean Square, RMS, is a measure of the data central tendency:

$$RMS = \sqrt{\frac{1}{n}\sum_{i=1}^{n} x_i^2} \qquad (6.12),$$

Where, x_i corresponds to the amplitude value of each of the n values,

The Root Mean Square Deviation, RMSD, and root mean square deviations of the normalized, RMSDN, data can be expresses as:

$$RMSD = \sqrt{\frac{\sum_{i=1}^{n}(w_i - d_i)^2}{n}} \qquad (6.13),$$

$$RMSDN = \sqrt{\frac{\sum_{i=1}^{n}\left(\frac{w_i}{|w|_{max}} - \frac{d_i}{|d|_{max}}\right)}{n}} \quad (6.14),$$

In which, w_i and d_i are the potential amplitude values, for a given time-point, for the reference electrode (Ag/AgCl) and the working electrode (Ag/AgCl or PEDOT), respectively. $|w|_{max}$ and $|d|_{max}$ are the maximum values of amplitudes obtained. With RMSD, it is possible to evaluate the similarity or discrepancy, in absolute amplitude, between the measurements recorded in the same test for different electrodes. With RMSDN, enables comparison of signal shapes.

The Spearman Correlation coefficient:

$$C_{Spearmann} = \frac{\sum_i (w_i - \bar{w})\,(d_i - \bar{d})}{\sqrt{\sum_i (w_i - \bar{w})^2 \sum_i (d_i - \bar{d})^2}} \quad (6.15),$$

Where, $\bar{w}$ and $\bar{d}$ are the average of the points i of the registered signal between the reference electrode (Ag/AgCl) and the working electrode (Ag/AgCl or PEDOT), respectively. Each coefficient is a measurement of the correlation between the two variables: the obtained signals for both electrodes, where the upper limit 1 corresponds to a perfect correlation between both variables.

Chapter VII

7. Results and Discussion

7.1. Refining the parameters of the VPP process

7.1.1. Selection of the solvent and concentration for the oxidant solutions

The effect of the solvent was studied by using two suitable solvents, namely ethanol and methanol, for the Fe(III) salts that were used as oxidants. Looking at **figure 7. 1**, it is possible to notice that each oxidant has a different behaviour in the two solvents. $FeCl_3$ produced more homogeneous films, lower standard deviations, on both 20wt% and 40wt% concentration in methanol, whereas $Fe(Tos)_3$ was in ethanol and was the oxidant with lowest surface resistivities.

In what regards the concentration effect, the $FeCl_3$ had a sizable decrease in the surface resistivity (SRy) with the increase of concentration, from 184±14 Ω/□ to 36±7 Ω/□, which was ascribed to a more efficient oxidation of the EDOT. Regarding the $Fe(Tos)_3$, the inverse trend was observed, but the decrease was not significant from 40wt% (48±1 Ω/□) to 20wt% (24±4 Ω/□). To note that the with $Fe(Tos)_3$, a particularly low SRy is achieved with 20% concentration in both solvents.

For this work, it was favoured to operate with methanol as the solvent for the $FeCl_3$ and ethanol for the $Fe(Tos)_3$. For the concentrations for both oxidants a concentration of 40wt% was preferred. On one hand, in the $FeCl_3$, a higher concentration produces a lower SRy. On other hand in the $Fe(Tos)_3$, even with the increase of concentration it does not form a lower SRy but the films were more homogeneous because of the lowered standard deviations.

7.1.2. Samples drying

For the drying of the samples after immersion three techniques were chosen: to dry the samples inside an oven at 100ºC, using an air blower while rotating and drying the sample, also with an air blower, in an inverted position compared to the position when the sample is hanged inside the oxidant solution. The samples were left to dry from 1 min to 2 min in all techniques. The oven technique produced no film on the sample because the sample was too dry and as

mentioned in the chapter 5, water plays a crucial role in the PEDOT film formation. The drying technique in an inverted position still generated heterogeneous films, which is not desired. The usage of an air blower while rotating was the best of all three because an even film on the sample was produced. This drying technique was chosen for the following of the research.

For times of drying three-time intervals were analysed: 30s, 1 minute and 2 minutes. This step is crucial for the formation of PEDOT films since an excess of water leads to a significant formation of crystals, resulting in films heterogeneous and consequently, less conductive. Also, there must be some water to deprotonate the EDOT dimers for the polymerization to take place.

Looking at the **figure 7. 2**, it is possible to notice that the time of 1-minute produces films with the lowest SRy in comparation to the times of 30 s and 2 minutes in the two oxidants. In the case of $FeCl_3$ was 36±7 Ω/□ and in $Fe(Tos)_3$ was 28±3 Ω/□ for 1 min of immersion. For this reason, the 1-minute drying time was the chosen for the next tests.

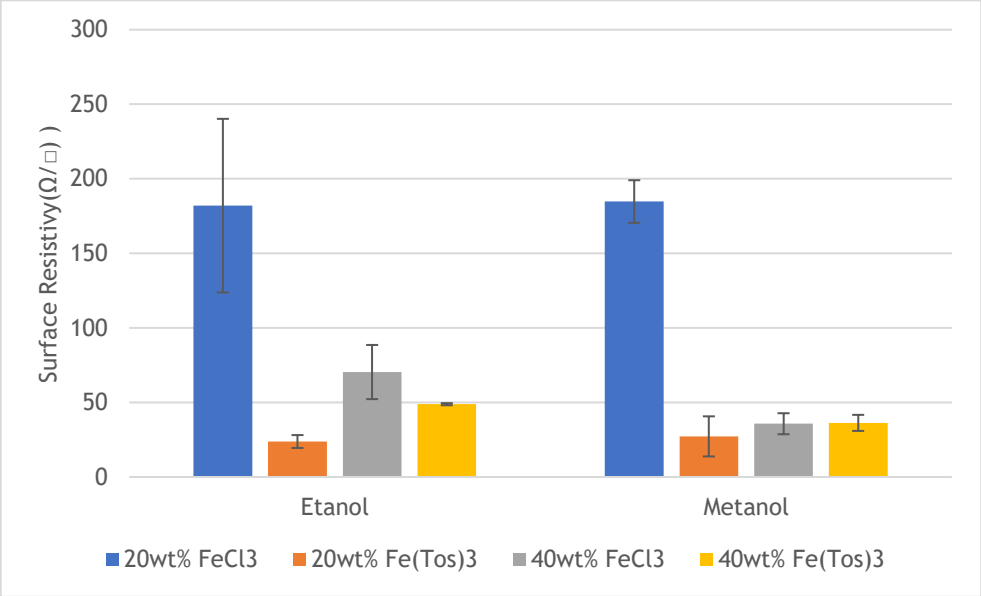

Figure 7. 1-Surface Resistivity in ethanol and methanol at 20 wt % or 40wt% for $Fe(Tos)_3$ and FeCl3 with 1 min of immersion

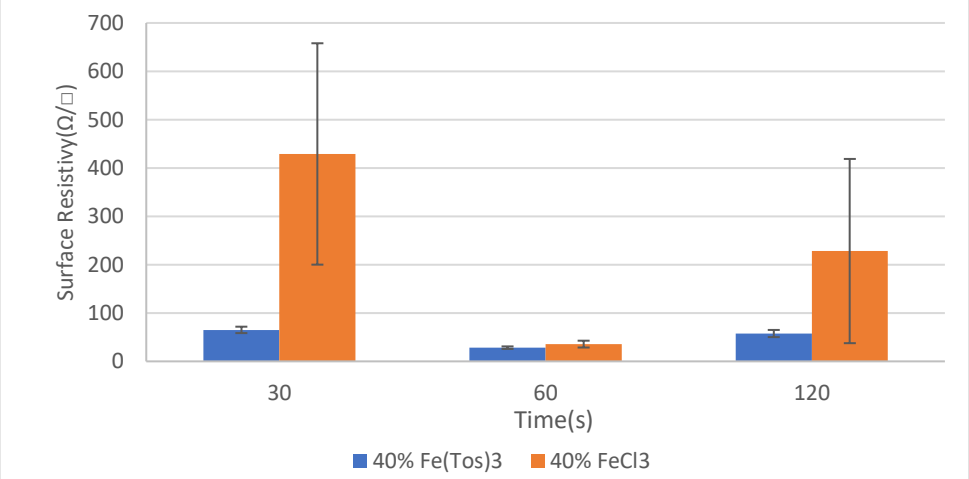

Figure 7. 2- -Surface Resistivity in different drying times (30,60 and 120 seconds) for 40wt% $Fe(Tos)_3$ in ethanol and $FeCl_3$ in methanol

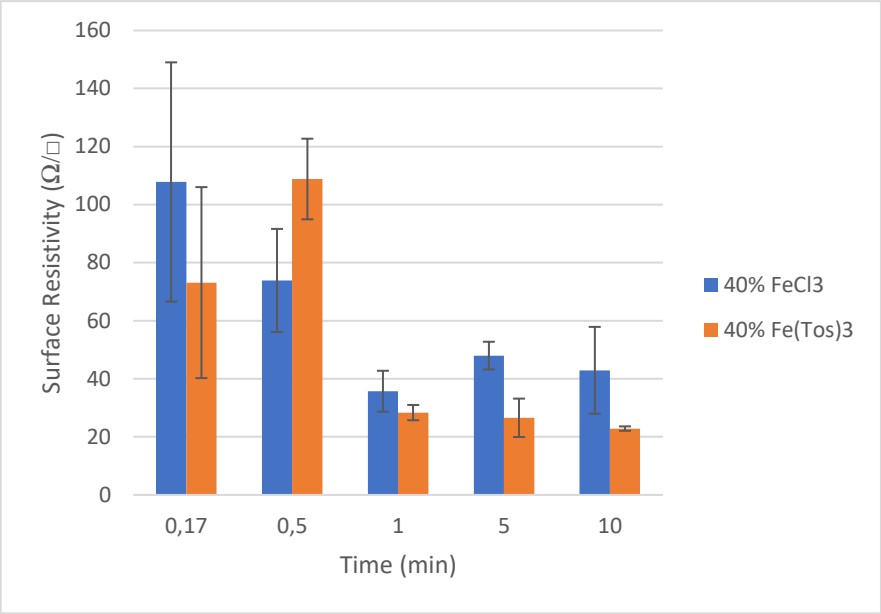

Figure 7. 3-Surface Resistivity in 0.17, 0.5, 1, 5 and 10-min immersion in the oxidant solution

7.1.3. Immersion time in the oxidant solution

During immersion of the PU samples in the oxidant solution there is adsorption of the oxidant on the polymer and also diffusion of iron inside the polymer. Analysing **figure 7. 3**, the immersion times of 10s (0.17 min), and 30s displayed the highest SRy (for the $Fe(Tos)_3$ was 73±33 Ω/□ and 109±14 Ω/□ for 0.17min and 0.5min, respectively, and for $FeCl_3$ 108±41 Ω/□ and 74±18 Ω/□ for 0.17min and 0.5min, respectively) in relation to 1, 5 and 10 minutes. This can be due to lower integration of the oxidant into the substrate surface layer, which results in a lower amount of PEDOT and subsequently, a higher SRy. Then at 5 and 10 minutes for the $FeCl_3$ samples, they presented a higher SRy in relation to 1 minute (36±7 Ω/□ for the $FeCl_3$ and 28±3 Ω/□ for the $Fe(Tos)_3$). Relative to the $Fe(Tos)_3$ samples, they presented a gradual decrease in SRy along the chosen times, reaching the lowest value at 10 min, 23±1Ω/□ .Finally, 1 minute was preferred in this study because it is less time consuming and provides excellent results.

7.2. Conductivity enhancement techniques

7.2.1. Action of additives

Now with the best parameters prior VPP, namely 1 min of immersion and drying with an air blower in a multidirectional position for 1 min, the next step was the addition of additives. In this part of the work only the $Fe(Tos)_3$ oxidant in ethanol was analyzed since most the works in the literature work with this oxidant and it is not possible to add pyridine to $FeCl_3$ due to a precipitation of a solid compound.

In this work three additives were experimented namely: pyridine and PEG-PPG-PEG and H_2SO_4 post-treatment. From all the additives, pyridine and H_2SO_4 had a successful result in decreasing the SRy (from 74±17 Ω/□ in $Fe(Tos)_3$ to 52±13 Ω/□ and 47±4 Ω/□ for pyridine and H_2SO_4 repetitively). The PEG-PPG-PEG did not work as well as the two other additives and the final films even displayed a higher SRy (105±11 Ω/□) in relation to the $Fe(Tos)_3$ without any additive, as it is possible to notice **in figure 7. 4**. The samples with added PEG-PPG-PEG displayed a lower PEDOT deposition when

compared to pyridine and H_2SO_4 since the top of the sample it is not completely covered, **figure 7. 5**.

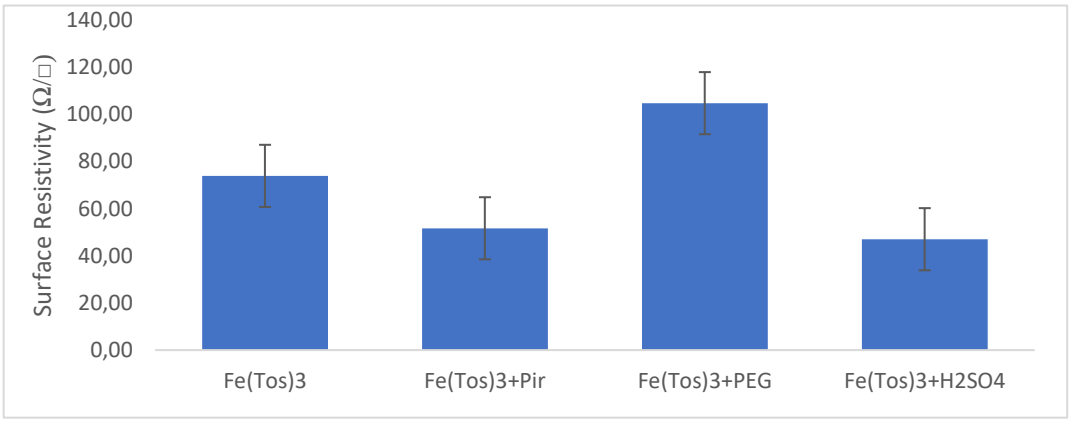

Figure 7. 4-Surface Resistivity. $Fe(Tos)_3$ sample without additive; Fe(Tos)3+Pir sample with pyridine; Fe(Tos)3+PEG sample with the copolymer PPG-PEG-PPG; $Fe(Tos)3+H_2SO_4$ sample after H_2SO_4 post-treatment

Figure 7. 5-Samples after VPP with PEG (left), pyridine (middle), and after H_2SO_4 treatment(right)

7.2.2. Influence of number of layers

Xia et al [78] studied the application of several layers of PEDOT, by repeating the VPP deposition process. It was observed that there was a significant decrease in the SRy and consequently an increase in conductivity. So, this technique was tested in this work, resulting in a significant decrease in the SRy (from 32±3 Ω/□ to 19±2 Ω/□) just after two layers, in **figure 7. 6**. There is even a further decrease(16±1 Ω/□) with the addition of a third layer but less significant. Therefore, this technique was tested in the addition of additives.

In the addition of one more layer of PEDOT,**figure 7. 7**, the SRy was reduced to almost one half in some cases, for example in pyridine it went from 52±13 Ω/□ to 24±2Ω/□. The lowest accomplished SRy was obtained with pyridine with a value of 24±2 Ω/□.

This influence of layers has two positive outcomes on one hand it decreases the SRy and on other hand it creates films more robust due to the addition of another layer. Though, the increase of thickness has a significant influence in decreasing the conductivity of the films.

There was a significant difference in terms of SRy in $Fe(Tos)_3$ in the test of the number of layers and in the addition of additives but one point that must be considered is that, here only SRy is taken into account and not the thickness of the film. The thickness of the films would help to

accurately show that samples with pyridine have less thickness than samples without pyridine since it is reported in the literature.

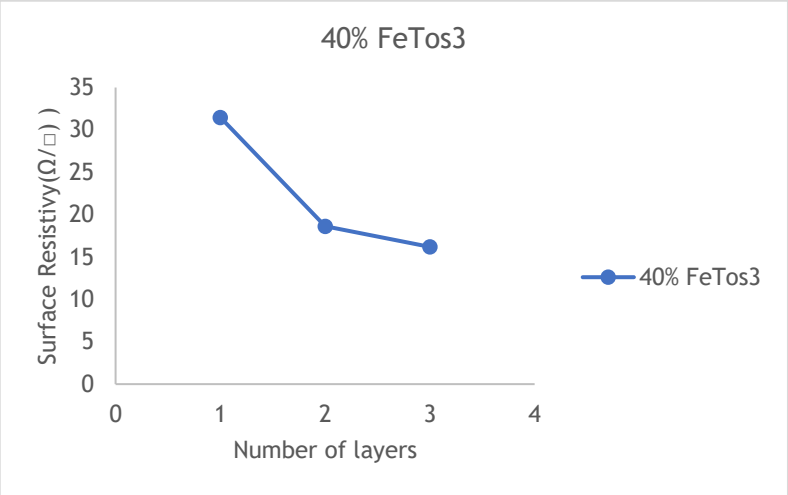

Figure 7. 6- Surface Resistivity of 40% $Fe(Tos)_3$ in different layers

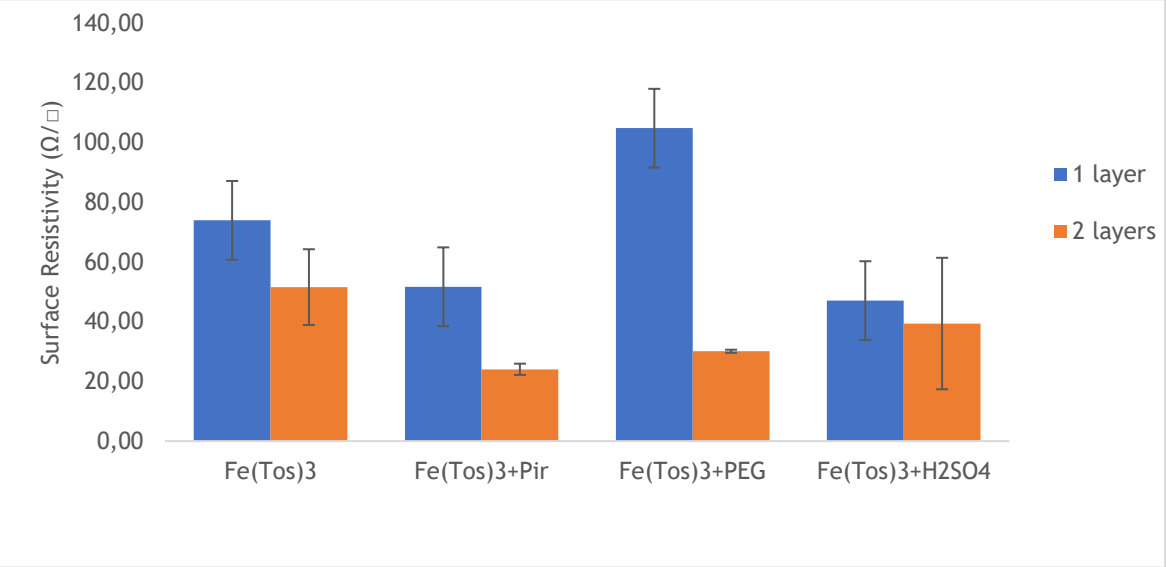

Figure 7. 7-Influence of two layers in the additives

7.2.3. Post-treatment H_2SO_4 after the two layer formation

A post-treatment with H_2SO_4, was also tested to reduce even more the resistivity, and to see if there was any significant decrease in the SRy, **figure 7. 8**. It is apparent that there was no relevant effect of this treatment on the SRy.

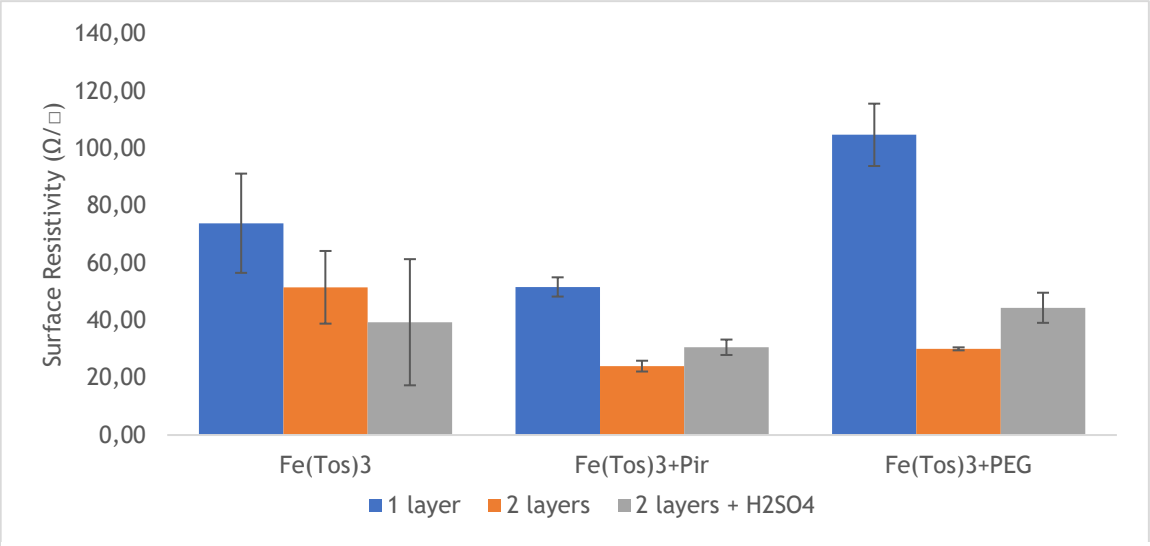

Figure 7. 8-H_2SO_4 treatment after the formation of two layers in all additives

7.3. FTIR

The FTIR spectrum of PU and PEDOT is shown in **figure 7. 9**. Samples were characterized by PU for polyurethane and PEDOT for samples which has 2 layers of PEDOT with pyridine.

The PEDOT spectra is similar with those reported in the literature with the peak at 1550 cm^{-1} due to $C_{\alpha}{=}{=}C_{\beta}$ stretching in the thiophene ring[109]. The peak at 1294 cm^{-1} is due to $C_{\beta}{-}C_{\beta}$ stretching[109]. Peaks at 1168, 1046 and 966 cm^{-1} are due to C—O—C bending vibrations in ethylenedioxyl group[12, 109]. The band at 950 cm^{-1} is due to ethylenedioxy ring deformation[110]. The peaks at 867, 767 and 673 cm^{-1} are due to C—S—C bond stretching in the thiophene ring[109, 111].

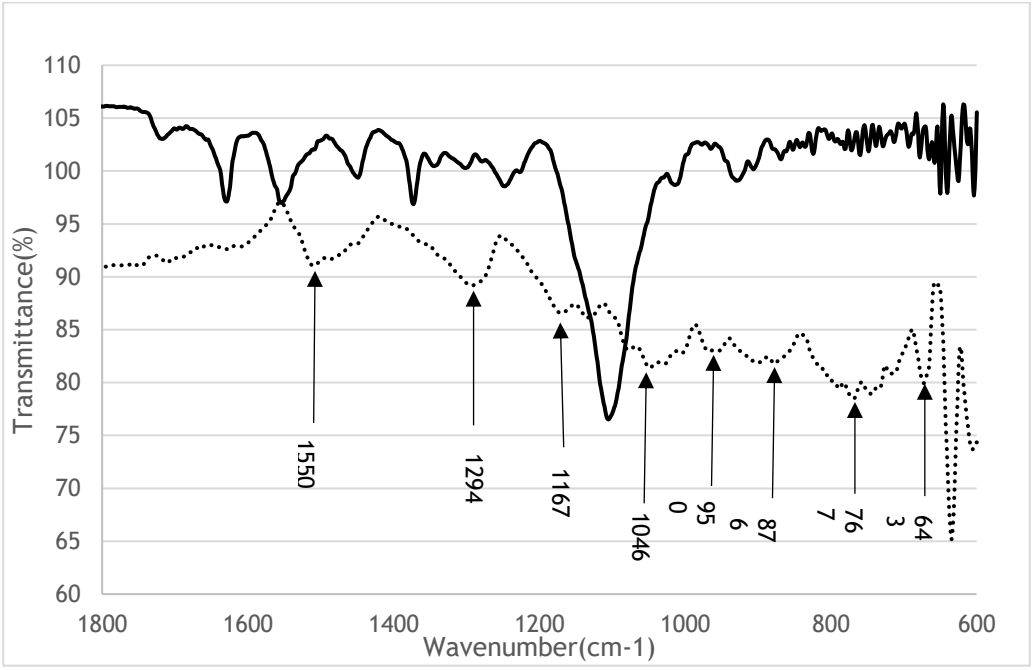

Figure 7. 9- PU (solid line) and PEDOT(dash line) FTIR spectrum

7.4. SEM

For SEM analysis only the best samples in terms of surface resistivity was selected, namely the samples with pyridine with two layers of PEDOT.

In **figure 7. 10**, it is possible to observe a PU sample without any film and in the **figure 7. 11** there is the presence of the PEDOT layer on the samples. In **figure 7. 11** it is observed a thickness between 1.550 to 1.900 µm which results in films with conductivities from 209 to 268 S/cm, with a surface resistivity of 24 Ω/□.

In literature the PEDOT films have thickness in the nm range, [79, 83, 91], and not in the µm. This was not expected to happen, but one advantage is the robustness of the films. The PEDOT films are going to be subjected to some high pressures when put them in scalp to keep a good contact with the skin. If the films were in the nm range this could have an undesired effect by breaking and then, resulting in unreliable electrodes for EEG.

The PU/PEDOT interface is represented in **figure 7. 12**, from where two zones were analysed named Z3 and Z4 in order to confirm the presence of a PEDOT film. The presence of PEDOT in the zone Z3 is verified by its elemental analysis, **figure 7. 13**, with higher amounts of S. In Z4, **figure 7. 14**, there is no PEDOT film due to a higher presence of C and absence of S.

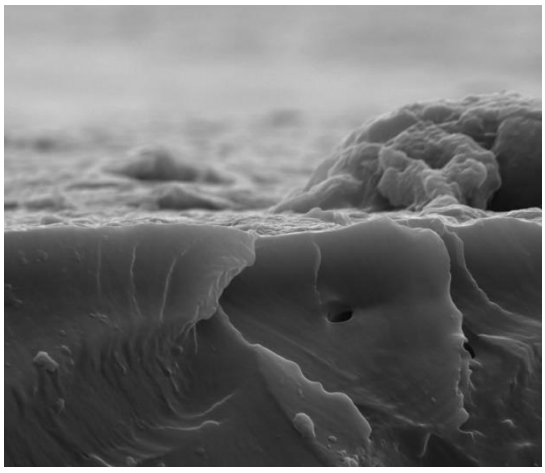

Figure 7. 10- SEM fracture image of a sample without film

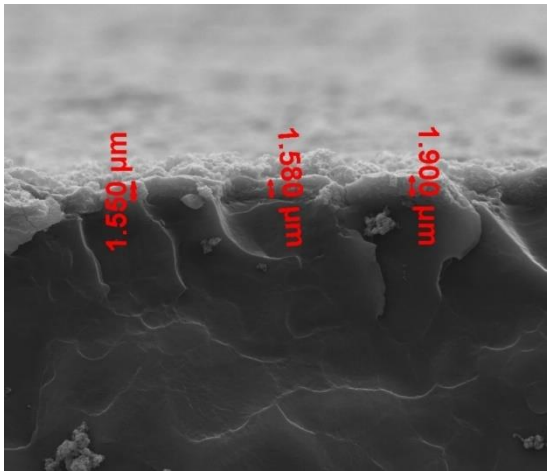

Figure 7. 11-SEM fracture image of a sample with PEDOT film and its thicknesses

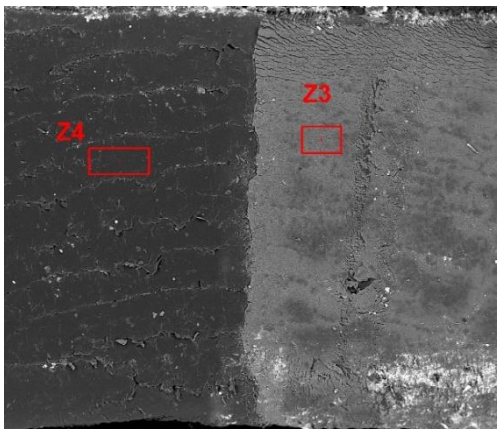

Figure 7. 12- SEM surface image with two distinct zones. Z3 with film. Z4 without any film

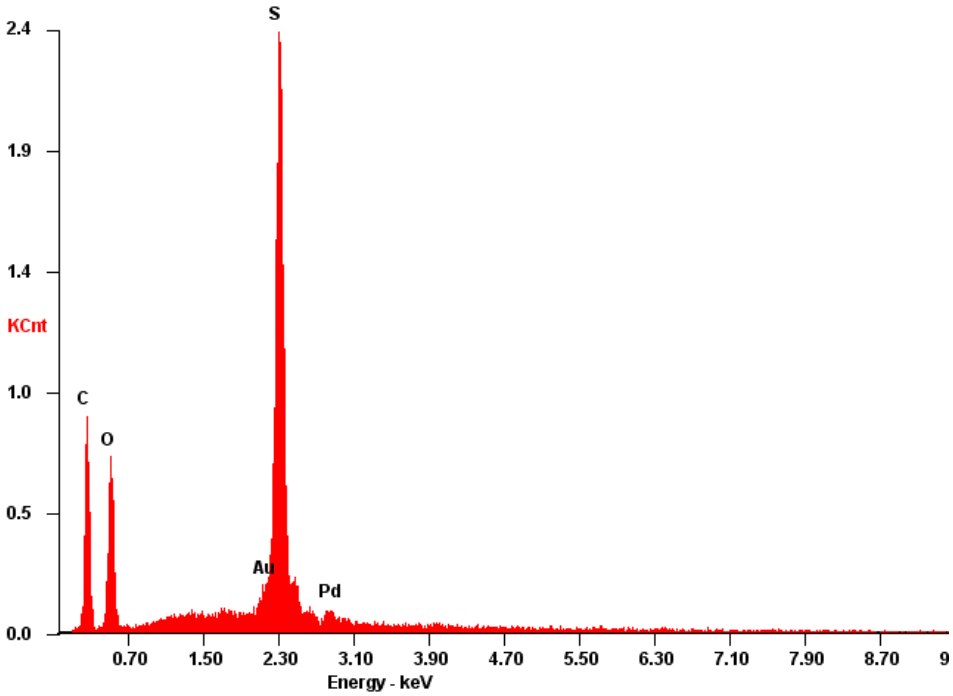

Figure 7. 13-Z3 zone EDS

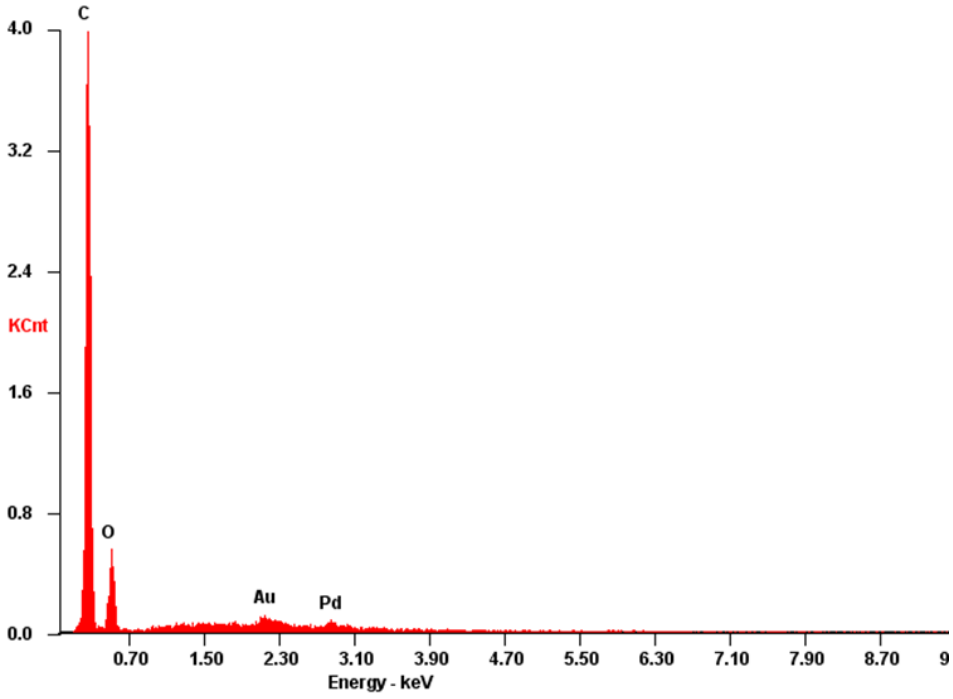

Figure 7. 14- Z4 zone EDS

7.5. Electrical wire connection with the multipin electrode

An araldite® adhesive charged with graphite powder was used to glue the plate top of the PEDOT multipin electrode with a copper wire, see in **figure 7. 15**. A multimeter was used to evaluate the success of the electrical connection, by measuring the electrical resistance. The 50 w/w % presented a higher resistance in relation to 70 w/w %, but each presented a quite low electrical resistance. To accurately evaluate this result each pin was submitted to EIS measurements.

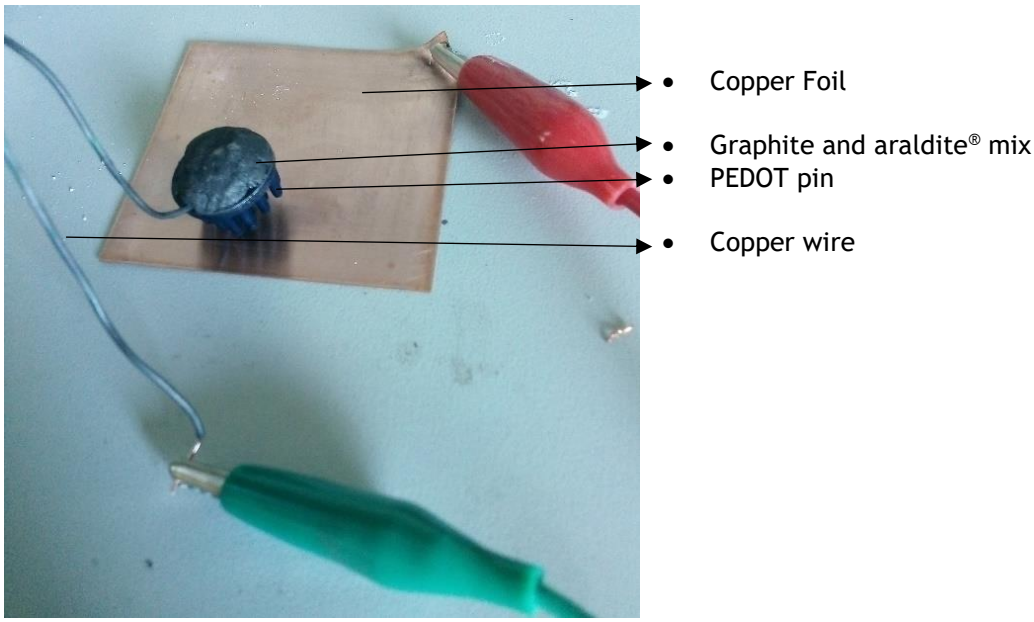

Figure 7. 15-PEDOT pin montage

7.6. EIS measurements

7.6.1. Electrical connection with the graphite/ araldite® composite

For the EIS test of the adhesive composite/multipin interface each multipin sample was tested from 0,01 Hz to 10 kHz. Looking at **figure 7. 16**, it is possible to notice that with an increase from 50 to 70 w/w % in araldite® there is a decrease in impedance, 1200 Ω to 400 Ω. This was in accordance with the study of reference [106]. In terms of phase, both are quite similar with 0º phase until 100 Hz and then the phases differed between 0.4º to -0.8 º, for the 50 w/w % and 0.2º to -0.4º, for the 70 w/w %, up till to 100 kHz. These values are not significant, but it can be assumed that 70 w/w % will have a more homogeneous resistive behaviour in the range of frequency applied in this work. Thus, the mix of 70 w/w % graphite on araldite® was chosen for attaching the copper wire to the PEDOT pin resulting in a fully operationalized EEG electrode.

7.6.2. PEDOT pins on the copper foil

The multipin electrodes (three) were first tested for their contact impedance in contact with a copper foil. The EIS experiments showed that all impedances were bellow to 90 Ω, **figure 7. 17**, and a phase approximately zero in all frequency range. It is noticeable that the sample 1 has a

higher impedance as well as a stronger variance in terms of phase. Therefore, for the in-vivo tests only sample 2 and sample 3 were selected.

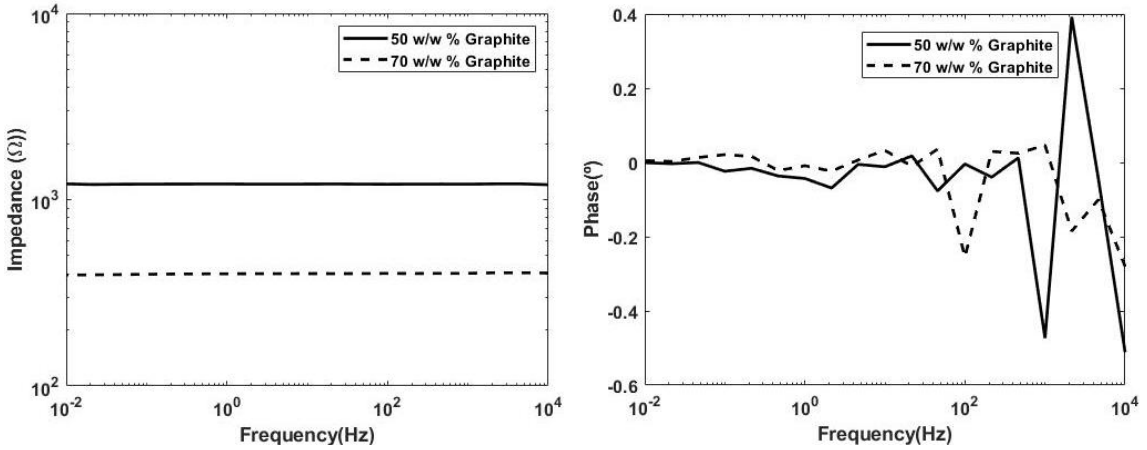

Figure 7. 16-Bode (left) and phase(right) diagram for 50 and 70 w/w% mix of graphite on araldite®

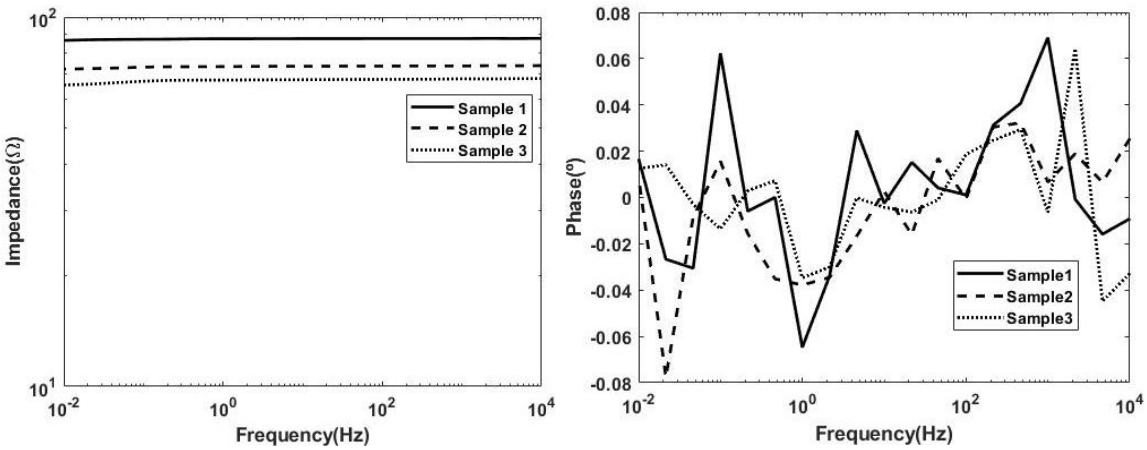

Figure 7. 17- Bode (left) and phase(right) diagram for PEDOT pins on the copper foil

7.6.3. Electrochemical tests of the PEDOT coated PU samples

Electrochemical tests of PEDOT coated PU samples were performed in contact with a saline solution, in order to simulate the electric behaviour of the electrodes in contact with skin sweat. From the plots of **figure 7. 18**. it is possible to notice that there is some variance between the three samples in terms of impedance as well as phase. In terms of impedance, it is kept the same in all range of frequency with only a small increase at 1 Hz. Then, at the phase diagram is evident that the phase angle changes at 1Hz, decreasing to values from -25º to -5º. Therefore, it can be assumed that the impedance variability between samples is due to the VPP fabrication technique and the impedance is, for each sample, essentially independent of frequency. The phase remains also invariant for high frequencies and only starts increasing below 1 Hz, an indication that the system adopts a capacitive component.

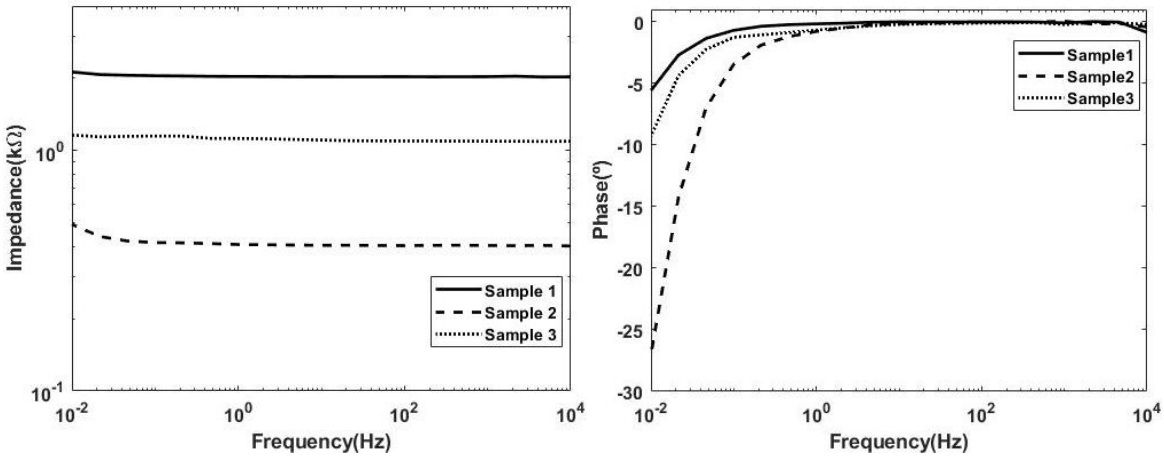

Figure 7. 18- Bode (left) and phase(right) diagram for PEDOT samples

7.6.4. In-vivo tests of the PEDOT coated multipin electrodes on the forearm

In **figure 7. 19,** the mean of all measurements, black line, indicates that, in the case of impedance, most of the samples will have a constant impedance bellow to 40kΩ, which it is a good value according with the literaure for dry electrodes [112], and at 100Hz there is a slowly decrease. In terms of phase, until 10Hz, approxemitelly, the samples will have a phase close to zero and then decreases graddually up to 10kHz. In this work the interested range of frequency is between 0,01 to 40 Hz and until 40 Hz the phase only reaches -15°, meaning it is mostly resistive.

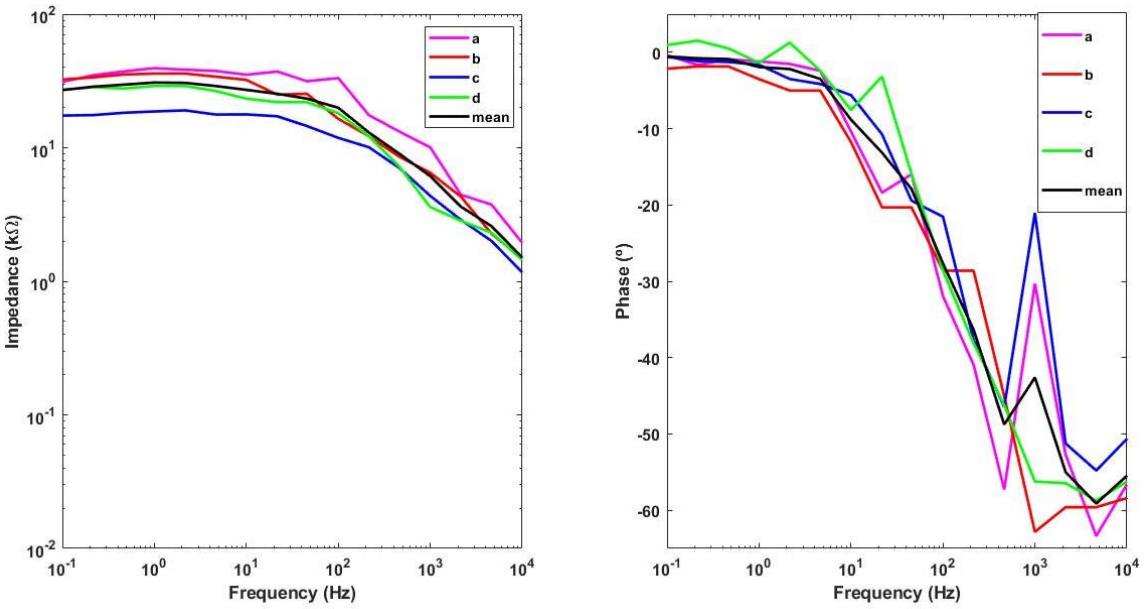

Figure 7. 19- Bode (left) and phase (right) diagram for PEDOT pins on forearm. From a to b with PEDOT sample 2. From c to d with PEDOT sample 3. Black line the mean of all measurements

EEG Data Analysis

For EEG recordings only measurements with the eyes close are going to be discussed in this chapter and the results from the eyes opened are going to be moved to the annex chapter they do not differ significantly from each other.

7.6.5. Fp1 position

In **figure 7. 20** are plotted the EEG signals of two AgCl gelled electrodes placed on the forehead (Fp1), about 2 cm apart. It is apparent that the signals have the same shape in the 5 second interval, though the difference between them in terms of amplitude varies randomly between -10 and 10 μV, as it is possible to see from the difference between them. At **figure 7. 21**, a very similar behaviour can be seen with a AgCl reference electrode and a PEDOT working electrode. Since the residual signals are very similar for both couples, it can be concluded that the PEDOT based electrode is very promising to measure EEG signals. These results also show that even between two electrodes of the same type there is some difference, while they are separated by 2 cm from each other. In EEG measurements it is quite difficult to obtain two perfectly similar signals because of the low amplitude value (μV), thus any type of noise can easily alter the signal. The same kind of results happened in **annex 4**, the two AgCl gelled electrodes, and **annex 5, t**he AgCl reference electrode and a PEDOT working**,** with the eyes opened

Another option to evaluate the effectiveness of the PEDOT electrode, it is to do a blink test (eyes open/close).

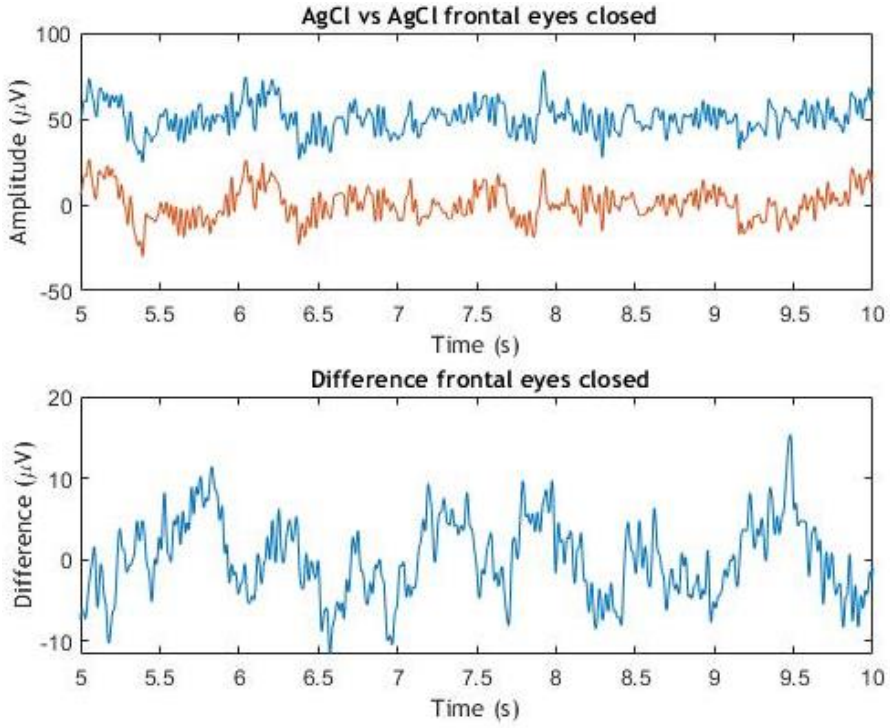

Figure 7. 20 - Fp1 EEG recording AgCl reference electrode (blue) vs AgCl working electrode (orange)

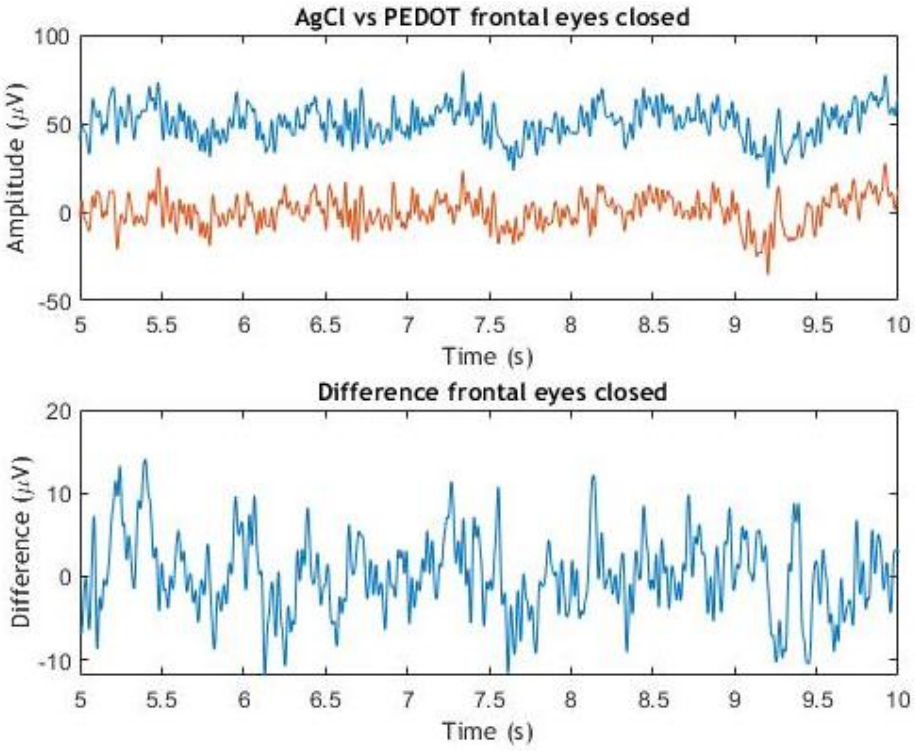

Figure 7. 21 - Fp1 EEG recording AgCl reference electrode (blue) vs PEDOT working electrode (orange)

In **figure 7. 22**, it is shown an example of the eyes blink test for the AgCl reference electrode, and PEDOT, working electrode, and it is noticeable that when there is a blink the amplitude reaches a high value and then stabilized again. Both recorded signals are very similar meaning that the PEDOT electrode can successfully record the shape of the signal, although the amplitude it is not similar. Indeed, in the AgCl electrode the amplitude is about 300 μV and with the PEDOT electrode the amplitude is 200 μV. However, it shouldn't be forgotten that PEDOT is a dry electrode and does not have a gel like AgCl, increasing the impedance of charge transfer, furthermore, the resistance of the PEDOT electrode is much higher than the resistance of the AgCl electrode.

In figure 7. 23, the amplitudes and shape between the two electrodes of AgCl for the blink test is almost identical.

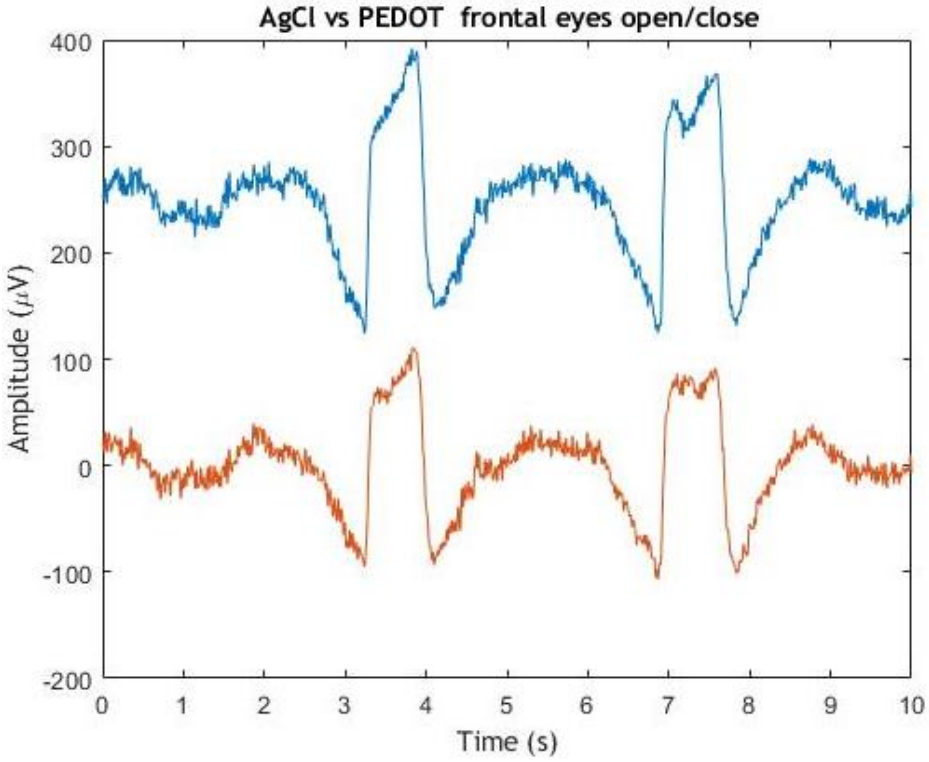

Figure 7. 22 - Fp1 EEG recording blink test AgCl reference electrode (blue) vs PEDOT working electrode (orange)

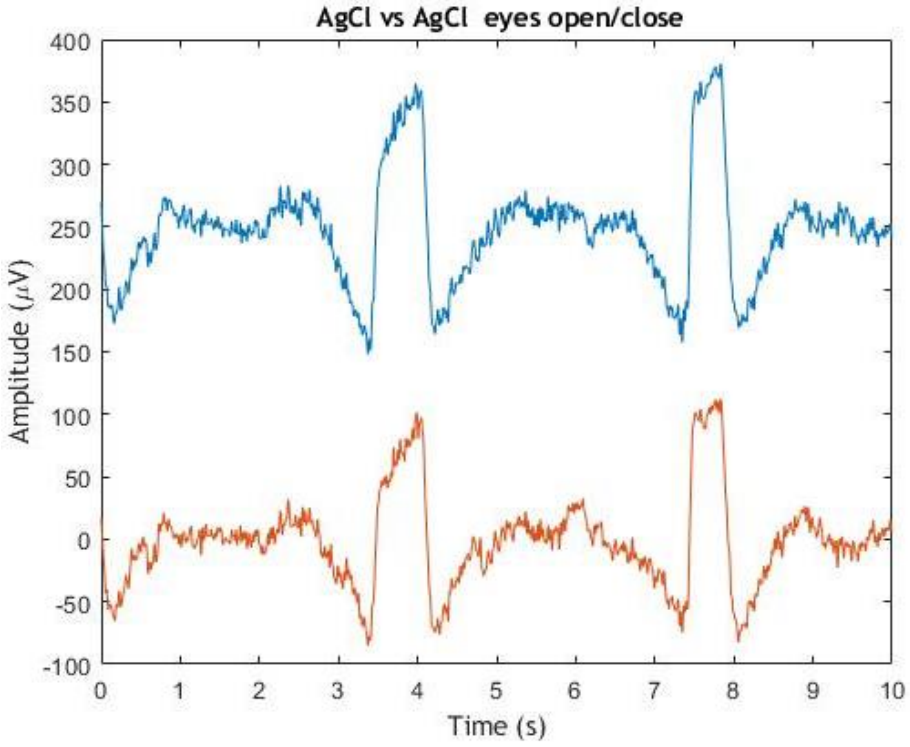

Figure 7. 23 - Fp1 EEG recording blink test AgCl reference electrode (blue) vs AgCl working electrode (orange)

7.6.6. O1 position

For the occipital EEG recording the electrodes were positioned in the O1 position next to each other, following a scheme similar to that adopted for the frontal position. Looking at **figure 7. 24**, it can be seen that the results are quite distinct from the frontal position with more noise in the signals, which is due to the presence of hair. In **figure 7. 24**, the signals have almost the same shape, additionally, there is the presence of repetitive peaks that may come from a grounding problem. Without counting the presence of the amplitude of the peaks the difference varies from 5 μV to -5 μV. For the PEDOT multipin, **figure 7. 25** ,the shape of the wave is almost identical but the difference between the two fluctuates from 10 μV to -5 μV. Although, the noise was not that predominant. The analogous of results happened in **annex 6**, the two AgCl gelled electrodes, and **in annex 7, t**he AgCl reference electrode and a PEDOT working**,** with the eyes opened.

The PSD was calculated for the PEDOT and AgCl electrodes in the eyes closed condition, in order to look for the alfa activity, which is usually found in the 8-12 Hz range. Analysing the **figure 7. 26**, the existence of a peak between 8-12 Hz is not clear, to deduce that it is alpha activity. Though, both PSD spectrum are mostly the same from 0.5-40 Hz with only a small difference at 5 Hz. This result of the PSD spectrum is not completely unexpected since some individuals cannot have this alpha activity present in their EEG recording [17] and for that reason it is not possible to assume if the PEDOT multipin is able or not to record alpha activity.

The PSD spectrum of the Fp1 position was also calculated for the eyes closed, **annex 8,** and it is possible to see that there is not any significant difference between the PEDOT and AgCl electrodes.

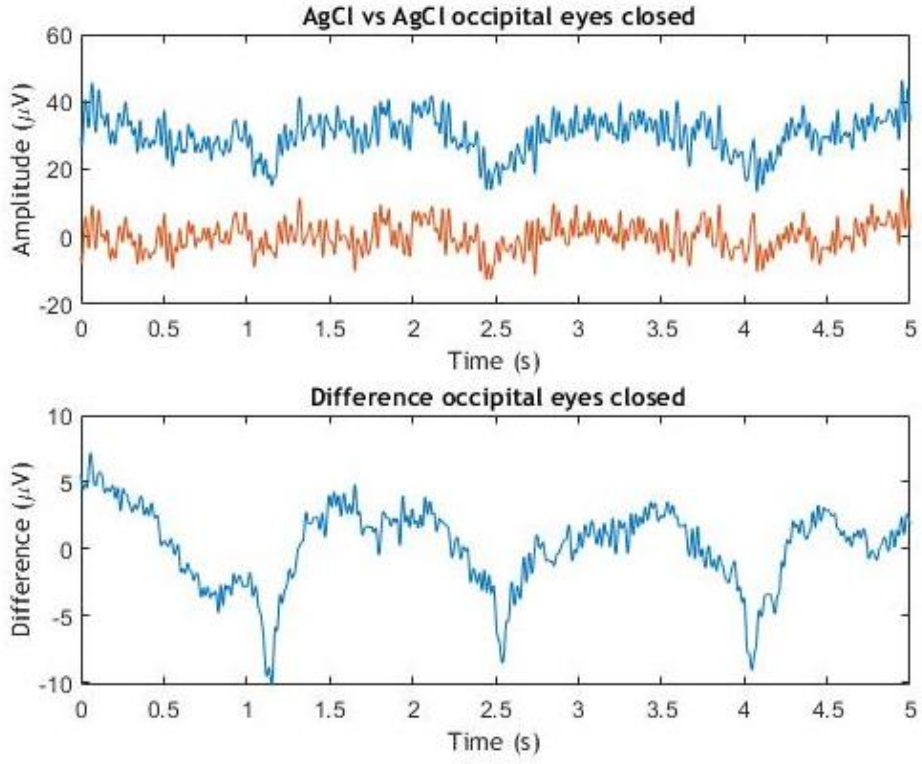

Figure 7. 24 - O1 EEG recording AgCl reference electrode (blue) vs AgCl working electrode (orange)

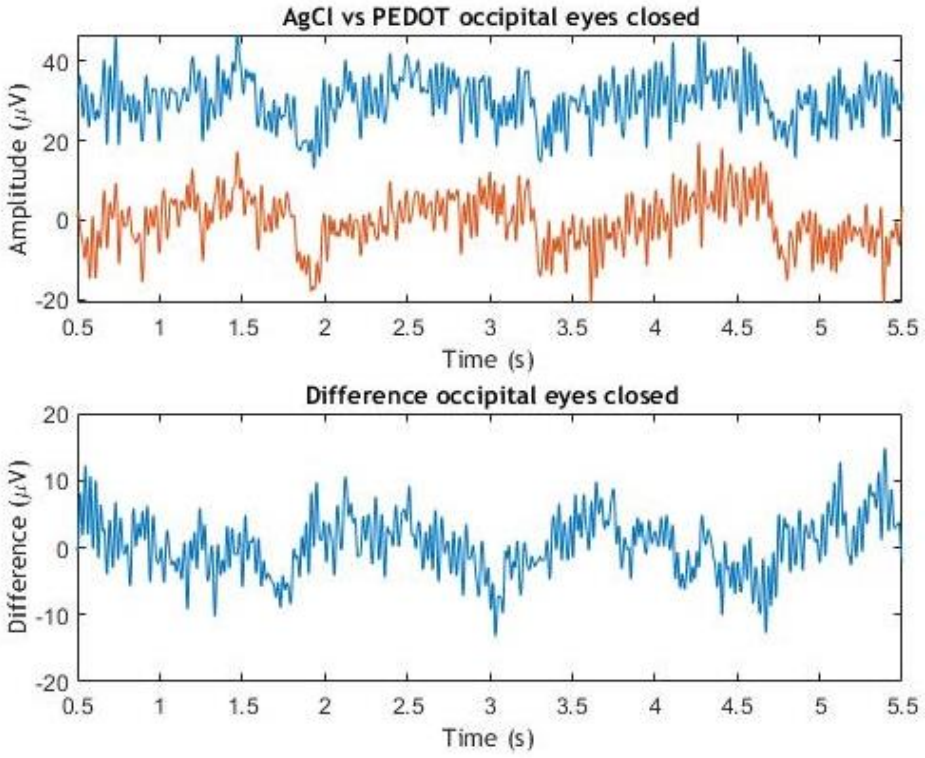

Figure 7. 25 - O1 EEG recording AgCl reference electrode (blue) vs PEDOT electrode (orange)

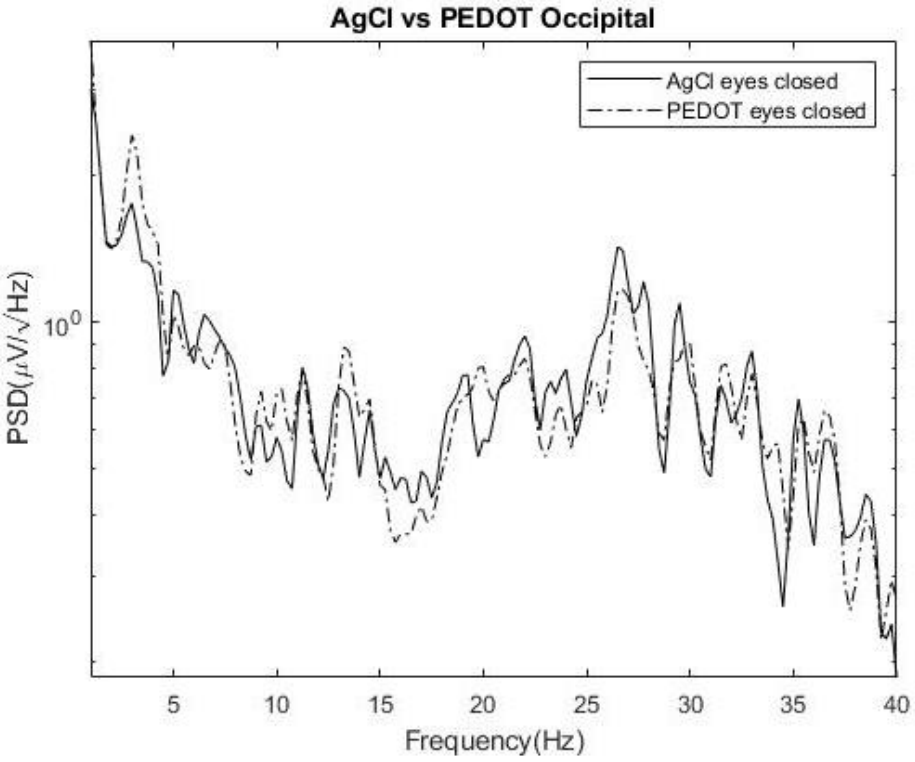

Figure 7. 26- PSD spectrum of Ag electrode (-) and PEDOT(-.-) for alpha detection

The quantification of the differences between EEG signals of the AgCl/AgCl and AgCl/PEDOT electrodes was done through the calculation of the RMSD, RMSDN and Pearson correlation coefficient, **table 7. 1** and **table 7. 2**.In the frontal region, both EEG signals of the AgCl/AgCl and AgCl/PEDOT electrodes were very similar signals between the pairs of electrodes, in terms of amplitude and shape of the signals. The correlation is slightly lower in the case of the eyes open condition. The results are superior in the case of eye blink because the signals have much higher amplitudes and a better signal-to-noise ratio.

Table 7. 1 - Signal evaluation parameters results in the Fp1 position

	AgCl vs AgCl				AgCl vs PEDOT			
	RMSD (µV)	**SD (±)**	**RMSDN**	**Corr (%)**	**RMSD (µV)**	**SD (±)**	**RMSDN**	**Corr (%)**
Eyes Closed	4,83	0,53	0,17	81	5,29	0,51	0,16	86
Eyes Open	4,54	0,62	0,17	84	4,83	0,87	0,16	76
Eyes Open /Close	11,89	1,00	0,08	97	14,26	1,48	0,08	97

The occipital region results differ from the frontal results with higher values of RMSD and RMSDN and lower values of the Pearson correlation, meaning more dissimilar signals in terms of amplitude and shape and, consequently, a lower correlation between signals. This is valid for the couples AgCl vs AgCl and AgCl vs PEDOT and should be ascribed to the presence of hair. Furthermore, it is apparent that in the occipital results the AgCl vs PEDOT measurements show a greater similarity in relation to the AgCl vs AgCl, with lower values of RMSD and RMSDN and higher values of correlation. This result was not expected because due to the presence of hair it should be more reliable to establish a connection with the scalp by using the gel than just my mechanical coupling as it is done by using PEDOT. This experiment should be repeated for validation.

Table 7. 2 – Signal evaluation parameters results in the O1 position

	AgCl vs AgCl				AgCl vs PEDOT			
	RMSD (µV)	**SD (±)**	**RMSDN**	**Corr (%)**	**RMSD (µV)**	**SD (±)**	**RMSDN**	**Corr (%)**
Eyes Closed	5,83	3,02	0,23	73	4,32	0,01	0,21	76
Eyes Open	5,70	2,10	0,35	63	4,37	0,54	0,21	78

Chapter VII

8. Conclusions and Future Developments

8.1. Conclusions

VPP has demonstrated to be a successful technique to produce conductive PEDOT films on PU substrates. VPP is a simple technique that has lot of parameters to be work over. In this work, only the parameters prior VPP were optimized, namely immersion time, drying technique and time, addition of additives and H_2SO_4 post-treatment, and the VPP parameters during polymerization (temperature, pressure) were kept constant. The optimized surface resistivity was 25 Ω/□, corresponding to a conductivity of from 209 to 268 S/cm for a film thickness from 1.550 to 1.900 μm, respectively.

The obtained conductivities were clearly lower than the reported values for PEDOT in the literature. However, the films produced in the current work display thicknesses in the μm range, unlike the literature films that display thicknesses up to 100 nm. The main advantage of this high thickenss is the robustness of the film, which is needed to resist mechanical effors during EEG recording. It was confirmed that the multipins had similar impedances after several EEG measurements, indicating their good stability. Futher mechanical tests should be done to evaluate the strengh of this thicker films to see if this is advantageous or not.

In terms of EEG data, and after performing EEG tests in the frontal and occipital positions, it was demonstrated that the PEDOT coated PU electrodes were able to record EEG data with similar results in terms of signal amplitude, shape and PSD, to AgCl gelled electrodes. However, further tests are requided to fully characerize the new electrodes.

8.2. Future Developments

For future tests it is proposed:

- For VPP:
    1. By using the already optimized parameters prior VPP it would be interesting to study VPP parameters, like amount of used EDOT, the influence of temperature, pressure and time as well.
    2. Work with PEDOT:PSS to evaluate the difference in terms of the counter ion and evaluate it with other already existent electrodes for EEG and ECG.
- For the montage of PEDOT multipin electrodes:
    1. Improvement of the attachment of the mix of graphite and araldite® to the PEDOT pins. This was not one point that was considered but when the multipin electrodes were fixed to the head of the subject with the rubber strips, the amount of glue compromised in some situations the positioning.
- For EEG data:
    1. Perform more measurements, by using more volunteers;
    2. In the eye blinking test, to use cyclic intervals of time for better recording;
    3. To perform the recording in an controlled environment, like an illumination controlled and silent room in order to facilitate the focus of the patients.

Annex

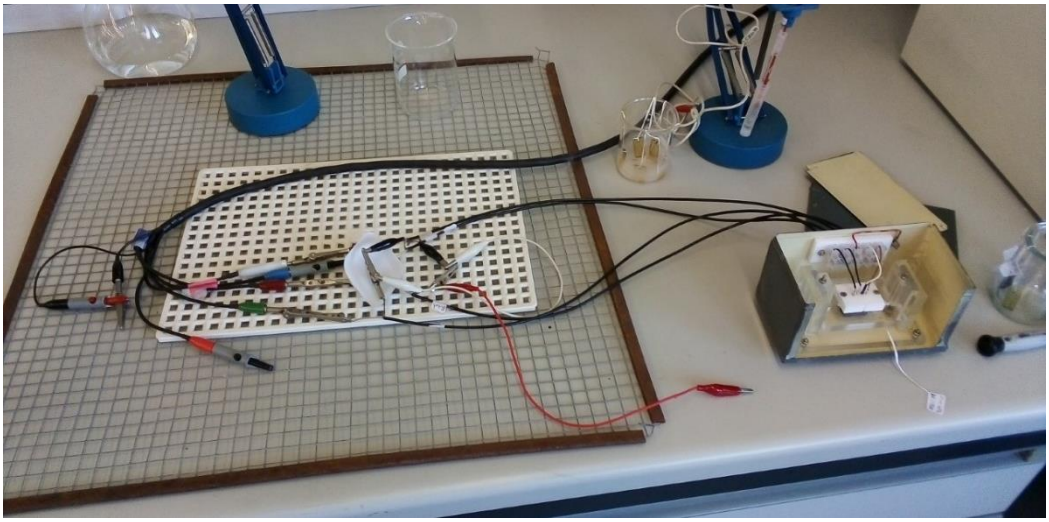

Annex 1- Potentiostat Gamry G300

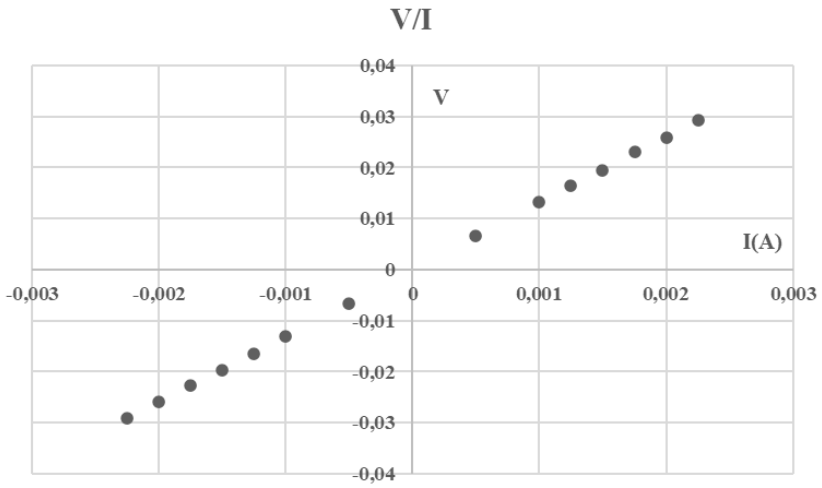

Annex 2- Voltage(V) over Current (I)

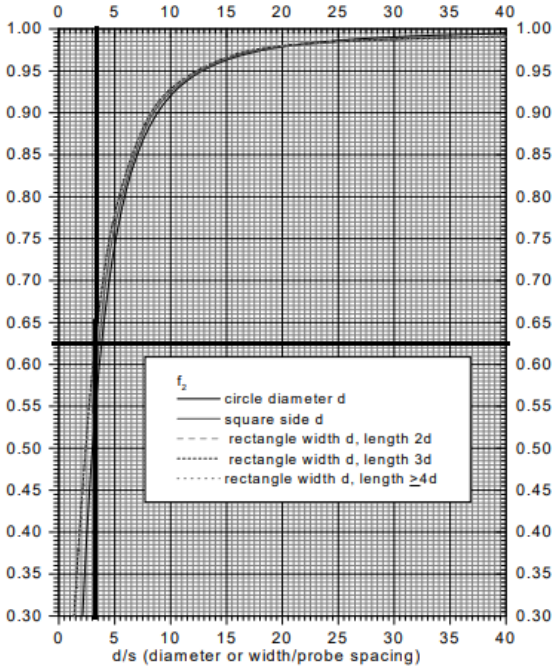

Annex 3- *Selection of the value of f2*

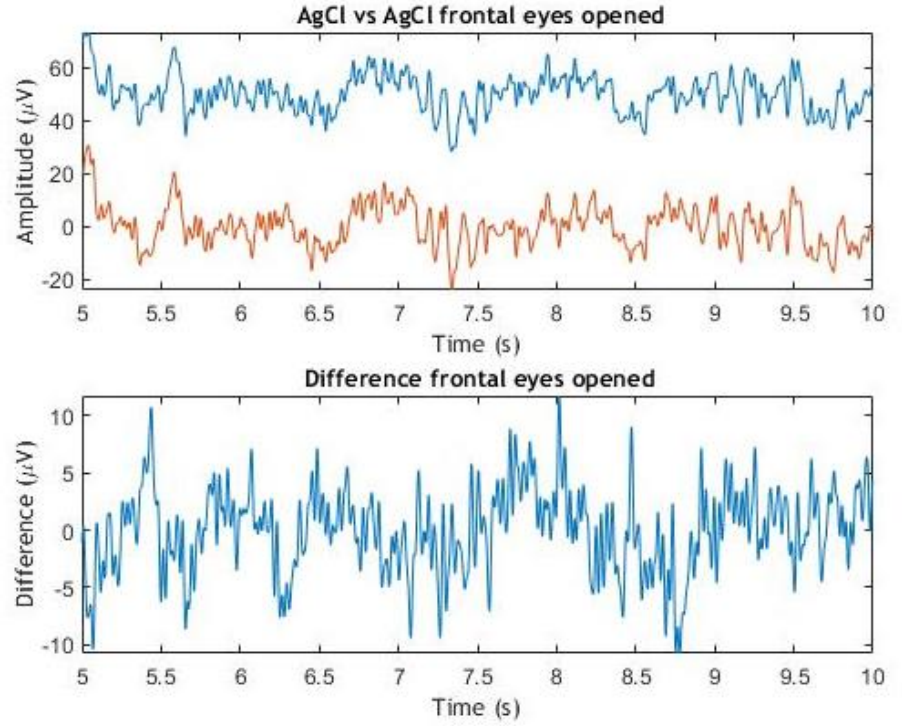

Annex 4 - Fp1 EEG recording AgCl reference electrode (blue) vs AgCl working electrode (orange) eyes opened

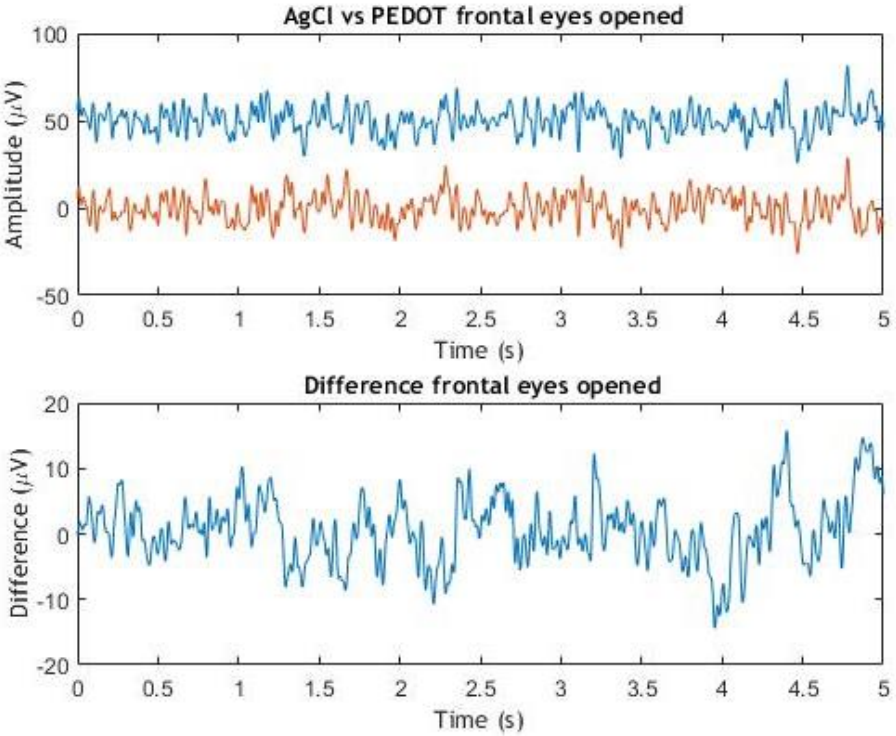

Annex 5 - Fp1 EEG recording AgCl reference electrode(blue) vs PEDOT electrode (orange) eyes opened

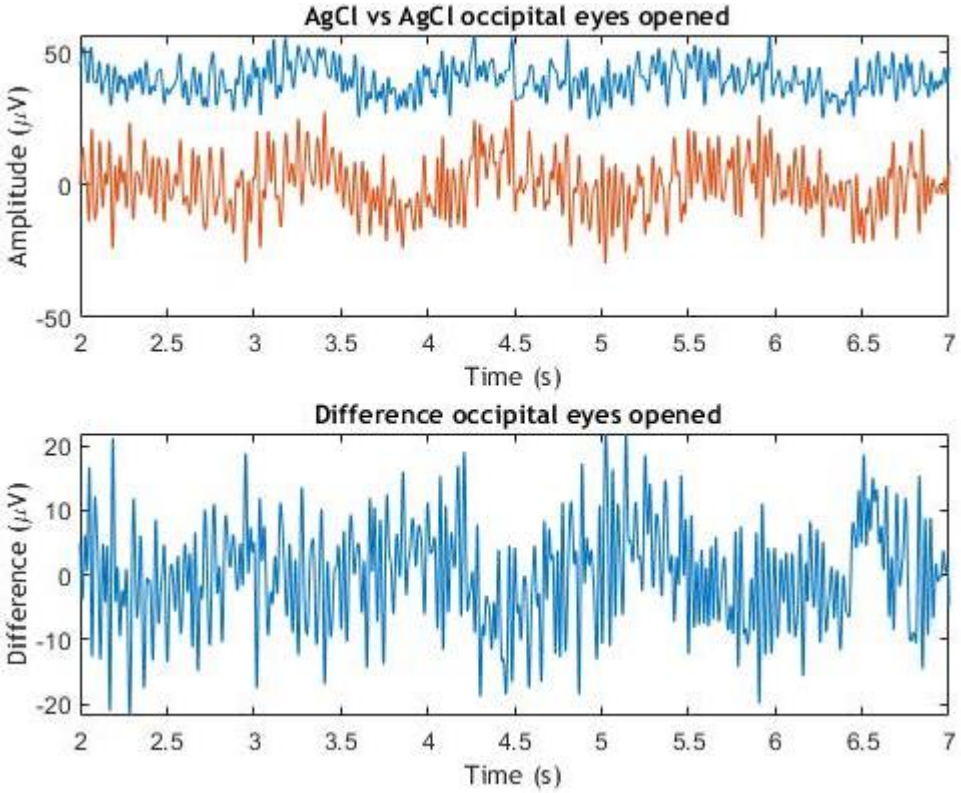

Annex 6 - O1 EEG recording AgCl reference electrode(blue) vs AgCl working electrode (orange) eyes opened

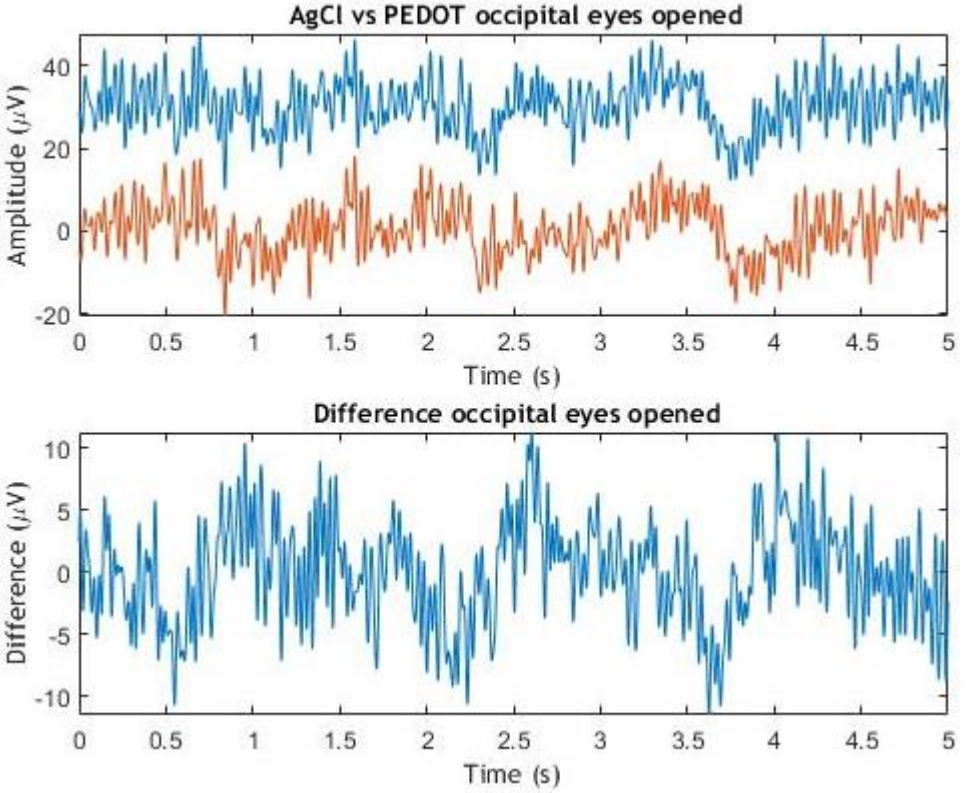

Annex 7 - O1 EEG recording AgCl reference electrode(blue) vs PEDOT electrode (orange) eyes opened

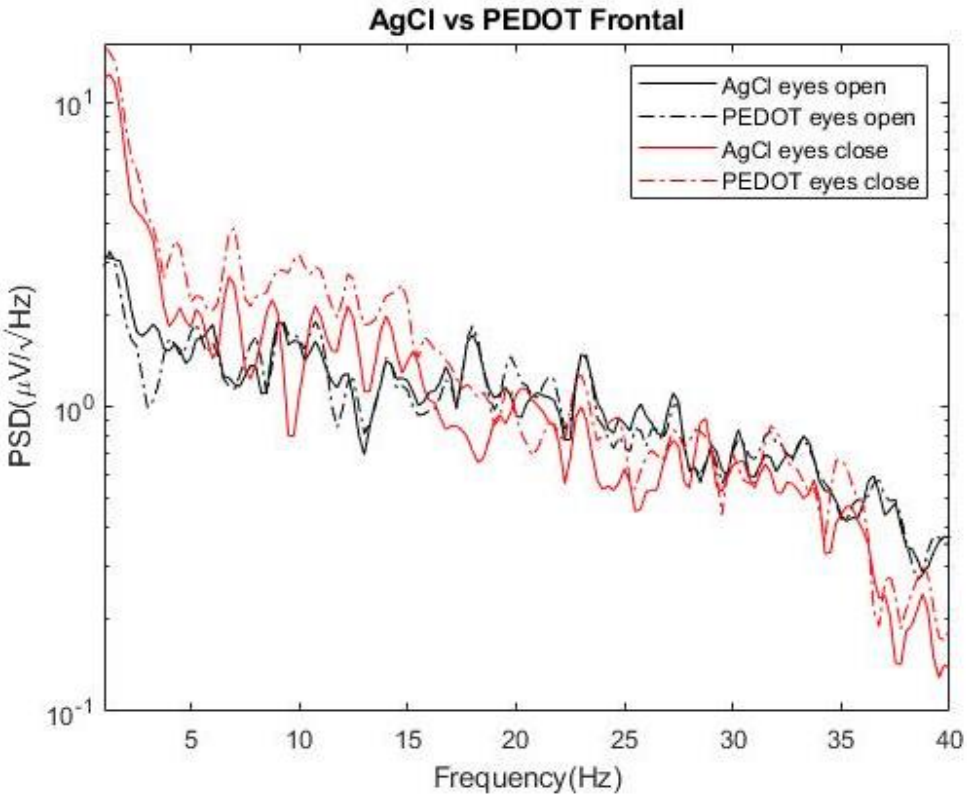

Annex 8 - PSD of Fp1 position O1 EEG recording

References

[1] Im, C. and J.-M. Seo, "A review of electrodes for the electrical brain signal recording." Biomedical Engineering Letters,vol. 6,n. 3, p. 104-112, 2016..

[2] Webster, J., *22. Webster, J. G. (ed.), Medical instrumentation: application and design, Fourth edition,* John Wiley & Sons, Hoboken, NJ, 2010. 2010.

[3] Khandpur, R., *Biomedical Instrumentation: Technology and Applications*. 2004: Mcgraw-hill.

[4] Teplan, M., "Fundementals of EEG measurement". Measurement Science Review, vol. 2, p.1-11, 2002.

[5] Lopez, M., D. Morillo, and F. Pelayo, "*Dry EEG electrodes"*. Sensors (Basel, Switzerland), vol. 14, p. 12847-12870, 2014.

[6] Ray, W.J. and S. Slobounov, *Fundamentals of EEG Methodology in Concussion Research*, in *Foundations of Sport-Related Brain Injuries*, p. 221-240. S. Slobounov and W. Sebastianelli, Editors. 2006, Springer US: Boston, MA..

[7] Ko, W.H. "Active electrodes for EEG and evoked potential". in *Proc. of the 20th Annu. International Conference of the IEEE Engineering in Medicine and Biology Society. Vol.20 Biomedical Eng. Towards the Year 2000 and Beyond (Cat. No.98CH36286)*. 1998.

[8] Chen, Y.H., et al., "Soft, comfortable polymer dry electrodes for high quality ECG and EEG recording". Sensors (Basel), vol. 14, n.12, p. 23758-80, 2014.

[9] Jeong, J.W., et al., "Soft materials in neuroengineering for hard problems in neuroscience." Neuron, vol. 86, n. 1, p. 175-86, 2015.

[10] Cogan, S.F., "Neural stimulation and recording electrodes". *Annu Rev Biomed Eng*, vol.10, p. 275-309, 2008.

[11] Merrill, D.R., M. Bikson, and J.G. Jefferys, "Electrical stimulation of excitable tissue: design of efficacious and safe protocols", J. Neurosci Methods, vol.141, n.2, p. 171-98, 2005.

[12] Leleux, P., et al., "Conducting polymer electrodes for electroencephalography". Adv Healthc Mater, vol.3 n.4, p. 490-3, 2014.

[13] Chen, Y., et al.,"Poly(3,4-ethylenedioxythiophene) (PEDOT) as interface material for improving electrochemical performance of microneedles array-based dry electrode." Sensors and Actuators B: Chemical, vol.188, p. 747-756, 2013.

[14] Fiedler, P., et al., "Novel flexible dry PU/TiN-multipin electrodes: first application in EEG measurements." Conf. Proc. IEEE Eng. Med. Biol. Soc., p. 55-8, 2011.

[15] Jung, H.C., et al., "CNT/PDMS composite flexible dry electrodes for long-term ECG monitoring." IEEE Trans Biomed Eng, vol.59, n.5, p. 1472-9, 2012.
[16] Albajes-Eizagirre, A., et al., *EEG/ERP Analysis: Methods and Applications*. CRC Press, 2014.
[17] Greenfield, L.J., J.D. Geyer, and P.R. Carney, *Reading EEGs: A Practical Approach*. Lippincott Williams & Wilkins, 2009.
[18] Libenson, M., *Practical Approach to Electroencephalography*. Chapter 9, Elsevier, 2009.
[19] Angel, A., "Processing of sensory information". Progress in Neurobiology, vol.9, n.1, p. 1-122, 1977.
[20] *QEEG*. Available from: https://www.amenclinics.com/services/qeeg/.Cited on April 2020;
[21] Nunez, P.L. and R. Srinivasan, *Electric fields of the brain: the neurophysics of EEG*. 2006. Oxford University Press, USA.
[22] Jin-Chern, C., et al." Using novel MEMS EEG sensors in detecting drowsiness application". 2006 *IEEE Biomedical Circuits and Systems Conference*. 2006.
[23] Ruffini, G., et al., "First human trials of a dry electrophysiology sensor using a carbon nanotube array interface." Sensors and Actuators A: Physical, vol.144, n.2, p. 275-279, 2008.
[24] Grozea, C., C.D. Voinescu, and S. Fazli, "Bristle-sensors--low-cost flexible passive dry EEG electrodes for neurofeedback and BCI applications." J. Neural Eng., vol.8 n.2, p. 025008, 2011.
[25] Liao, L.D., et al., "Design, fabrication and experimental validation of a novel dry-contact sensor for measuring electroencephalography signals without skin preparation". Sensors (Basel), vol. 11, n.6, p. 5819-34, 2011.
[26] H.N., N., *The Biomedical Engeneering Handbook*, J. D.Bronzino, Editor. 1995, CRC Press: Florida. p. 1185-1195.
[27] H.N., N., The Biomedical Engeneering Handbook, J. D.Bronzino, Editor. 1995, CRC Press: Florida. p. 201-212.
[28] Picton, T., et al., "Guidelines for Using Human Event-Related Potentials to Study Cognition: Recording Standards and Publication Criteria." Psychophysiology, vol.37, p. 127-52.2000.
[29] Klem, G.H., et al., "The ten-twenty electrode system of the International Federation. The International Federation of Clinical Neurophysiology." Electroencephalogr Clin Neurophysiol Suppl, vol. 52, p. 3-6, 1999.
[30] Freye, E., *Cerebral Monitoring in the Operating Room and the Intensive Care Unit — An Introductory for the Clinician and a Guide for the Novice Wanting to Open a Window to the Brain*, in *Cerebral Monitoring in the OR and ICU*, E. Freye, p. 77-168. Editor. Springer Netherlands: Dordrecht. 2005.
[31] Heeger, A.J., "Semiconducting and Metallic Polymers: The Fourth Generation of Polymeric Materials (Nobel Lecture) ". Angewandte Chemie International Edition, vol. 40, n.14, p. 2591-2611, 2001.
[32] Elschner, A., et al., "PEDOT: principles and applications of an intrinsically conductive polymer". CRC Press. 2010.
[33] Ouyang, J., "Recent advances of intrinsically conductive polymers". Wuli Huaxue Xuebao/ Acta Physico - Chimica Sinica, vol.34, p. 1211-1220, 2018.
[34] Skotheim, T.A. and J. Reynolds, *Handbook of Conducting Polymers, 2 Volume Set*. 2007.

[35] Su, W.P., J.R. Schrieffer, and A.J. Heeger, "Solitons in Polyacetylene". Physical Review Letters, vol.42, n.25, p. 1698-1701, 1979.
[36] Ouyang, J. and Y. Li, "Effect of electrolyte solvent on the conductivity and structure of as-prepared polypyrrole films". Polymer, vol.38, n.8, p. 1971-1976, 1997.
[37] Ouyang, J. and Y. Li, "Great improvement of polypyrrole films prepared electrochemically from aqueous solutions by adding nonaphenol polyethyleneoxy (10) ether". Polymer, vol.38, n.15, p. 3997-3999, 1997.
[38] Yongfang, L. and Q. Renyuan, "On the nature of redox processes in the cyclic voltammetry of polypyrrole nitrate in aqueous solutions". Journal of Electroanalytical Chemistry, vol.362, n.1, p. 267-272, 1993.
[39] *Ho, K.-S.,* "Effect of phenolic based polymeric secondary dopants on polyaniline". Synthetic Metals, vol.126, p. 151-158, 2002.
[40] Chan, H.S.O., et al., "A New Water-Soluble, Self-Doping Conducting Polyaniline from Poly(o-aminobenzylphosphonic acid) and Its Sodium Salts: Synthesis and Characterization". Journal of the American Chemical Society, vol.117, n.33, p. 8517-8523, 1995.
[41] Armour, M., et al., "Colored electrically conducting polymers from furan, pyrrole, and thiophene". Journal of Polymer Science Part A-1: Polymer Chemistry, vol. 5, n. 7, p. 1527-1538, 1967.
[42] Tourillon, G. and F. Garnier, "New electrochemically generated organic conducting polymers". Journal of Electroanalytical Chemistry and Interfacial Electrochemistry, vol.135, n.1, p. 173-178, 1982.
[43] Roncali, J., et al., "Effects of steric factors on the electrosynthesis and properties of conducting poly(3-alkylthiophenes)". The Journal of Physical Chemistry, vol.91, n.27, p. 6706-6714, 1987.
[44] Tourillon, G., "Structural effect on the electrochemical properties of polythiophene and derivatives". Journal of Electroanalytical Chemistry - J ELECTROANAL CHEM, vol. 161, p. 51-58, 1984.
[45] Daoust, G. and M. Leclerc, "Structure-property relationships in alkoxy-substituted polythiophenes". Macromolecules, vol. 24, n. 2, p. 455-459, 1991.
[46] Hagiwara, T., et al., "Synthesis and properties of poly(3,4-dimethoxythiophene)". Synthetic Metals, vol. 32, n. 3, p. 367-379, 1989.
[47] Fréchette, M., et al., "Monomer reactivity vs. regioregularity in polythiophene derivatives." Macromolecular Chemistry and Physics, vol. 198, n.6, p. 1709-1722.1997.
[48] F. Jonas, G.H.a.W.S., "Novel polythiophenes, process for their preparation, and their use", DE3813589A1, Bayer AG, Germany, 1988.
[49] F. Jonas, G.H.a.W.S., "Process for the preparation of Polythiophenes", European Patent 0339340B1, *Bayer AG*, 1999.
[50] Corradi, R. and S.P. Armes, "Chemical synthesis of poly(3,4-ethylenedioxythiophene)".Synthetic Metals, vol. 84, n.1, p. 453-454, 1997.
[51] Im, S.G., et al., "Conformal Coverage of Poly(3,4-ethylenedioxythiophene) Films with Tunable Nanoporosity via Oxidative Chemical Vapor Deposition". ACS Nano, vol. 2, n.9, p. 1959-1967, 2008.
[52] Moriarty, R.M. and O. Prakash, "Hypervalent iodine in organic synthesis". Accounts of Chemical Research, vol. 19, n.8, p. 244-250, 1986.
[53] Groenendaal, L., et al.,"Poly(3,4-ethylenedioxythiophene) and Its Derivatives: Past, Present, and Future". Advanced Materials, vol. 12, n.7, p. 481-494, 2000.

[54] Jonas, F. and L. Schrader, "Conductive modifications of polymers with polypyrroles and polythiophenes". Synthetic Metals, vol. 41, n.3, p. 831-836, 1991.

[55] Winther-Jensen, B., D.W. Breiby, and K. West, "Base inhibited oxidative polymerization of 3,4-ethylenedioxythiophene with iron(III)tosylate". Synthetic Metals, vol. 152, n.1, p. 1-4, 2005.

[56] Dobrynin, A.V. and M. Rubinstein, "Counterion Condensation and Phase Separation in Solutions of Hydrophobic Polyelectrolytes". Macromolecules, vol. 34, n. 6, p. 1964-1972, 2001.

[57] Spiteri, M.N., C.E. Williams, and F. Boué, "Pearl-Necklace-Like Chain Conformation of Hydrophobic Polyelectrolyte: a SANS Study of Partially Sulfonated Polystyrene in Water". Macromolecules, vol. 40, n.18, p. 6679-6691, 2007.

[58] Jonas, F. and W. Krafft." New polythiophene dispersions, their preparation and their use", *European Patent* 0440957A2, Bayer AG, 1991.

[59] Jonas, F. and R. Dhein, "Sheets for transparent plastic and glass useful as heat protection windows - are coated with poly-thiophene(s) or their salts", European Patent 4229192, Bayer AG,1993.

[60] F. Louwet, E.V. Thillo, and B. Groenendaal.,"Process for preparing electroconductive coatings" European Patent 1639607A1, *Agfa-Graevert,* 2004.

[61] Jonas, F., et al.,"Conductive coatings", European Paten 0686662A2, Bayer AG, 1994.

[62] Mohammadi, A., et al., "Chemical vapour deposition (CVD) of conducting polymers: Polypyrrole". Synthetic Metals, vol. 14, n.3, p. 189-197, 1986.

[63] Fabretto, M., et al., "Influence of PEG-ran-PPG Surfactant on Vapour Phase Polymerised PEDOT Thin Films". Macromolecular Rapid Communications, vol. 30, n.21, p. 1846-1851, 2009.

[64] Chen, Y.-s., et al., "Gas sensitivity of a composite of multi-walled carbon nanotubes and polypyrrole prepared by vapor phase polymerization". Carbon, vol. 45, n. 2, p. 357-363.2007.

[65] Ali, M.A., et al., "Effects of solvents on poly(3,4-ethylenedioxythiophene) (PEDOT) thin films deposited on a (3-aminopropyl)trimethoxysilane (APS) monolayer by vapor phase polymerization". Electronic Materials Letters, vol. 6, n. 1, p. 17-22, 2010.

[66] Wu, D., et al., "Temperature dependent conductivity of vapor-phase polymerized PEDOT films". Synthetic Metals, vol. 176, p. 86-91, 2013.

[67] Glenis, S., G. Tourillon, and F. Garnier, "Photoelectrochemical properties of thin films of polythiophene and derivatives: Doping level and structure effects". Thin Solid Films, vol. 122, n. 1, p. 9-17, 1984.

[68] Mitchell, G.R., F.J. Davis, and C.H. Legge, "The effect of dopant molecules on the molecular order of electrically-conducting films of polypyrrole". Synthetic Metals, vol. 26, n.3, p. 247-257, 1988.

[69] Ali, M.A., et al.,"Effects of the FeCl3 concentration on the polymerization of conductive poly(3,4-ethylenedioxythiophene) thin films on (3-aminopropyl) trimethoxysilane monolayer-coated SiO2 surfaces". Metals and Materials International, vol. 15, n. 6, p. 977-981, 2009.

[70] Subramanian, P., et al., "Vapour phase polymerisation of pyrrole induced by iron(III) alkylbenzenesulfonate salt oxidising agents". Synthetic Metals, vol. 158, n. 17, p. 704-711, 2008.

[71] Jang, K.-S., et al., "Fabrication of Poly(3-hexylthiophene) Thin Films by Vapor-Phase Polymerization for Optoelectronic Device Applications". ACS Applied Materials & Interfaces, vol. 1, n. 7, p. 1567-1571, 2009.
[72] Kim, J., et al., "The preparation and characteristics of conductive poly(3,4-ethylenedioxythiophene) thin film by vapor-phase polymerization". Synthetic Metals, vol. 139, n.2, p. 485-489, 2003.
[73] Fabretto, M.V., et al., "Polymeric Material with Metal-Like Conductivity for Next Generation Organic Electronic Devices". Chemistry of Materials, vol. 24, n.20, p. 3998-4003, 2012.
[74] Brooke, R., et al., "Recent advances in the synthesis of conducting polymers from the vapour phase". Progress in Materials Science, vol. 86, p. 127-146, 2017.
[75] Ouyang, J., "Solution-Processed PEDOT:PSS Films with Conductivities as Indium Tin Oxide through a Treatment with Mild and Weak Organic Acids". ACS Applied Materials & Interfaces, vol. 5, n. 24,p. 13082-13088, 2013.
[76] Nevrela, J., et al., "Secondary doping in poly(3,4-ethylenedioxythiophene):Poly(4-styrenesulfonate) thin films". Journal of Polymer Science Part B: Polymer Physics, vol. 53, n. 16, p. 1139-1146, 2015.
[77] Wang, J., K. Cai, and S. Shen, "Enhanced thermoelectric properties of poly(3,4-ethylenedioxythiophene) thin films treated with H2SO4". Organic Electronics, vol.15, n. 11, p. 3087-3095, 2014.
[78] Xia, Y., K. Sun, and J. Ouyang, "Solution-Processed Metallic Conducting Polymer Films as Transparent Electrode of Optoelectronic Devices". Advanced Materials, vol. 24, n. 18, p. 2436-2440, 2012.
[79] Winther-Jensen, B. and K. West, "Vapor-Phase Polymerization of 3,4-Ethylenedioxythiophene: A Route to Highly Conducting Polymer Surface Layers." Macromolecules, vol. 37, n. 12, p. 4538-4543, 2004.
[80] Truong, T.L., et al., "Poly(3,4-ethylenedioxythiophene) vapor-phase polymerization on glass substrate for enhanced surface smoothness and electrical conductivity". Macromolecular Research, vol. 15, n. 5, p. 465-468, 2007.
[81] Winther-Jensen, B., et al., "Vapor Phase Polymerization of Pyrrole and Thiophene Using Iron(III) Sulfonates as Oxidizing Agents". Macromolecules, vol. 37, n.16, p. 5930-5935, 2004.
[82] Fewings, K., et al., "Supramolecular interactions in metal tosylate complexes". Polyhedron, vol. 20, p. 643-649, 2001.
[83] Fabretto, M., et al., "High Conductivity PEDOT Using Humidity Facilitated Vacuum Vapour Phase Polymerisation". Macromolecular Rapid Communications, vol. 29, n. 16, p. 1403-1409, 2008.
[84] Zuber, K., et al., "Improved PEDOT Conductivity via Suppression of Crystallite Formation in Fe(III) Tosylate During Vapor Phase Polymerization". Macromolecular Rapid Communications, vol. 29, n.18, p. 1503-1508, 2008.
[85] Ha, Y.-H., et al., "Towards a Transparent, Highly Conductive Poly(3,4-ethylenedioxythiophene)". Advanced Functional Materials, vol. 14, n. 6, p. 615-622, 2004.
[86] von Helden, G., T. Wyttenbach, and M.T. Bowers, "Conformation of macromolecules in the gas phase: use of matrix-assisted laser desorption methods in ion chromatography". Science, vol. 267, n. 5203, p. 1483-5, 1995.

[87] Wyttenbach, T., G. von Helden, and M.T. Bowers," Conformations of alkali ion cationized polyethers in the gas phase: polyethylene glycol and bis[(benzo-15-crown-5)-15-ylmethyl] pimelate". International Journal of Mass Spectrometry and Ion Processes, vol. 165 p. 377-390, 1997.

[88] Wang, J., et al., "Simultaneously enhanced electrical conductivity and Seebeck coefficient in Poly (3,4-ethylenedioxythiophene) films treated with hydroiodic acid". Synthetic Metals, vol. 220, p. 585-590, 2016.

[89] Massonnet, N., et al., "Metallic behaviour of acid doped highly conductive polymers". Chemical Science, vol. 6, n. 1, p. 412-417, 2015.

[90] Saxena, N., et al., "Facile Optimization of Thermoelectric Properties in PEDOT:PSS Thin Films through Acido-Base and Redox Dedoping Using Readily Available Salts". ACS Applied Energy Materials, vol. 1, n. 2, p. 336-342, 2018.

[91] Jia, Y., et al., "Efficient enhancement of the thermoelectric performance of vapor phase polymerized poly(3,4-ethylenedioxythiophene) films with poly(ethyleneimine)". Journal of Polymer Science Part B: Polymer Physics, vol. 57, n. 5, p. 257-265, 2019.

[92] Massonnet, N., et al., "Improvement of the Seebeck coefficient of PEDOT:PSS by chemical reduction combined with a novel method for its transfer using free-standing thin films". Journal of Materials Chemistry C, vol. 2, n. 7, p. 1278-1283, 2014.

[93] Crispin, X., et al., "Conductivity, morphology, interfacial chemistry, and stability of poly(3,4-ethylene dioxythiophene)-poly(styrene sulfonate): A photoelectron spectroscopy study". Journal of Polymer Science B Polymer Physics, vol. 41, p. 2561-2583, 2003.

[94] Gueye, M.N., et al., "Structure and Dopant Engineering in PEDOT Thin Films: Practical Tools for a Dramatic Conductivity Enhancement". Chemistry of Materials, vol. 28, n. 10, p. 3462-3468, 2016.

[95] Zuber, K., et al., "Influence of Postsynthesis Heat Treatment on Vapor-Phase-Polymerized Conductive Polymers". ACS Omega, vol. 3, p. 12679-12687, 2018.

[96] Fabretto, M., et al., "In-situ QCM-D analysis reveals four distinct stages during vapour phase polymerisation of PEDOT thin films". Polymer, vol. 51, n. 8, p. 1737-1743, 2010.

[97] Fabretto, M., et al., "High conductivity PEDOT resulting from glycol/oxidant complex and glycol/polymer intercalation during vacuum vapour phase polymerisation". Polymer, vol. 52, p. 1725-1730, 2011.

[98] Mueller, M., et al., "Vacuum vapour phase polymerization of high conductivity PEDOT: Role of PEG-PPG-PEG, the origin of water, and choice of oxidant". Polymer, vol. 53, n. 11, p. 2146-2151, 2012.

[99] Smits, F.M., "Measurement of sheet resistivities with the four-point probe". The Bell System Technical Journal, vol. 37, n. 3, p. 711-718, 1958.

[100] Valdes, L.B., "Resistivity Measurements on Germanium for Transistors". Proceedings of the IRE, vol. 42, n. 2, p. 420-427,1954.

[101] Swapp, S. *Scanning Electron Microscopy (SEM)*. Available from: https://serc.carleton.edu/research_education/geochemsheets/techniques/SEM.html.Cited on May 2020;

[102] Goodge, J. *Energy-Dispersive X-Ray Spectroscopy (EDS)*. Available from: https://serc.carleton.edu/msu_nanotech/methods/eds.html. Cited on May 2020;

[103] Bradley, M. *FTIR Basics*. Available from: https://www.thermofisher.com/pt/en/home/industrial/spectroscopy-elemental-isotope-

analysis/spectroscopy-elemental-isotope-analysis-learning-center/molecular-spectroscopy-information/ftir-information/ftir-basics.html. Cited on April 2020.
[104] Xiao, Y., X. Cui, and D.C. Martin, "Electrochemical polymerization and properties of PEDOT/S-EDOT on neural microelectrode arrays". Journal of Electroanalytical Chemistry, vol. 573, n. 1, p. 43-48, 2004.
[105] *Basics of Electrochemical Impedance Spectroscopy*. Available from: https://www.gamry.com/application-notes/EIS/basics-of-electrochemical-impedance-spectroscopy/. Cited on April 2020.
[106] Calixto, C., et al., "Development of graphite-polymer composites as electrode materials."Materials Research-ibero-american Journal of Materials, vol. 10, 2007.
[107] Rampil, I.J., "A primer for EEG signal processing in anesthesia". Anesthesiology, vol. 89, n. 4, p. 980-1002, 1998.
[108] Cutmore, T.R.H. and D.A. James, "Identifying and reducing noise in psychophysiological recordings". International Journal of Psychophysiology, vol. 32, n. 2, p. 129-150, 1999.
[109] Khan, Z.U., et al., "Acido-basic control of the thermoelectric properties of poly(3,4-ethylenedioxythiophene)tosylate (PEDOT-Tos) thin films". Journal of Materials Chemistry C, vol. 3, n. 40, p. 10616-10623, 2015.
[110] Selvaganesh, S.V., et al., "Chemical Synthesis of PEDOT–Au Nanocomposite". Nanoscale Research Letters, vol. 2, n. 11, p. 546, 2007.
[111] Cho, W., et al., "Synthesis and characterization of bicontinuous cubic poly(3,4-ethylene dioxythiophene) gyroid (PEDOT GYR) gels". Physical Chemistry Chemical Physics, vol. 17, n. 7, p. 5115-5123, 2015.
[112] Ferree, T.C., et al., "Scalp electrode impedance, infection risk, and EEG data quality".Clin Neurophysiol, vol. 112, n. 3, p. 536-44, 2001.